UNIV. OF MICHIGAN
MAR 10 1953
EAST ENGINEERING

Electrochemical Society

ELECTROCHEMICAL INDUSTRY

The Niagara Frontier

Electrolytic Aids to INSECTICIDE MANUFACTURE

Chlorine and caustic soda, products of the electrolytic industry, are essential to insecticide manufacture.

Uniformly high quality **GLC Graphite Anodes** are equally important to the chlorine and caustic soda production of many leading electrochemical manufacturers. The performance of **GLC Graphite Anodes** in electrolytic cell operations is unsurpassed.

ELECTRODE DIVISION

Great Lakes Carbon Corporation

Niagara Falls, N. Y. GLC Morganton, N. C.

Courtesy Piper Aircraft

Graphite Anodes, Electrodes and Specialties

Sales office: Niagara Falls, N. Y. • **Other offices:** New York, N. Y., Chicago, Ill., Pittsburgh, Pa

Sales Agents: J. B. Hayes Company, Birmingham, Ala., George O'Hara, Wilmington, Cal.

EDITORIAL STAFF

R. M. BURNS, *Chairman*
NORMAN HACKERMAN, *Technical Editor*
RUTH G. STERNS, *Managing Editor*
CECIL V. KING, *Associate Editor*
U. B. THOMAS, *News Editor*
MARY F. MURRAY, *Assistant Editor*

DIVISIONAL EDITORS

M. A. STREICHER, *Corrosion*
ABNER BRENNER, *Electrodeposition*
N. C. CAHOON, *Battery*
H. C. FROELICH, *Electronics*
W. C. GARDINER, *Industrial Electrolytic*
S. J. SINDEBAND, *Electrothermic*
JOHN J. CHAPMAN, *Electric Insulation*
L. B. ROGERS, *Theoretical*
SHERLOCK SWANN, JR., *Electro-Organic*

REGIONAL EDITORS

JOSEPH SCHULEIN, *Pacific Northwest*
J. C. SCHUMACHER, *Los Angeles*
O. W. STOREY, *Chicago*
G. W. HEISE, *Cleveland*
PAUL S. BRALLIER, *Niagara Falls*
OLIVER OSBORN, *Houston*
EARL A. GULBRANSEN, *Pittsburgh*
A. C. HOLM, *Canada*
J. W. CUTHBERTSON, *Great Britain*
T. L. RAMA CHAR, *India*

ADVERTISING OFFICE

JACK BAIN
Advertising Manager
545 Fifth Avenue
New York 17, N. Y.
PHONE—*Murray Hill 2-3345*

Journal of the
Electrochemical Society

MARCH, 1953 VOL. 100 · NO. 3

CONTENTS

Regional Features

The Niagara Frontier—Editorial. *R. M. Burns* 53C

Electrochemical Industry: The Niagara Frontier 57C–64C
Four articles by *Paul S. Brallier, M. S. Kircher, W. T. Dunlap, Jr., and G. R. Finlay and J. A. Upper.*

Technical Papers

Correlations between Parabolic Oxidation of Metals and Properties of Oxides. *Andrew Dravnieks* 95

The Diffusion and Solubility of Nitrogen in Beta Zirconium. *M. W. Mallett, E. M. Baroody, H. R. Nelson, and C. A. Papp* 103

Electrodeposition of Tin-Nickel Alloy Plate from Chloride-Fluoride Electrolytes. *J. W. Cuthbertson, N. Parkinson, and H. P. Rooksby* 107

The Hot-Wire Process for Zirconium. *Robert B. Holden and Bernard Kopelman* 120

The Electrochemistry of Gallium. *William M. Saltman and Norman H. Nachtrieb* 126

Electrodeposition Behavior of Cadmium and of Thallium at Mercury Cathodes. *L. B. Rogers and Charles Merrit, Jr.* .. 131

A New Electrochemical Process for Indium. *J. R. Mills, B. G. Hunt, and G. H. Turner* 136

Current Affairs

New York Meeting Combines Fine Technical Program with Attractive Entertainment Features 67C

News Notes 68C
Division News 69C
Section News 70C
Personals 72C
New Members 72C
Book Reviews 73C
Literature from Industry .. 75C
Employment Situations ... 76C

Published monthly by The Electrochemical Society, Inc., Mount Royal and Guilford Aves., Baltimore 2, Md., combining the JOURNAL and TRANSACTIONS OF THE ELECTROCHEMICAL SOCIETY. Editorial offices: 235 West 102nd Street, New York 25, N. Y. Statements and opinions given in articles and papers in the JOURNAL OF THE ELECTROCHEMICAL SOCIETY are those of the contributors, and The Electrochemical Society assumes no responsibility for them. Subscription $11.25 to members, $15.00 to nonmembers. Single copies $1.25 to members, $1.50 to nonmembers. Copyright 1953 by The Electrochemical Society, Inc. Entered as second-class matter November 15, 1947, at the Post Office at Baltimore, Md., under the act of August 24, 1912.

"Check your air, Sir?"

Air compressor and tank are at right. Long cylinders on rack dry air before it enters cables.

He's checking the air pressure in a branch cable, one of scores serving a town. The readings along the cable are plotted as a graph to find low-pressure points which indicate a break in the protecting sheath.

Master meters keep watch over the various cable networks which leave a telephone office in all directions to serve a community. Air enters the system at 7 pounds pressure, but may drop to 2 pounds in outermost sections—still enough to keep dampness out.

To keep voices traveling strongly through telephone cables, you have to keep water out. This calls for speed in locating and repairing cable sheath leaks—a hard job where cable networks fork and branch to serve every neighborhood and street.

At Bell Telephone Laboratories, a team of mechanical and electrical engineers devised a way to fill a complex cable system with dry air under continuous pressure. Pressure readings at selected points detect cracks or holes, however small. Repairman can reach the spot before service is impaired.

It's another example of how Bell Laboratories works out ways to keep your telephone service reliable—and to keep down the cost to you.

BELL TELEPHONE LABORATORIES

Improving telephone service for America provides careers for creative men in mechanical engineering

Editorial

The Niagara Frontier

"*ALTHOUGH* Philadelphia may with right claim to be the birthplace of the American Electrochemical Society, Niagara Falls may with equal right claim to be the home *par excellence* of the American electrochemical industry" wrote Professor Joseph W. Richards, in the first issue of *Electrochemical Industry*, which appeared in September 1902. He writes further in this enterprising journal, the ancestor of our esteemed neighbor *Chemical Engineering*, as follows: "No field in the whole range of applied sciences is succeeding more signally, promising more attractively, or so pregnant with suggestions of future applications than electrochemistry."

There follows an interesting description of the electroprocess industry at the beginning of the century and brief accounts of the operations of the following companies: Castner, Electrolytic Alkali, Niagara Electrochemical, Norton Emery Wheel, International Acheson Graphite, United Barium, Oldbury Chemical, Electrical Lead Reduction, National Electrolytic, Atmospheric Products, and the Union Carbide Company. Professor Richards appears to have been particularly impressed by the achievements of the Ampere Electrochemical Company for he writes ". . . if one considers the combination of forces which this company commands—some veteran inventors, some college professors, some college-trained chemists and electricians, some business men, all enthusiastic persevering workers—it is safe to predict that many more valuable processes will be brought to light as their reward." To the Pittsburgh Reduction Company and its organizers, R. B. Mellon, Charles M. Hall, G. H. Clapp, and Arthur V. Davis he offers: "Our congratulations to the enterprising pioneers of the aluminum industry in America!" Finally, in the account of the Carborundum Company is a picture of the first commercial furnace—an impressive relic which we ourselves had the privilege of being shown by the late Frank J. Tone in the last year of his life.

So this month, we salute Niagara Falls, the home of electrochemical industry! Well nurtured there in the early years, the industry has long been world-wide in location. The prophetic vision of Joesph W. Richards is well demonstrated in America alone by that reliable index of industrial growth and activity, the chlor-alkali industry. From 40 tons a day from five plants in 1900, the production of chlorine has grown to over 5,000 tons a day from 58 plants. In the case of electrolytic caustic soda, the annual output has increased from about 10,000 tons in 1901 to more than a million and a half last year.—RMB

DOW

DOW ADDS NEW EXPORT COMPANIES

Dow has recently formed two subsidiary export companies to serve foreign industry's increasing demands for high-quality chemicals

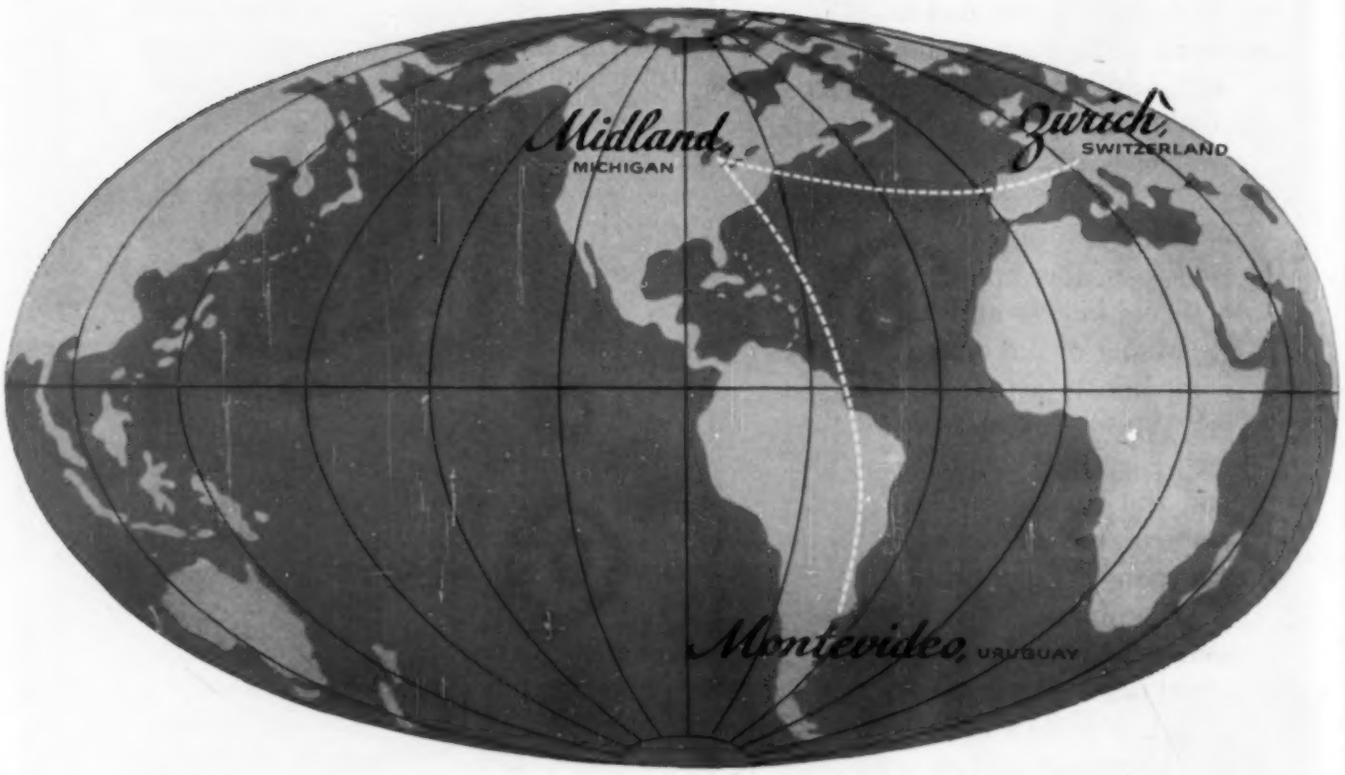

In the Western Hemisphere, Dow Chemical Inter-Ameri an Limited with sales offices in Montevideo, Uruguay will supply chemicals to Mexico and to many countries in Central and South America.

Industries in other continents—Europe, Asia, Africa, and Australia—will be served by Dow Chemical International Limited. The first sales office of this company will be opened in Zurich, Switzerland.

These two new export companies are only one example of the continued growth taking place at Dow. Each year finds new Dow plant facilities, increased production, new products developed . . . an over-all growth and expansion that keeps Dow high among the world leaders in the chemical industry.

you can depend on DOW CHEMICALS

DOW

Correlations between Parabolic Oxidation of Metals and Properties of Oxides[1]

ANDREW DRAVNIEKS

Standard Oil Company (Indiana), Chicago, Illinois

ABSTRACT

From the literature and the author's data on the parabolic oxide formation rates, kinetic constants are correlated with some physical properties of oxides. The parabolic rate constants, taken at $0.6T_m$ and reduced to the same number of diffusion paths and jumps, and the same driving force per jump, fall into logical groups. In the divalent oxides, the reduced rate constant, r, increases with decreasing cation size, for the same lattice type; values of r for the wurtzite lattice type are smaller than for the NaCl type. In the tri-and four-valent oxides, the value of r increases with the cation size. These relations are explained on the basis of Jost's rules. The value of log r is found to vary systematically with $\frac{\Delta F^*}{RT}$ term, where ΔF^* is the free energy of activation. Correlation between the frequency factor in the Arrhenius equation and the so-called reduced activation energy $\frac{E}{T_m}$ found by Dienes for the diffusion in metals, is found to hold also for the oxides. The activation energies for the divalent oxides are found to be a function of the total electron concentration. The activation energy plot vs. Klemm's volume increment shows a concentration of the low E values around the low increments. An explanation of these last two findings on the basis of polarization energies is attempted.

INTRODUCTION

The oxidation of metals has been shown to follow parabolic, linear, logarithmic, and some other specific rate laws (1–13). The present paper deals with the parabolic law

$$\frac{dw}{dt} = \frac{k^1}{w} \qquad w^2 = kt \qquad k^1 = \frac{k}{2} \qquad \text{(I)}$$

(w = weight increase; t = time; k, k^1 = constants) which is traditionally derived from the diffusion of reactants through the oxide as the rate limiting step (7, 14). The most direct proof, by means of radioactive tracers, has been obtained thus far only in a few cases (15–17). Wagner's electrochemical theory of tarnishing (10, 18–21), together with the vacancy diffusion mechanism, successfully relates the parabolic rate constant k to the electrical properties of the oxide, and explains the dependence of this constant on the oxygen pressure for several cases. Thus, it seems permissible to assume, at least for the purpose of seeking correlations between the rates of formation and other properties of oxides, that the parabolic oxidation is diffusion-controlled. Hence, the parabolic rate constants, the Arrhenius activation energies, and the pre-exponential factors for the oxide formation may be tentatively associated with diffusion phenomena. The purpose of the present paper is to demonstrate that the empirical parabolic oxidation constants, if interpreted in the above sense and correlated with certain properties of the oxides, integrate into comparatively coherent trends. These trends may be explained on the basis of concepts issuing from the present knowledge about the diffusion in solids.

DATA

All available literature was searched for cases where the parabolic formation of oxides was either reported or evident from the experimental data. In addition, oxidation of Cu, Ni, and Co was studied experimentally to clarify some uncertainties.

A few words must be said initially about the factors which might cause complications.

The initial oxidation rate may depend especially strongly on surface roughness, stresses, pretreatment, cleanliness (17, 22–25), and other surface factors. Growth of thin films, especially at somewhat lower temperatures, may also be complicated by space charges and potential fields (12, 13) which cause deviations from the parabolic relationship. For these reasons, data pertaining to very thin films were not used.

At larger thicknesses, cracking and other mechanical types of film failures (11, 26) may interfere. If the parabolic relation is evident from plotted

[1] Manuscript received December 16, 1951. This paper was prepared for delivery before the Detroit Meeting, October 9 to 12, 1951. A part of this paper was prepared in 1947–1949 in the course of work at the Chemistry Department, Illinois Institute of Technology, Chicago, Ill., under a contract of the U. S. Navy, Office of Naval Research.

points and the data are used with discrimination, this interference is actually not too important.

Furthermore, impurities in metals pass into the oxides and may change the oxidation rates (21, 27, 28). Similarly, orientation effects modify the rates of oxidation, e.g., in case of Cu and Fe by as much as 20 per cent (29).

Finally, the pressure of oxygen, both by an eventual rate-limiting process on the surface of oxide and by changing the vacancy equilibria in the oxide, may modify the oxidation rates. The first factor does not seem to be very significant at usual pressures (30, 31), and the second factor changes the rates only proportionally to a fractional power of oxygen pressure (18, 19, 32).

Generally, even with the same investigator, the reproducibility of the oxidation measurements is rarely better than a few per cent, and with samples of varying purity, the variations in the oxidation rates reported for the same metal may be much larger.

All of these factors command considerable caution in selecting data from literature. Even so, some apparently parabolic cases might happen to result from a fortuitous combination of nondiffusion processes.

However, in experimenting and in examining the literature data, one gains a certain confidence that, even if the separate values reported vary by a factor of 2 or 3, *it is the identity of the metal and the oxide which primarily determines the magnitude of the oxidation rate*. Other factors, inherent or incidental, only modulate these values and should be averaged out or overlooked if generalizations are attempted. As one sees from Table I, the oxide formation rates at $0.6T_m$ (T_m = absolute melting point of oxide) where the spread of the values is less than at some arbitrary common temperature, are still in a ratio of 1:1000. The reason for choosing $0.6T_m$ as the reference point will be seen from the later discussion.

With this principle in mind, the data summarized in Table I were compiled. The parabolic rates in some cases are not amenable to the experimental study at $0.6T_m$. In such cases, the data from the region where the parabolic law holds were extrapolated to $0.6T_m$. The table contains the Arrhenius activation energies, E, and the frequency factors, A, as related by the equation

$$k = Ae^{-E/RT}. \qquad \text{(II)}$$

Also entered are the entropies of activation, ΔS^*, and the free energies of activation, ΔF^*, for $0.6T_m$, from Eyring's equations (33) introduced into oxidation kinetics by Gulbransen (34)

$$k = \frac{2(k)T}{h} d^2 e^{\Delta S^*/R} e^{-\Delta H^*/RT} \qquad \text{(III)}$$

$$\Delta F^* = \Delta H^* - T\Delta S^* \qquad \text{(IV)}$$

where: k = diffusion rate constant, cm^2 sec^{-1}; (k) = Boltzmann's constant; T = absolute temperature; h = Planck's constant; d = distance between the diffusion sites; ΔS^* = entropy of activation, per mole; ΔH^* = enthalpy of activation, per mole; ΔF^* = free energy of activation, per mole; and R = gas constant.

In using equation (III) a choice of d must be made. Since the crystals of the oxide in the scale are more or less disoriented, it appears reasonable to put $d = V^{\frac{1}{3}}N^{-\frac{1}{3}}$, as is done in treating the diffusion in liquids. V is the volume per mole of diffusion sites; N is Avogadro's number. A choice of the diffusing species also must be made. However, the calculations showed that ΔF^* changes by less than one kcal if oxygen is chosen instead of metal, so this choice is not too significant. In the present work, the metal ions were assumed to diffuse in Me_2O and MeO oxides, and the oxygen ions in Me_2O_3 and MeO_2 oxides, on grounds to be seen in the discussion.

Free energies of oxide formation at $0.6T_m$ were calculated from the equations given by Thompson (35) and by Kubaschewski and Evans (36). The values are given per equivalent of the oxide, so that they correspond, except for the units, to the F_o in Wagner's equation for the parabolic rate constant:

$$k = B\frac{(\bar{n}_1 + \bar{n}_2)\bar{n}_3\bar{n}}{96500} \cdot F_o. \qquad \text{(V)}$$

(B is a constant dependent on the units employed; $\bar{n}_1$, $\bar{n}_2$, and $\bar{n}_3$ are the mean transport numbers of the cations, anions, and electrons, respectively; $\bar{n}$ is the mean electrical conductivity of the oxide; and F_o is the free energy of formation of the oxide under conditions of oxidation). For oxides, $\bar{n}_1$ and $\bar{n}_2$ are very small, and $\bar{n}_3$ is very close to unity (99).

The characteristic frequencies were obtained by applying the T^3 (Debye) law to the heat capacities at 50°K, taken from Kelly (100). The absolute scale for these frequencies was determined by comparing this series of values with another, obtained from the melting points, the molecular weights, and mole volumes by the methods of Lindemann (101) and Herz (102). The actual physical meaning of these frequencies is obscured by the atomic heterogeneity and the anharmonicity of the lattice vibrations. Nevertheless, they may prove convenient in planning models for the diffusion mechanisms.

Discussion

Table I represents a seemingly incoherent assembly of numbers. However, it is clear that certain relations between the kinetic constants and other properties must be implicit in these data, although

TABLE I. *Parabolic rates and related constants for the formation of metal oxides*

Oxide	T_m melting point °K	V molecular volume, cm³	F kcal per equiv. at 0.6 T_m	Log k at 0.6 T_m k = g²cm⁻⁴ sec⁻¹ g = grams of oxygen	Log A see eq. (II) units of A as k	E kcal per mole	ΔS^* eq. (III) kcal	ΔF^* eq. (IV) kcal	Charact. frequency[d] units: 10^{13}	Lattice type
Al_2O_3	2310	26.1	49	−11.3	−7.7	23	−30.8	67	17.8	corundum
BeO	2803	8.3	55	−9.1	−1.9	55	−4.9	63	22.6	wurtzite
CbO	[ass. 1800]	11.5		−2.7	−2.7	25				own
CdO	subl. 1663	15.6	18	[−8 to −9]					7.6	NaCl
CoO	2083	13.2	17	−8.0	−0.7	42	+2.6	39	8.8	NaCl
Cr_2O_3	2263	29.2	31	−9.9	−1.3	53	−2.0	55	13.4	corundum
Cu_2O	1505	23.8	13	−9.4	−2.3	29	−1.9	31	6.2	own
CuO[a]	1609	12.3	5[a]	<−9.2	[−2.5]	<30	−5.5	<36	8.8	own
FeO[b]	1633	12.5	1 [24][b]	−9.1	−2.4	30	−5.0	35	9.0	NaCl
Fe_2O_3	1570	30.5	26	−10.9	−5.6	23	−18.9	42	9.8	(corundum)
Fe_3O_4	1530	44.6	24	−8.4	[−1.2]	<30			9.8	spinel
MnO[c]	2058	13.7	5 [39][c]	−9.4	−1.3	46	−0.1	46	7.5	NaCl
Mn_3O_4	1833	49.0	31	−8.4	−1.2	36			9.0	spinel
MoO_2	[ass. 1500]	28.3	24	[−9.3]	−0.5	37	+3.3	34		rutile
NiO	2263	11.0	13	−9.2	−5.2	25	−18.6	50	11.1	NaCl dist. (37)
PbO	1163	23.3	18[e]	[−11.3][e]					6.5	own
TiO_2	2048	20.8	43	−10.2	−5.1	29	−19.2	52	10.3	rutile
V_2O_3	2243	30.9	42	−8.0	−3.0	31	−9.0	43	11.2	corundum
WO_2	1543	17.8	24	−9.7	+1.4	47	+8.7	38	[7]	rutile
ZnO	2248	14.9	26	−11.1	−6.4	29	−23.6	61	8.2	wurtzite
ZrO_2	2973	22.5	45	−8.8	−6.6	18	−26.6	65	10.9	several

[a] Formation from Cu_2O.
[b] Formation from Fe-Fe_3O_4; F° in parentheses for direct formation.
[c] Formation from Mn-Mn_3O_4; F° in parentheses for direct formation.
[d] From Lindemann's and Herz method.
[e] At 0.5 T_m.

Note on Sources of Data for Table I

Al_2O_3—Parabolic 350°–450°C (38), extrapolation.
BeO—Averages from (39) and (40), extrapolation.
CbO—From (41), extrapolation; oxide CbO (42), also (43).
CdO—Parabolic 300°C (7). For k, assumed $\frac{E}{T_m}$ = 4–4.5, which holds for NaCl type oxides.
CoO—From (44), for pure Co, scale above 850°C is CoO; other data: (24, 45–47, and author's).
Cr_2O_3—From (48); other data: (45, 49).
Cu_2O—Author's data (30); other data: (7, 8, 9, 15, 16 19, 50–70).
CuO—Estimates from Cu_2O/CuO ratios in scale (57), using Jost (71) and Valensi (57) methods.
FeO—Forms on Fe in steam (72) above 550°C. Extrapolated from average of (73) and (17), taking into account oxide ratios in the scale; also (26, 74, 75).
Fe_2O_3—Prevalent on Fe 300°–400°C (76), extrapolated with E = 23. From (17), E at higher temperatures 30–35; cf. Ref. (74).
Fe_3O_4—At 497°C only oxide on Fe (73). From this value and relative thicknesses of oxide layers at higher temperatures; cf. Ref. (74).
MnO—By Valensi method (77) from (78), extrapolation to lower temperature from the high temperature end.
Mn_3O_4—From (78), below 900°C where prevalent in the scale.
MoO_2—From (79); the only oxide in thin films above 400°C (80).
NiO—Author's data (pure Ni courtesy International Nickel Company), with parabolic law obeyed ideally; other data: (7, 19, 45, 48, 54, 61, 81–83).
PbO—From (7), data for 0.5 T_m only; E not known.
TiO_2—Parabolic below 600°C (84, 85), extrapolated. Oxygen soluble in Ti, so that k for the oxide must be lower than the summary constant given. At higher temperature linear (86).
V_2O_3—k is the summary constant for oxide and solid solution in V (87). For oxide alone, k should be smaller.
WO_2—From (25). Scale above 700°C is WO_2 (80, 88); E from (25) and (89).
ZnO—Data scattered and difficult to reproduce (7, 19, 23, 82, 90–92). Data from (90), parabolic law observed 375°–400°C above 10 cm O_2 pressure; crude extrapolation.
ZrO_2—From (93), summary constant. Oxygen dissolution in Zr rapid, so that at advanced oxidation k refers to oxidation of Zr-O alloy; other data: (85, 93–98).

they might be obscured by the uncertainty of some of the data. Nevertheless, one may hope that the number of systems suffices to outline some relationships. By operating on the parameters from Table I, as well as on some others, certain correlations emerged. Principal concern is with three kinetic parameters: parabolic rate constants, pre-exponential factors, and activation energies.

Comparison of Rate Constants

The values of the rate constants are determined primarily by the nature of oxide and the temperature. If the parabolic oxide formation is regarded as diffusion-controlled, some of the most obvious parameters may be accounted for, so as to compare the oxides more equitably.

Temperature.—There have been many attempts to relate the mechanisms of diffusion and of melting (71, 103). It appears natural to compare the diffusion rates at a certain fraction of the melting point of the matrix. The fraction $0.6T_m$ was found to be a good choice. It falls above $0.5T_m$, which usually is considered to be the limit below which the disorder equilibria in oxides are frozen (104), and it is also

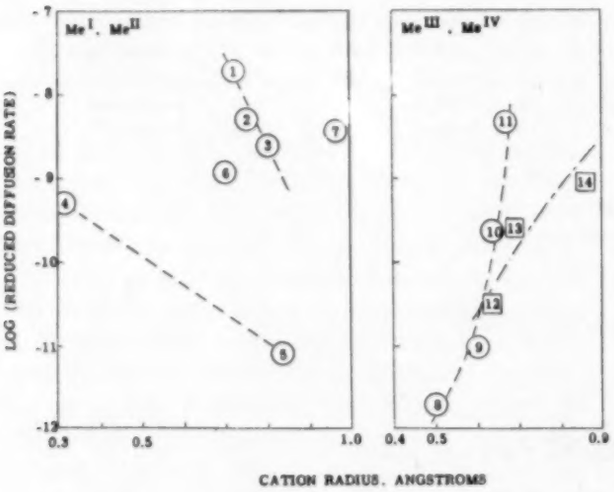

FIG. 1. Variation of r with cation charge, size (107–109), and lattice type. NaCl type: 1—CoO, 2—FeO, 3—MnO; wurtzite type: 4—BeO, 5—ZnO; own type: 6—NiO, 7—Cu_2O; trivalent: 8—Al_2O_3, 9—Fe_2O_3, 10—Cr_2O_3, 11—V_2O_3; tetravalent: 12—TiO_2, 13—WO_2, 14—ZrO_2.

above 0.53–$0.59T_m$, which is reported as the lowest empirical limit for sintering of simple ionic solids (105, 106). It is also the range in which many of the oxidation reactions have been studied and found to proceed with well-measurable rates. Incidentally, at higher or lower corresponding temperatures the relationships which result[1] are much less readily explainable.

Diffusion paths.—If one mole volume of MeO is made into a cube and placed on the surface of the metal, one can imagine N metal ions arranged in N^1 paths, each N^1 ions long. By applying stoichiometry and algebra, one obtains a diffusion rate, r^1, referred to the same arrangement and number of paths and jumps. Because of reasons which will be shown later, metal ion diffusion was assumed in Me_2O and MeO oxides, and oxygen diffusion was assumed in Me_2O_3 and MeO_2 oxides.

Driving force.—The driving force in the diffusion, from equation (V), is the free energy of oxide formation, F_o (Table I). Dividing r^1 by F_o, one obtains the diffusion rate, r, referred to the same driving force per jump, and taken at $0.6T_m$.

An examination of the relative magnitudes of r, plotted diagrammatically in Fig. 1, reveals interesting correlations. The ion charges determine the influence which the ion sizes have on the value of r.

MnO, FeO, and CoO have the sodium chloride structure, and the reduced diffusion rates increase with decreasing cation size. BeO and ZnO have the wurtzite structure, and the smaller Be^{++} ion diffuses faster than the larger Zn^{++} ion. In addition, the diffusion in the wurtzite structure, with four openings between the surrounding oxygen ions facing each cation, is slower than in the sodium chloride structure, with eight openings available for the cation jumps. NiO has a slightly distorted sodium chloride structure, with some openings smaller than others, and this causes slower diffusion, despite the smaller size of the cation. Thus, in the divalent oxides, the reduced diffusion rate is larger if the cation is smaller.

In the Me_2O_3 and MeO_2 oxides, the situation is opposite. With an increase in the cation size, the reduced diffusion rate increases.

These relationships agree with many other indications if one assumes cation diffusion in the mono- and divalent oxides, and oxygen ion diffusion in the higher oxides. Jost (110) has pointed out that in halides the ion with the smaller charge is the diffusing species. Furthermore, the ion diffusivity is larger if the ion of the opposite kind is made more polarizable. The ion polarizability is, very approximately, proportional to the cube of the radius, so that, if oxygen diffuses, its diffusivity would be higher if the partner cation were larger. This actually holds for the Me_2O_3 and MeO_2 types. Recently, oxygen diffusion has been demonstrated in Fe_2O_3 and TiO_2 (17, 86, 104) and cation diffusion in FeO (17) and Cu_2O (15, 16). Oxygen vacancy mechanism would be a natural type of disorder in oxides of higher valences, where the electrical neutrality may be readily maintained by demoting cations to the next lower valence. Such mechanism has been demonstrated for a number of higher oxides (10, 104, 111).

The reduced diffusion rates are expected to be essentially proportional to the concentration of the activated species, which most probably are lattice site vacancies. This thesis may be tested for consistency as follows. The mole fraction concentration (more exactly the thermodynamic activity) of the activated sites is formally connected to the equilib-

rium constant of activation and the free energy of activation by the relations:[2]

$$K^* = \frac{(c^*)}{(c)} = \text{const}\, e^{-\Delta F^*/RT}, \qquad c^* \sim r \quad \text{(VI)}$$

where c is the practically constant concentration (activity) of the normal sites. From these equations, $\log r$ must vary $e^{-\Delta F^*/RT}$ linearly with $\frac{\Delta F^*}{RT}$. This is borne out by the plot in Fig. 2.

Magnitude of the Pre-exponential Factor A

Many attempts have been made to attribute physical significance to the value of A in the Arrhenius equation (II), and to relate A and the activation energy E. An excellent review of these attempts is given by Barrer (112). More recent interpretations are due to Dienes (113) and to Zener and Wert (114–116).

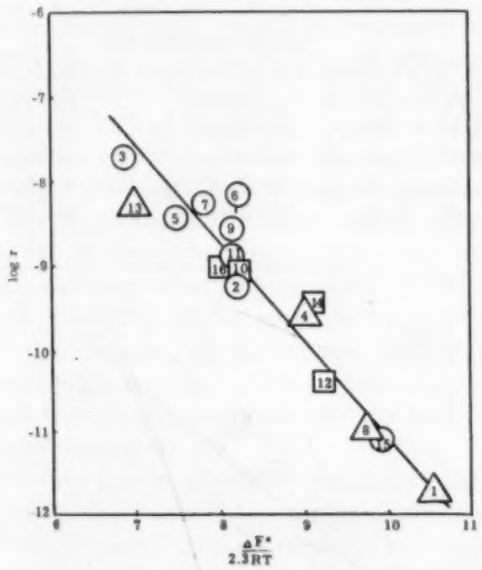

FIG. 2. Correlation between rate of diffusion and free energy of activation.

1—Al_2O_3	5—Cu_2O	9—MnO	13—V_2O_5
2—BeO	6—CuO	10—MoO_2	14—WO_3
3—CoO	7—FeO	11—NiO	15—ZnO
4—Cr_2O_3	8—Fe_2O_3	12—TiO_2	16—ZrO_2

From the interrelations proposed, the one fashioned after Dienes' plot for metal diffusion in metals was found to hold also for the diffusion in oxides as shown in Fig. 3. Here ν is the characteristic frequency, d is the distance between diffusion sites, derived from the mole volumes of oxides, and $\frac{E}{T_m}$ is the so-called "reduced activation energy." The quality of correlation is similar to the correlation found for metals. The plot appears to be an additional indication that the rate controlling mechanism in parabolic oxidation is the volume diffusion.

[2] In certain activation types, a $(c^*)^2$ term must be used (117, 118), but in the present case, the accuracy is not sufficient to distinguish the proper exponent.

Activation Energies

According to Frenkel (117) and Jost (112, 118–121), the energy requirement for diffusion is

$$E = aE^1 + U \qquad \text{(VII)}$$

where E^1 is the energy to create one activated unit, U is the energy to move the activated unit around; and $a = 1$ for Schottky, and 0.5 for Frenkel disorder. The term E^1 is made up of the sum of several other terms:

$$E^1 = E_{coul} + E_{rep} + E_{pol}. \qquad \text{(VIII)}$$

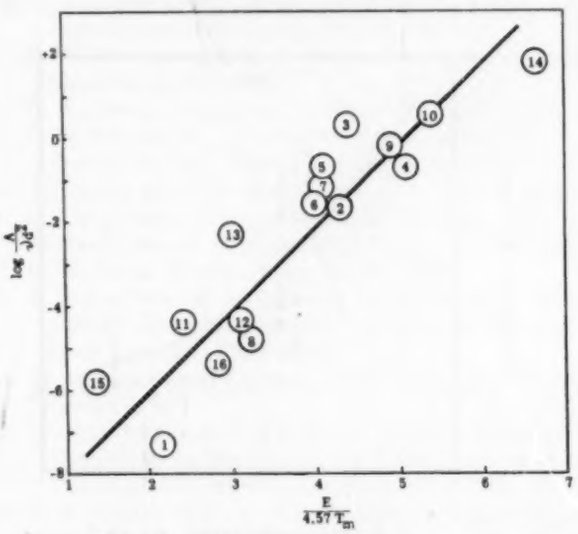

FIG. 3. Correlation between frequency factor and reduced activation energy.

1—Al_2O_3	5—Cu_2O	9—MnO	13—V_2O_5
2—BeO	6—CuO	10—MoO_2	14—WO_3
3—CoO	7—FeO	11—NiO	15—ZrO_2
4—Cr_2O_3	8—Fe_2O_3	12—TiO_2	16—ZnO

E_{coul} is the energy difference due to coulombic forces between the normal and the activated site; E_{rep} is a similar difference because of the repulsion forces, and it usually decreases the first term by 10–20 per cent; E_{pol} is the difference in the polarization energies between both sites, and it also decreases the total energy requirement. The polarization here accomplishes a similar function to the water dipole polarization in breaking up the coulombic forces of an ionic crystal during the solution process. The E_{coul} is of the order of the lattice energy. The variation of the activation energy E thus is caused mainly by the variation of the difference between the coulombic and the polarization energies. Unfortunately, the polarization term involves effects such as mutual polarization of the activated ion and its surroundings, and of the vacant sites and their

surroundings which cannot be evaluated readily. Nevertheless, the above concepts appear to be useful in understanding two correlations which were found in attempts to discover some physical parameters which in some indirect way would interlock with the polarization energies.

One would expect that the total electron density might have a bearing on the polarization energies in an oxide. Atom cores, that is nuclei with surrounding electrons other than the valence electrons, are polarizable and it is believed, for instance, that in the compression of other than alkali metals, the distortion of cores plays a considerable role (122). From this standpoint, a higher electron concentration would tend to increase the polarization energy. For the divalent oxides considered, the lattice energies have a maximum spread of fifteen per cent,

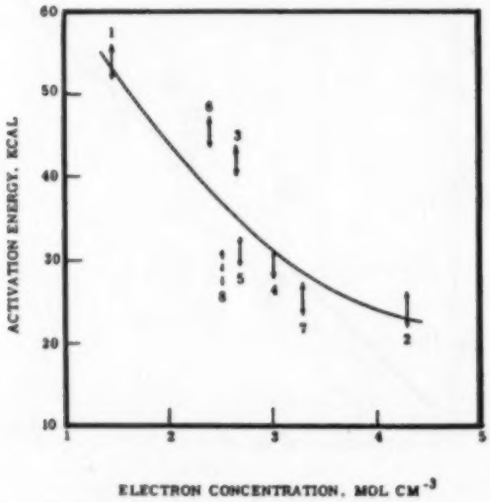

FIG. 4. Variation of activation energy with total electron concentration in divalent oxides.

1—BeO	3—CoO	5—FeO	7—NiO
2—CbO	4—CuO	6—MnO	8—ZnO

as obtained from the approximate formula of Kapustinskii (123):

$$U_L = 256.1 \frac{mn}{r_c + r_a}, \qquad \text{(IX)}$$

where U_L is the lattice energy in kcal, m and n are the coefficients in the compound formula Me_mX_n, and r_c and r_a are the *univalent* (Pauling's) radii of the cation and anion, respectively. This also should be, approximately, the amount of the maximum spread in the value of the complex $(E_{coul} + E_{rep})$ term. Then the activation energy, which is the difference between the latter term and the polarization energy, should decrease with an increase in the total electron density. Fig. 4 indicates that this expectation holds. Higher valency oxides do not fit into this plot, probably because of the more complex distribution of the polarization energies arising from the fact that not all of the sites used by the cations in the MeO type oxides are occupied here.

Fig. 5 illustrates the variation of the activation energy with volume increment. Biltz and Klemm

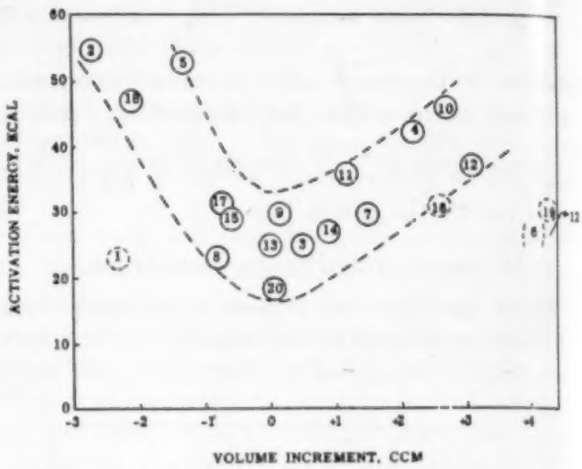

FIG. 5. Variation of E with volume increment.

1—Al_2O_3	6—Cu_2O	11—Mn_3O_4	16—ThO_2 (126)
2—BeO	7—FeO	12—MoO_2	17—V_2O_3
3—CbO	8—Fe_2O_3	13—NiO	18—WO_2
4—CoO	9—Fe_3O_4	14—Ta_2O_5 (41, 125)	19—ZnO
5—Cr_2O_3	10—MnO	15—TiO_2	20—ZrO_2

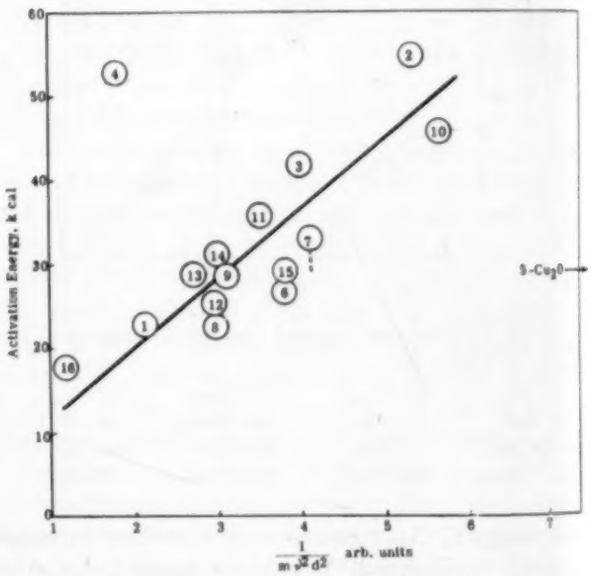

FIG. 6. Activation energy vs. reciprocal of energy of arbitrary oscillator.

1—Al_2O_3	5—Cu_2O	9—Fe_3O_4	13—TiO_2
2—BeO	6—CuO	10—MnO	14—V_2O_3
3—CoO	7—FeO	11—Mn_3O_4	15—ZnO
4—Cr_2O_3	8—Fe_2O_3	12—NiO	16—ZrO_2

(124) attributed to one mole of $O^=$ in solids an average volume of 11 ccm. The difference between the actual volumes (Table I) and 11 ccm is the volume increment. A certain trend is evident: lower activation energies tend to group around the zero increment. The trend appears even more consistent if one considers that the points for Al_2O_3, ZnO, and ThO_2 are questionable, since for these oxides the parabolic law has been found to hold over quite

narrow temperature ranges, and that Cu_2O, the only monovalent oxide considered here, has a very specific lattice. The following explanation is proposed. Large negative or positive increments signify more mismatch in sizes, and more polarization and interionic strain in the lattice than occur for smaller increments. The additional polarization upon activation is then smaller, which makes the activation energy larger.

In closing, Fig. 6 illustrates what happens if one attempts to treat ions as harmonic oscillators. It was assumed that the cations vibrate harmonically with their characteristic frequency, according to the equation:

$$E_{osc} = 2\pi^2 m\nu^2 x^2 \qquad (X)$$

where m is the vibrator mass, ν its frequency, and x its amplitude. The question was asked, what energy would be required to reach an amplitude proportional to one half of the Me-Me distance as taken from the mole volumes of oxides. Naively, one would expect that the larger this energy requirement is, the larger should be the activation energy. However, exactly the reverse situation obtains. This appears to be an indication that the frequency is a function of the amplitude and that the restoring force changes due to the loosening of the oxygen framework as the amplitude increases, which in fact is stating in different terms that one must take account of the polarization energies.

Fig. 1 to 5 give a gratifying realization that the assembly of the empirical metal oxidation data is not such a formless mass of numbers as it appears to be at first sight. Certain trends are evident and are in agreement with some of present diffusion concepts.

Any discussion of this paper will be included in a Discussion Section, to be published in the December 1953 issue of the JOURNAL.

REFERENCES

1. W. H. J. VERNON, *Chemistry & Industry*, **1943**, 314.
2. U. R. EVANS, *Trans. Electrochem. Soc.*, **83**, 335 (1943).
3. K. FISCHBECK, *Chem. Fabrik*, **1938**, 525.
4. B. LUSTMAN, *Trans. Electrochem. Soc.*, **81**, 359 (1942).
5. N. F. MOTT, *Nature*, **145**, 996 (1940).
6. H. A. MILEY, *Trans. Electrochem. Soc.*, **81**, 391 (1942).
7. N. B. PILLING AND R. E. BEDWORTH, *J. Inst. Metals (London)*, **29**, 529 (1923).
8. A. L. DIGHTON AND H. A. MILEY, *Trans. Electrochem. Soc.*, **81**, 321 (1942).
9. H. DUNEWALD AND C. WAGNER, *Z. physik. Chem. B*, **22**, 212 (1933).
10. C. WAGNER, "Diffusion and High Temperature Oxidation of Metals," in "Atom Movements," p. 153, American Society for Metals, Cleveland (1951).
11. U. R. EVANS, *Trans. Electrochem. Soc.*, **91**, 547 (1947).
12. N. CABRERA AND N. F. MOTT, *Repts. Progr. Phys.*, **12**, 163 (1949).
13. T. N. RHODIN, *J. Am. Chem. Soc.*, **72**, 5102 (1950).
14. G. TAMMANN, *Z. anorg. u. allgem. Chem.*, **111**, 78 (1920).
15. J. BARDEEN, W. H. BRATTAIN, AND W. SHOCKELY, *J. Chem. Phys.*, **14**, 714 (1946).
16. G. W. CASTELLAN AND W. J. MOORE, *J. Chem. Phys.*, **17**, 41 (1949).
17. M. H. DAVIES, M. T. SIMNAD, AND C. E. BIRCHENALL, *J. Metals*, **3**, 889 (1951).
18. C. WAGNER, *Z. physik. Chem. B*, **32**, 447 (1936).
19. C. WAGNER AND K. GRUNEWALD, *Z. physik. Chem. B*, **40**, 455 (1938).
20. L. E. PRICE, *Chemistry & Industry*, **1937**, 769.
21. C. WAGNER AND K. E. ZIMENS, *Acta Chem. Scand.*, **1**, 547 (1948).
22. A. PORTEVIN, E. PRETET, AND H. JOLIVET, *Rev. met.*, **31**, 101, 186, 219 (1934).
23. W. H. J. VERNON, E. I. AKEROYD, AND E. G. STROUD, *J. Inst. Metals*, **65**, 301 (1939).
24. E. A. GULBRANSEN AND K. ANDREW, *J. Electrochem. Soc.*, **98**, 241 (1951).
25. E. A. GULBRANSEN AND W. S. WYSONG, *Trans. Am. Inst. Mining Met. Engrs.*, **175**, 611 (1948).
26. B. W. DUNNINGTON, F. H. BECK, AND M. G. FONTANA, *Corrosion*, **8**, 2 (1952).
27. C. WAGNER, *Corrosion and Material Protect.*, **5**, 9 (1948).
28. F. N. RHINES, W. A. JOHNSON, AND W. A. ANDERSON, *Trans. Am. Inst. Mining Met. Engrs.*, **147**, 205 (1942).
29. J. BENARD AND J. TALBOT, *Compt. rend.*, **225**, 411 (1947).
30. A. DRAVNIEKS, *J. Am. Chem. Soc.*, **72**, 3761 (1950).
31. A. DRAVNIEKS, *J. Phys. & Colloid Chem.*, **55**, 540 (1951).
32. C. WAGNER, *Angew. Chem.*, **49**, 735 (1936).
33. S. GLASSTONE, K. J. LAIDLER, AND H. EYRING, "The Theory of Rate Processes," p. 477, McGraw-Hill Book Co., New York (1941).
34. E. A. GULBRANSEN, *Trans. Electrochem. Soc.*, **83**, 301 (1943).
35. M. KAY THOMPSON, "The Total and Free Energies of Formation of the Oxides of Thirty-two Metals," The Electrochemical Society, Inc., New York (1942).
36. O. KUBASCHEWSKI AND E. L. L. EVANS, "Metallurgical Thermochemistry," p. 217, Academic Press Inc., New York (1951).
37. H. P. ROOKSBY, *Nature*, **152**, 304 (1943).
38. E. A. GULBRANSEN, *Trans. Electrochem. Soc.*, **91**, 573 (1947).
39. D. D. CUBICCIOTTI, "The Oxidation of Beryllium at High Temperature," Techn. Rep. No. 1, U. S. Navy Office of Naval Research, Contract N7-ONR-329 (1949); also in press.
40. E. A. GULBRANSEN AND K. F. ANDREW, *J. Electrochem. Soc.*, **97**, 383 (1950).
41. E. A. GULBRANSEN AND K. F. ANDREW, *J. Metals*, **188**, 586 (1950).
42. C. W. Balke, in the "Corrosion Handbook," p. 620, John Wiley & Sons, Inc., New York (1948).
43. R. T. PHELPS, E. A. GULBRANSEN, AND J. W. HICKMAN, *Ind. Eng. Chem. Anal. Ed.*, **18**, 391 (1946).
44. C. R. JOHNS AND W. M. BALDWIN, JR., *Metals Transactions, AIME*, **185**, 720 (1949).
45. W. H. HATFIELD, *J. Iron Steel Inst., London*, **115**, 483 (1927).
46. G. CHAUVENET AND M. G. VALENSI, *Compt. rend.*, **205**, 317 (1937).
47. V. I. ARKHAROV AND G. D. LOMAKIN, *Zhur. Tekh. Fiz.*, **14**, 155 (1944).
48. Y. MATSUNAGA, *Japan Nickel Rev.*, **1**, 347 (1935).
49. V. I. ARKHAROV AND M. M. SELICHOV, *Zhur. Priklad. Khim.*, **14**, 81 (1941).

50. W. G. Palmer, *Proc. Roy. Soc. (London) A*, **103**, 444 (1923).
51. E. A. Gulbransen, *Trans. Electrochem. Soc.*, **83**, 301 (1943).
52. P. B. Holmesland, *Kgl. Norske Videnskab. Selskabs Forh.*, **12**, 129 (1940).
53. J. H. W. Vernon, *J. Chem. Soc.*, **1926**, 2275.
54. Y. Utida and M. Saito, *Science Repts. Tôhoku Univ., I*, **13**, 391 (1925).
55. F. O. Hudson, M. T. Herbert, E. F. Ball, and H. E. Bucknall, *J. Inst. Metals*, **42**, 221 (1929).
56. A. Krupkowski and J. Jascurowski, *Congr. intern. mines met. et geol. appl. Paris, Met. II*, **VII**, 6 (1925).
57. G. Valensi, Pittsburgh Intern. Conf. on Surface Reactions, **1948**, 156.
58. J. Benard, *ibid.*, 167.
59. W. Feitknecht, *Z. Elektrochem.*, **35**, 142 (1929).
60. W. Feitknecht, *ibid.*, **36**, 16 (1930).
61. W. B. Campbell and U. B. Thomas, *Trans. Electrochem. Soc.*, **91**, 623 (1947).
62. F. J. Wilkins, *Proc. Roy. Soc. London, A*, **128**, 407 (1930).
63. F. J. Wilkins and E. K. Rideal, *Proc. Roy. Soc. London, A*, **128**, 394 (1930).
64. F. J. Wilkins, *Z. Elektrochem.*, **35**, 500 (1929).
65. B. Lustman and R. F. Mehl, *Trans. Am. Inst. Mining Met. Engrs.*, **143**, 246 (1941).
66. K. H. Moore, *Ann. Physik*, **33**, 133 (1938).
67. J. S. Dunn, *Proc. Roy. Soc. London, A*, **111**, 203 (1926).
68. J. S. Dunn, *Proc. Roy. Soc. London, A*, **111**, 210 (1926).
69. D. H. Bangham, *J. Sci. Instr.*, **22**, 230 (1945).
70. A. T. Gwathmey and A. F. Benton, *J. Phys. Chem.* **46**, 969 (1942).
71. W. Jost, "Diffusion und Chem. Reaktion in festen Stoffen," p. 166, Verlag von Theodor Steinkoff, Dresden (1937).
72. K. Fischbeck, L. Neundeubel, and F. Salzer, *Z. Elektrochem.*, **40**, 517 (1934).
73. J. K. Stanley, J. von Hoene, and R. T. Huntoon, *Trans. Am. Soc. Metals*, **43**, 426 (1951).
74. P. Paidassi, *J. Metals*, **4**, 536 (1952). (Discussion to Ref. 87.)
75. L. B. Pfeil, *J. Iron Steel Inst. London*, **64**, No. I, 504 (1929).
76. E. A. Gulbransen and J. W. Hickman, *Am. Inst. Mining Met. Engrs.*, **171**, 306 (1947).
77. M. G. Valensi, *Compt. rend.*, **203**, 1252, 1354 (1936).
78. R. S. Gurnick and W. M. Baldwin, Jr., *Trans. Am. Soc. Metals*, **42**, 308 (1950).
79. E. A. Gulbransen and W. S. Wysong, *Am. Inst. Mining Met. Engrs.*, **175**, 628 (1948).
80. J. W. Hickman and E. A. Gulbransen, *Am. Inst. Mining Met. Engrs.* **171**, 371 (1947).
81. N. B. Pilling and R. E. Bedworth, *Ind. Eng. Chem.*, **17**, 372 (1925).
82. C. F. Downey, J. K. Lee, and W. J. Moore, "Kinetics of Oxidation of Nickel and Zinc Foils," paper presented at the 116th meeting of the American Chemical Society, Atlantic City, N. J., Sept. 1949; also private communication.
83. O. Kubaschewsky and O. Goldbeck, *Z. Metallkunde*, **39**, 158 (1948).
84. J. W. Hickman and E. A. Gulbransen, *J. Anal. Chem.*, **20**, 158 (1948).
85. E. A. Gulbransen and K. F. Andrew, *Trans. Am. Inst. Mining Met. Engrs.*, **185**, 741 (1949).
86. M. H. Davies and C. E. Birchenall, *J. Metals*, **3**, 877 (1951).
87. E. A. Gulbransen and K. F. Andrew, *J. Electrochem. Soc.*, **97**, 396 (1950).
88. J. W. Hickman, *Am. Inst. Mining Met. Engrs.*, **180**, 547 (1949).
89. J. S. Dunn, *J. Chem. Soc.*, **1929**, 1149.
90. W. S. Moore, private communication.
91. G. I. Finch and A. G. Quarell, *Proc. Roy. Soc. London*, **46**, 168 (1934).
92. G. I. Finch and A. G. Quarell, *Proc. Roy. Soc. London, A*, **141**, 398 (1933).
93. E. A. Gulbransen and K. F. Andrew, *Trans. Am. Inst. Mining Met. Engrs.*, **185**, 515 (1949).
94. W. G. Guldner and L. A. Wooten, *J. (and Trans.) Electrochem. Soc.*, **93**, 223 (1948).
95. J. H. DeBoer and J. D. Fast, *Rec. trav. chim.*, **59**, 161 (1940).
96. J. H. DeBoer and J. D. Fast, *Rec. trav. chim.*, **55**, 459 (1936).
97. D. D. Cubicciotti, U. S. Navy Office of Naval Research, Contr. N7-ONR-329, Yearly Report, April 1949; also in press.
98. D. J. McAdam and G. W. Geil, *J. Research Natl. Bur. Standards*, **28**, 593 (1942).
99. A. Dravnieks and H. J. McDonald, *J. (and Trans.) Electrochem. Soc.*, **93**, 177 (1948).
100. K. K. Kelly, "Entropies of Inorganic Substances," U. S. Department of Interior, Bureau of Mines, Bulletin 477 (1950).
101. F. A. Lindemann, *Physik. Z.*, **11**, 609 (1910).
102. W. Herz, *Z. anorg. u. allgem. Chem.*, **163**, 221 (1927).
103. C. E. Birchenall, in "Atom Movements," p. 118, Am. Soc. Metals, Cleveland (1951).
104. D. J. M. Bevan, J. P. Shelton, and J. S. Anderson, *J. Chem. Soc.*, **1948**, 1729.
105. G. Tammann, *Z. anorg. Chem.*, **157**, 321 (1926).
106. G. Tammann and Q. A. Mansuri, *Z. anorg. Chem.*, **126**, 119 (1926).
107. A. F. Wells, *Quarterly Rev. Chem. Soc. (London)* **2**, 185 (1948).
108. L. Pauling, "Nature of the Chemical Bond," p. 346, Cornell University Press, Ithaca (1948).
109. J. D'Ans and E. Lax, "Taschenbuch für Chemiker und Physiker," p. 184, Berlin (1943).
110. W. Jost, "Diffusion und Chemiche Reaktion in Festen Stoffen," pp. 78–80, Verlag Th. Steinkopff, Dresden (1937).
111. P. Ehrlich, *Z. Elektrochem.*, **45**, 362 (1939).
112. R. M. Barrer, "Diffusion in and through Solids," p. 238, Cambridge University Press, London (1941).
113. G. J. Dienes, *J. Appl. Phys.*, **21**, 1189 (1950).
114. C. Zener, *J. Appl. Phys.*, **22**, 372 (1951).
115. C. Wert and C. Zener, *Phys. Rev.*, **76**, 1169 (1949).
116. C. Wert, *Phys. Rev.*, **79**, 601 (1950).
117. J. Frenkel, *Z. Physik.*, **35**, 652 (1926).
118. W. Jost, *J. Chem. Physics*, **1**, 466 (1933).
119. W. Jost, "Diffusion in Solids, Liquids, Gases," p. 135, Academic Press, New York (1952).
120. W. Jost, *Z. physik. Chem.*, **169**, 129 (1934).
121. W. Jost, *Trans. Faraday Soc.*, **34**, 860 (1938).
122. A. H. Wilson, "Semi-Conductors and Metals," p. 36, Cambridge Univ. Press, London (1939).
123. A. F. Kapustinskii, *Z. physik. Chem. B*, **22**, 261 (1933).
124. W. Biltz, "Raumchemie d. festen Stoffen," p. 192, Verlag Th. Steinkoff, Dresden-Leipzig (1936).
125. J. T. Weber, G. E. Sturdy, E. M. Wise, and C. R. Tipton, Jr., *J. Electrochem. Soc.*, **99**, 121 (1952).
126. P. Levesque and D. D. Cubicciotti, *J. Am. Chem. Soc.*, **73**, 2028 (1951).

The Diffusion and Solubility of Nitrogen in Beta Zirconium[1]

M. W. Mallett, E. M. Baroody, H. R. Nelson, and C. A. Papp

Battelle Memorial Institute, Columbus, Ohio

ABSTRACT

A study has been made of the diffusion of nitrogen in beta zirconium in the temperature range of 900° to 1600°C at one atmosphere pressure. Diffusion-rate calculations based on a solution of the usual diffusion equation gave a diffusion coefficient, $D_\beta = 3 \times 10^{-2}\, e^{-33,600/RT}$ cm²/sec. The energy of activation of diffusion, 33,600 cal/mole, has a probable error of 1,600 cal/mole. The limiting solubilities of nitrogen in beta zirconium were determined from the diffusion data.

Introduction

In the course of a program on gas-zirconium studies, the interaction of nitrogen and zirconium was considered. It was found that the over-all reaction of nitrogen with zirconium has been described by Gulbransen and Andrew (1) in the temperature range 400° to 825°C, and by Dravnieks (2) at 860° to 1050°C. Fast (3) has reported the solubility of nitrogen in zirconium to be about 20 weight per cent. This is apparently the saturation limit in the alpha-zirconium phase. The authors found no other reference to the solubilities of nitrogen in zirconium, nor to the rates of diffusion of nitrogen in zirconium. Therefore, an investigation of the diffusion of nitrogen in zirconium was started. The work on diffusion in the beta phase of the metal and the solubility limits in this phase are described below.

Experimental Procedure

Cylindrical zirconium specimens were machined from outgassed iodide zirconium crystal bars. A typical analysis of such zirconium is: zirconium 97.8 to 98.2 per cent, and hafnium 1.8 to 2.2 per cent, with traces of oxygen, nitrogen, hydrogen, iron, and silicon totaling less than 0.01 per cent. A zirconium cylinder about 4 cm long by 0.6 cm in diameter and weighing about 10 grams was placed in the reaction tube (fused silica or mullite) of a modified Sieverts apparatus. The system of approximately 100-ml volume was evacuated by a two-stage glass mercury-diffusion pump and a Hyvac mechanical pump. The reaction tube was heated by a resistance-wound furnace for temperatures up to 1000°C and by Globar elements for temperatures of 1050° to 1400°C. Still higher temperatures were reached by high frequency induction heating.

With the specimen at the desired temperature, commercial nitrogen (99.7% pure), dried by magnesium perchlorate, was admitted from a gas buret. Further nitrogen additions were made, as needed, to keep the pressure at 500 to 760 mm. The quantities of nitrogen absorbed ranged from 10 to 300 ml.

Upon completion of a run in which nitrogen was reacted with zirconium for a predetermined time, the system was evacuated, and the reaction chamber and specimen cooled as rapidly as feasible.

Lengths equal to the radius of the cylinder were cut from the ends of the specimen and discarded. The rest of the specimen was machined radially into several layers of equal weight which were then analyzed for nitrogen content by a modified Kjeldahl method.

Diffusion within the Metal

In considering the diffusion of nitrogen in beta zirconium, attention must first be given to the structure of the specimen after reaction. Rhines (4) has shown that a binary diffusion system consists of one-phase layers with the layer of highest content of diffusing matter on the surface. The nitrogen-zirconium system consisted of a beta solid-solution core surrounded by a thin alpha layer, and this in turn was surrounded by a thin gamma layer of ZrN. Metallographic examination showed the alpha and gamma layers to have a total thickness ranging from 0.05 to 0.08 mm, and x-ray analysis verified the presence of ZrN. Since 0.08 mm is only 3 per cent of the cylinder radius, it was not necessary to give further attention to the exact location of the interface between the surface film and the beta metal. In fact, in subsequent calculations it was possible to treat the original radius of the cylinder as synonymous with the radius to the interface between the beta core and the surface layers.

In order to determine the concentration gradients, and ultimately the diffusion coefficient, it was necessary to divide the specimens into a number of concentric layers and analyze each for nitrogen. A

[1] Manuscript received May 5, 1952. This paper was prepared for delivery before the Montreal Meeting, October 26 to 30, 1952. Work done under Contract No. W-7405-eng-92 for the U. S. Atomic Energy Commission.

surface layer including the alpha and gamma phases was first removed and the concentration in it was not used in subsequent calculations. The remaining metal, containing only nitrogen which had diffused as solute through beta zirconium, was machined into six additional layers of equal weight. For these layers, plots of weight per cent nitrogen vs. depth of penetration gave relatively smooth curves, as shown for a typical case in Fig. 1. Each of the concentration values is an average concentration, plotted midway in its respective layer.

When it is assumed that the diffusion coefficient is a constant, and that the concentration of diffusing

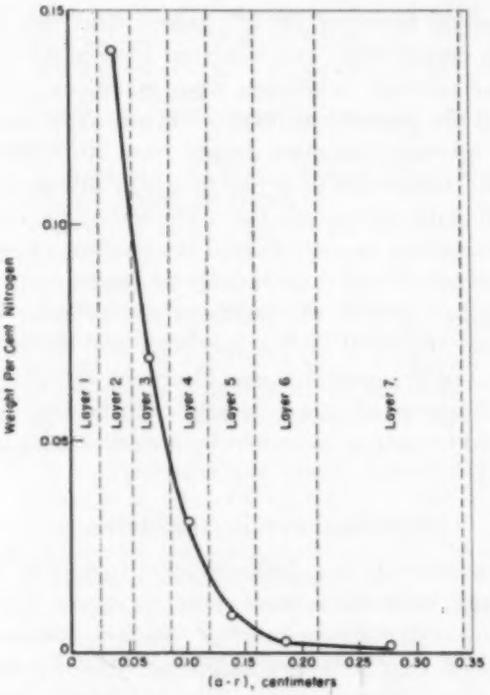

FIG. 1. Experimental average concentrations vs. depth of penetration at 1200°C for 2 hours.

matter, c, is a function of radius and time only, the partial differential equation for c takes the form:

$$\frac{\partial c}{\partial t} = D\left[\frac{\partial^2 c}{\partial r^2} + \frac{1}{r}\frac{\partial c}{\partial r}\right]. \qquad \text{(I)}$$

The solution of equation (I) for a cylinder of infinite length is (5):

$$\frac{c(r,t)}{c_o} = 1 + 2\sum_{n=1}^{n=\infty} \frac{J_o((r/a)\beta_n)}{\beta_n J_o'(\beta_n)}\, e^{-\beta_n^2(Dt/a^2)}, \qquad \text{(II)}$$

where: $c(r, t)$ = local concentration at radius, r, and time, t; c_o = constant concentration maintained at surface; D = diffusion coefficient; a = radius of cylinder; $J_o(\beta)$ = Bessel's function of the first kind and order zero; $J_o'(\beta)$ = first derivative of $J_o(\beta)$; β_n = roots of $J_o(\beta) = o$.

If we neglect the distinction between average concentration over a layer, as obtained by the experimental procedure, and local concentration at the middle of a layer, a simple graphical solution for the diffusion coefficient is available. Plotting c/c_o against r/a for various values of Dt/a^2 in equation (II) gives a family of curves, as shown in Fig. 2.

The experimental (r/a)'s were determined for each concentration in each specimen. A Dt/a^2 and a c_o were then so chosen to give the best fit of the

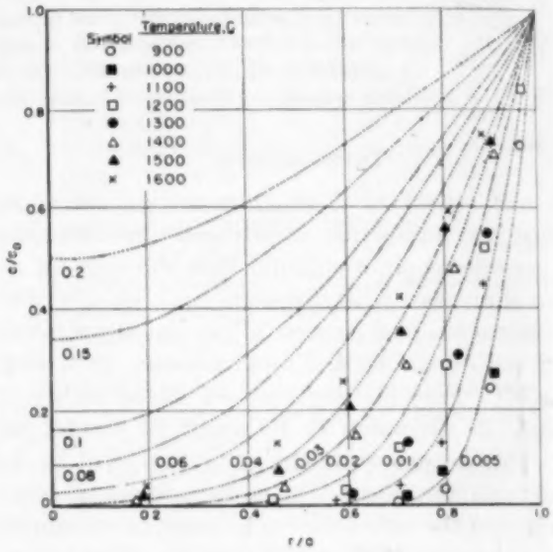

FIG. 2. Concentration distribution for various values of Dt/a^2 (as indicated by the numbers on the curves) in a cylinder of radius "a" with zero initial concentration and surface concentration c_o.

TABLE I. *Diffusion coefficients for nitrogen in zirconium*

Sample No.	Time, hours	Temperature, °C	c_o, weight per cent	$\frac{Dt}{a^2}$	$D \times 10^7$, cm²/sec
1	44.5	900	0.04	0.01	0.1
2	20	1000	0.08	0.02	0.4
3	5	1000	0.14	0.005	0.5
4	4.25	1100	0.16	0.015	1.1
5	2.5	1100	0.17	0.01	2.7
6	2	1200	0.26	0.015	2.4
7	1	1200	0.24	0.015	5
8	1	1300	0.35	0.015	6
9	1	1400	0.47	0.03	11
10	1	1500	0.53	0.05	17
11	0.5	1600	0.64	0.04	27

experimental data to theoretical. Representative experimental data at 100°C intervals are plotted in Fig. 2. The values Dt/a^2, c_o, and the diffusion coefficients obtained from them are listed in Table I.

The fact that it was not necessary to distinguish between the average concentration over a shell and the concentration at the midpoint is readily verified. For example, consider a thin shell of thickness 2δ centered at r/a. Writing $f(r/a)$ for c/c_o, one has for the average concentration:

$$\frac{\bar{c}}{c_o} = \bar{f} = \frac{a}{2r\delta}\int_{-\delta}^{\delta} f\left(\frac{r}{a}+x\right)\cdot\left(\frac{r}{a}+x\right)dx. \quad \text{(III)}$$

When this is evaluated approximately by first expanding the integrand in a Taylor series, the following expression is obtained:

$$\bar{f} = f\left(\frac{r}{a}\right) + f'\left(\frac{r}{a}\right)\cdot\frac{\delta^2 a}{3r} + f''\left(\frac{r}{a}\right)\cdot\frac{\delta^2}{6}. \quad \text{(IV)}$$

For purposes of illustration this may be applied to the case $Dt/a^2 = 0.02$ and $r/a = 0.9$. Taking $\delta = 0.05$, which is slightly larger than used in the

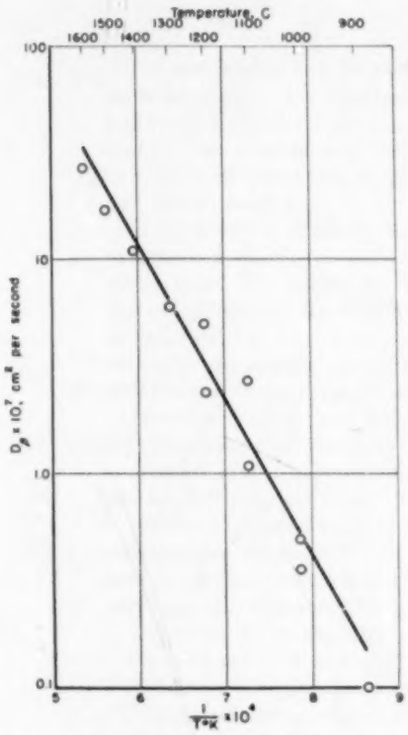

FIG. 3. Variation of diffusion coefficient with temperature.

experiments, and using equation (II) to evaluate $f(r/a)$ and its first two derivatives, one obtains:

$$\bar{f} - f\left(\frac{r}{a}\right) = 0.0016. \quad \text{(V)}$$

The corresponding value of $f(r/a)$ is about 0.65, making it evident that the small difference between local and average concentrations is not significant.

The logarithms of the diffusion coefficients listed in Table I were plotted against reciprocal temperature, as shown in Fig. 3. The equation of the best straight line through the points was then determined by the method of least squares, and identified with an equation of the Arrhenius type to obtain:

$$D_\beta = 3 \times 10^{-2} e^{-33,600/RT} \text{ cm}^2/\text{sec}. \quad \text{(VI)}$$

D_β is the diffusion coefficient for the β-phase in the temperature range 900° to 1600°C. The energy of activation of diffusion is 33,600 cal/mole, with a probable error of 1600 cal/mole. The frequency factor, 3×10^{-2}, is uncertain by about a factor 2.

Solubility of Nitrogen in Beta Zirconium

According to the description of the cross section of the specimen, the solubility limit of nitrogen in beta zirconium is the concentration just inside the interface between the beta and alpha phases. As stated before, this interface was very near the outer surface of the cylinder, the thickness of the high concentration phases being less than 3 per cent of the cylinder radius. Thus, no serious error was introduced in obtaining the maximum concentration in the beta phase by extrapolating to the outer surface rather than the interface.

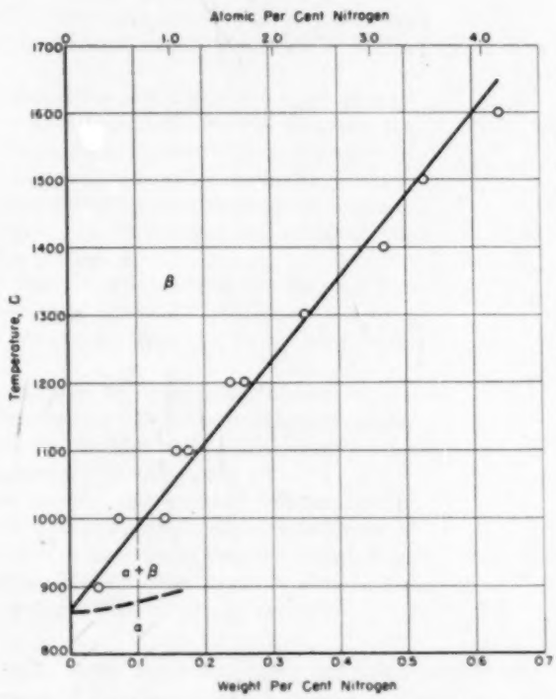

FIG. 4. Solubility limits (c_o's) of nitrogen in beta zirconium.

It is then evident that the c_o determined from equation (II) is the approximate limiting solubility of nitrogen in beta zirconium at the given temperature. The c_o's determined in this study were plotted in Fig. 4. A line which is considered the boundary between the beta and alpha-plus-beta phases was drawn through these points. The dashed line is intended only to indicate the possible boundary between the alpha and alpha-plus-beta phases.

Harris (6) and Breitbar (7) used a similar approach to determine the A_{cm} lines in the carbon-iron system. Recently, Wasilewski (8), working in our laboratory, also used this method for the nitrogen-titanium system. His c_o's fall on the line dividing the beta and the alpha-plus-beta phases as determined by a

metallographic technique and show that comparable results are obtained by each method.

Any discussion of this paper will appear in a Discussion Section, to be published in the December 1953 issue of the JOURNAL.

REFERENCES

1. E. A. GULBRANSEN AND K. F. ANDREW, *J. Metals*, **1**, 515 (1949).
2. A. DRAVNIEKS, *J. Am. Chem. Soc.*, **72**, 3568 (1950).
3. J. D. FAST, *Metallwirtschaft*, **17**, 641 (1938).
4. F. N. RHINES, "Surface Treatment of Metals," ASM Symposium Papers, p. 122, October (1940).
5. R. M. BARRER, "Diffusion in and Through Solids," p. 32, Cambridge Press, London (1941).
6. F. H. HARRIS, *Metal Prog.*, **44**, 265 (1943).
7. S. BREITBAR, *Metal Prog.*, **47**, 1121 (1945).
8. R. WASILEWSKI, private communication.

Electrodeposition of Tin-Nickel Alloy Plate from Chloride-Fluoride Electrolytes[1]

J. W. Cuthbertson and N. Parkinson

Tin Research Institute, Greenford, Middlesex, England

and

H. P. Rooksby

Research Laboratories, General Electric Company Limited, Wembley, England

ABSTRACT

Tin and nickel can be codeposited in approximately equi-atomic proportions from solutions containing stannous chloride, nickel chloride, and fluorides. The alloy deposits thus obtained are almost fully bright and are single phase, having a nickel arsenide type of structure. Below 300°C the deposits are quite stable, but on annealing at higher temperatures recrystallization takes place and a duplex structure of Ni_3Sn_2 and Ni_3Sn_4 results.

In the absence of fluorides, satisfactory alloy deposition is not possible from chloride solutions. Evidence is adduced that the fluorine complexes both the tin ions and the nickel ions. The constancy of composition of the cathode deposit that is a feature of the recommended electrolyte suggests that deposition is associated with the presence in the electrolyte of a tin-nickel-fluorine complex. Complex ion formation is followed through the medium of cathode potential-current density curves. The effect of the variables of the process on deposit composition is discussed.

The conductivity and throwing power of the electrolyte have been determined. The x-ray structure of tin-nickel alloy deposits covering a range of composition has been examined, and it is shown that bright deposits are characterized by a preferred orientation of the crystallites.

From solutions of this type, tin-nickel alloys can only be obtained by operating at a temperature above 45°C, the optimum temperature being 65°C. The metastable structure of these deposits is thought to be explained by the high activation energy of the discharging cations resulting from the high temperature of operation.

Tin-nickel alloy deposits as normally obtained contain approximately 65 per cent of tin and 35 per cent of nickel. Such deposits have a pleasing color, showing evidence of a faint rose-pink tint, and are equally as resistant, or even more resistant, than electrodeposited chromium to atmospheric tarnishing. The progress made to date in the industrial development of the tin-nickel alloy plating process is briefly reviewed.

Introduction

A method of codepositing tin and nickel in roughly equal atomic proportions was described recently by one of the present authors (1). The solution used contained stannous chloride, nickel chloride, ammonium bifluoride, and sodium fluoride, and the codeposition was dependent on the complexing action of the fluorides whereby the deposition potentials of the tin and nickel were brought sufficiently close to enable an alloy plate to be deposited. Much fundamental work was done in perfecting this process, and as the first report described only the essentials necessary to understand its technology it was thought that a description of the detailed research carried out might be of interest. The theory of alloy plating is still in the elementary stage, and most, if not all, of the successful processes of this type have been evolved by trial and error. The present process is not a complete exception to this, but its perfection is partly attributable to theoretical reasoning. Moreover, the experimental work, particularly that completed since the original paper was written, has shed some interesting information on the theory of alloy plating, suggesting that in this particular case an entirely novel mechanism of deposition is functioning.

Chloride-fluoride electrolytes will not deposit tin-nickel alloys over the whole composition range. It is a feature of these electrolytes, and apparently also of a more recently examined acetate type of electrolyte, that they favor the deposition of tin and nickel in roughly equal atomic proportions. With difficulty, it is possible to deposit alloys of other than this basic composition, the limiting tin contents being about 40 per cent and 90 per cent, respectively. It would not be practicable, however,

[1] Manuscript received October 17, 1951.

on a commercial basis, to use either of these electrolytes for depositing plate of other than the above standard composition.

The Tin-Nickel Alloy System

This system is characterized by a number of intermetallic compounds, of which Ni_3Sn_2 and Ni_3Sn_4 are important in connection with the present work. The alloy deposits with which we are concerned contain approximately 65 per cent of tin and 35 per cent of nickel. This composition corresponds closely with the formula NiSn and Rooksby (2) has established that such electrodeposited alloys are single phase and intermetallic compound in structure. The compound NiSn is metastable and is not therefore found in the equilibrium diagram. The structure of these alloy deposits will be discussed at greater length in a later section.

We do not at present know any method of making the alloy NiSn other than by electrodeposition, and for this reason we are at present recommending the use of tin and nickel anodes simultaneously to replenish the bath. A cast and annealed tin-nickel alloy containing 65 per cent of tin has a duplex structure consisting of Ni_3Sn_2 and Ni_3Sn_4, and if used as an anode the Ni_3Sn_2 phase dissolves preferentially. Single phase anodes consisting entirely of Ni_3Sn_2 or Ni_3Sn_4 dissolve satisfactorily but neither alloy is of the wanted composition.

Principles of the Plating Process

It is quite possible to codeposit tin and nickel from mixed simple salt solutions but under conditions more suited to the research laboratory than to the works. Parkinson has shown that while the difference between the normal electrode potentials of stannous tin and nickel is only about 0.1 volt the addition of stannous chloride to a nickel chloride solution causes the nobility of the cathode to increase rapidly until a point is reached where the cathode potential coincides with that for a simple acid stannous tin electrolyte. The mixed electrolyte then deposits almost pure tin. To deposit tin and nickel simultaneously from such solutions, the ratio of nickel to tin in the electrolyte must be maintained at a much higher value than their ratio in the deposit. Any change in the metal content of the electrolyte will then be accompanied by a much larger change in the composition of the deposit, and control of the latter within close limits becomes difficult or impossible. Parkinson has also shown that there are other objections to mixed simple salt baths.

By complexing the tin ions and the nickel ions or both, it is possible to bring the deposition potentials for tin and nickel close together and also, by the choice of a suitable complexing medium, to reduce the high acidity which necessarily characterizes straight stannous salt electrolytes.

Fluorides are known to exert a strong complexing influence on stannous tin ions in acid solution, and one electrotinning solution depends on this for its success (3). In the present work various complexing agents have been tried but, with the exception of an acetate type of electrolyte that has not yet been fully investigated, the best results have been obtained from fluoride-containing electrolytes. A process based on such an electrolyte has been perfected and is now coming into commercial use in Great Britain. The composition of the electrolyte decided on for development and hereafter referred to as the standard electrolyte is as follows: stannous chloride, 50 g/l; nickel chloride, 300 g/l; sodium fluoride, 28 g/l; ammonium bifluoride, 35 g/l.

Influence of Electrolyte Composition on Cathode Potential

It has previously been shown that the successful codeposition of tin and nickel from a mixed fluoride solution is dependent on the presence of fluorides to complex the stannous tin ions and, to a lesser extent, the nickel ions. In an attempt to explain the complexing action of the fluorides used, and in order to obtain further data on the effects of other variables of the cathode process, the cathodic polarization in electrolytes of various constitution was determined.

Experimental Procedure and Results

The electrolytes were contained in 5-liter Lucite cells maintained at a constant temperature. The cathodes were machined copper cylinders of constant superficial area having the ends stopped off to prevent edge effects. The anodes were concentric sheets of either tin or nickel, according to the electrolyte used. A capillary tube was pressed in close contact with the cathode, the reference electrode being a saturated calomel half-cell. The polarizing current was obtained from a storage battery and the emf of the cell was measured by a Marconi-type *p*H meter. All reagents were of high purity, the stannous chloride used throughout being the pure, anhydrous salt marketed under the name "Stannochlor." Deionized water was used for making up the electrolytes.

Complexing action of the fluoride ion on the stannous tin ion.—A stock solution containing 40 g/l of "Stannochlor," corresponding to a tin content of about 27 g/l, was prepared. Maintaining the temperature at 65°C, increasing amounts of sodium fluoride, up to a maximum of 80 g/l, were added to this solution and the cathode potential was deter-

mined over a range of current densities. The results obtained are shown in Fig. 1. Curves A to E show that the cathode potential becomes progressively more negative as the concentration of sodium fluoride is increased; with 60–80 g/l of sodium fluoride the cathode potential becomes more negative by 0.3–0.5 volt, according to the current density. Further additions of fluoride were found to produce no measurable change. With less fluoride, the tendency

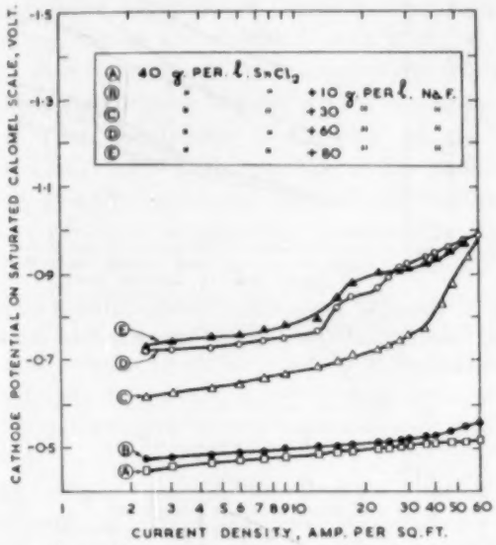

FIG. 1. Effect of adding sodium fluoride to a stannous chloride electrolyte on the cathode potential-current density relationship.

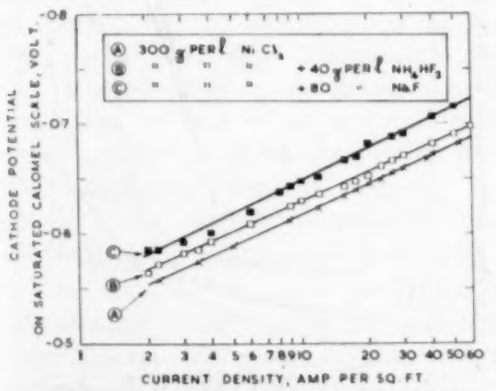

FIG. 2. Effect of adding fluorides to a nickel chloride electrolyte on the cathode potential-current density relationship.

toward complex formation diminishes and below 10 g/l is no longer clearly detectable. If ammonium fluoride is substituted for sodium fluoride, much the same results are obtained.

Complexing action of the fluoride ion on the nickel ion.—A stock solution containing 300 g/l of nickel chloride was prepared and the effect of adding thereto either sodium fluoride or ammonium bifluoride was examined. The results obtained are summarized in Fig. 2 from which it is seen that the change in cathode potential with fluoride concentration is small. Fluorides thus appear to exert less complexing action on nickel ions than on stannous tin ions.

Effect of adding nickel chloride to a stannous chloride-fluoride bath.—A stock solution containing 50 g/l of "Stannochlor," 28 g/l of sodium fluoride, and 35 g/l of ammonium bifluoride was prepared. Nickel chloride was added to this solution in increasing amounts up to a maximum of 300 g/l and the corresponding effect on the cathodic polarization was measured. Fig. 3 shows the polarization curves obtained alongside those for straight stannous chloride (curve A), straight nickel chloride (curve B), and stannous chloride plus fluorides (curve C). Curves D, E, and F show the effect of adding in-

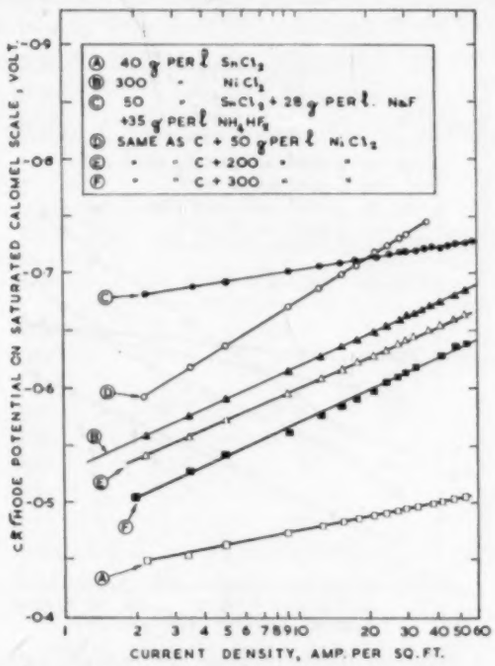

FIG. 3. Effect of adding nickel chloride to a stannous chloride-fluoride electrolyte on the cathode potential-current density relationship.

creasing amounts of nickel chloride to the stock solution. With 300 g/l of nickel chloride the cathode potential as compared with a stannous chloride-fluoride solution is ennobled by 0.09–0.17 volt according to the current density. The greater slope of curve D as compared with curves E and F may be due to concentration polarization effects arising from too low a concentration of nickel chloride.

Effect of temperature.—The optimum working temperature for tin-nickel alloy deposition is 65°C. Tin-nickel deposits can be obtained at temperatures as low as 45°C but only at relatively low current densities. Below 45°C almost pure tin tends to deposit except at very low current densities. Change in temperature has a marked effect on the cathode potential in a straight nickel chloride electrolyte,

which becomes more negative as the temperature is reduced. Temperature change has comparatively little effect on the potential in a stannous chloride-fluoride electrolyte (Fig. 4). The cathodic polarization for the standard tin-nickel bath is profoundly affected by a reduction change in temperature below about 50°C (Fig. 5). As the temperature is reduced, the cathode potential becomes more negative and ultimately the curve approaches that for the stannous chloride-fluoride bath (curve C, Fig. 3). This is in accordance with the observation that at room temperature the mixed chloride-fluoride bath deposits tin only.

Effect of surface active agents.—It has been shown earlier that many surface active agents when added to the standard tin-nickel electrolyte, unless present

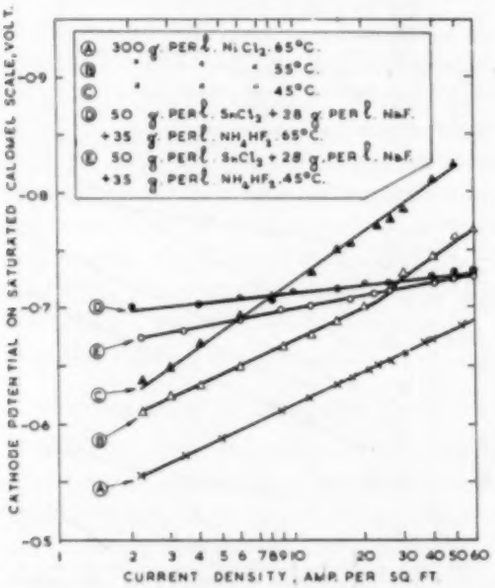
CATHODE POTENTIAL ON SATURATED CALOMEL SCALE, VOLT.
CURRENT DENSITY, AMP. PER SQ. FT.
Ⓐ 300 g PER ℓ. $NiCl_2$. 65°C.
Ⓑ " " " 55°C.
Ⓒ " " " 45°C.
Ⓓ 50 g PER ℓ. $SnCl_2$ + 28 g PER ℓ. NaF. +35 g PER ℓ. NH_4HF_2. 65°C.
Ⓔ 50 g PER ℓ. $SnCl_2$ + 28 g PER ℓ. NaF. +35 g PER ℓ. NH_4HF_2. 45°C.

FIG. 4. Effect of temperature on the cathode potential-current density relationship for electrolytes containing nickel chloride with and without addition of stannous chloride and fluorides.

in very small concentrations, inhibit the deposition of nickel except at low current densities. This effect has been further examined for the substance Lubrol W, a cetyl-alcohol polyethylene-oxide condensate, which is known to function satisfactorily as an addition agent in stannous chloride electrolytes.

The addition of 2 g/l of Lubrol W to a stannous chloride-sodium fluoride electrolyte causes the cathode potential to become less negative at low current densities and rapidly more negative at high current densities, the change over occurring at about 15 amp/ft² (compare curves A and B, Fig. 6). Addition of Lubrol W to a nickel-chloride-fluoride electrolyte causes the cathode potential to become about 0.10 volt more negative over the whole current density range (compare curve C, Fig. 6, with curves B and C, Fig. 2). If 2 g/l of Lubrol W is added to the standard tin-nickel electrolyte the cathode potential, which at the lowest current density is made more negative by about 0.06 volt, becomes progressively more negative as the current density is increased (compare curves D and E, Fig.

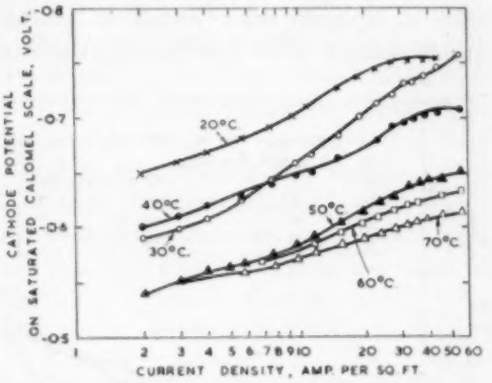

FIG. 5. Effect of temperature on the cathode potential-current density relationship for the standard tin-nickel electrolyte.

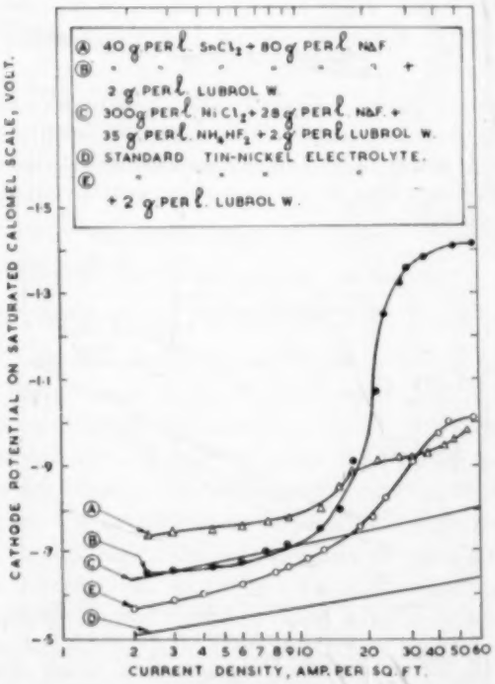
CATHODE POTENTIAL ON SATURATED CALOMEL SCALE, VOLT.
CURRENT DENSITY, AMP. PER SQ. FT.
Ⓐ 40 g PER ℓ. $SnCl_2$ + 80 g PER ℓ. NaF
Ⓑ " " " " " " + 2 g PER ℓ. LUBROL W.
Ⓒ 300 g PER ℓ. $NiCl_2$ + 28 g PER ℓ. NaF. + 35 g PER ℓ. NH_4HF_2 + 2 g PER ℓ. LUBROL W.
Ⓓ STANDARD TIN-NICKEL ELECTROLYTE.
Ⓔ " " " " + 2 g PER ℓ. LUBROL W.

FIG. 6. Effect of adding Lubrol W to fluoride-containing electrolytes on the cathode potential-current density relationship. Temperature: 65°C.

6). In form, curve E resembles curve B, the upward trend at high current densities being characteristic.

The addition of 2 g/l of Lubrol W to the standard tin-nickel bath completely suppresses the deposition of the nickel and only a dull tin deposit is obtained. In very small amounts Lubrol W acts as a brightener and does not interfere with alloy formation but the quantity permitted is so small that the use of this detergent could not be recommended safely.

Discussion of the Electrode Potential Measurements

Taken collectively, the cathode potential determinations indicate that a fundamental factor in the deposition of tin-nickel alloy is the complexing action of the fluoride ion on the stannous tin ions and, to a lesser extent, on the nickel ions. The potential of the cathode in a tin-nickel solution containing 0.23*M* tin is reduced by 0.25–0.4 volt by the presence of 1.42–2.0*M* of fluoride, the complexing action being a maximum at the latter concentration. Optimum results are obtained from a mixed stannous chloride-nickel chloride electrolyte when the fluoride concentration is 2.0*M* and it is possible that under these conditions a complex of the type $Na_2(SnCl_2F_2)$ exists in the electrolyte. By comparison with a straight stannous chloride electrolyte the amount of direct interaction between the fluoride ion and the nickel ion in a straight nickel chloride electrolyte appears to be small. It cannot be assumed, however, that in an electrolyte containing both tin ions and nickel ions addition of fluoride causes only the tin ions to be extensively complexed and, as mentioned later, there are indications to the contrary.

The cathode potential for the mixed metal chloride-fluoride electrolyte becomes progressively more negative as the temperature falls below 75°C, the decrease in potential being most marked below 50°C. If the temperature is reduced to 20°–30°C the cathode potential values are much the same as those obtained for the deposition of tin from a chloride-fluoride electrolyte. Temperature appears to exert far more effect on the deposition potential of nickel than on that of tin and this doubtless accounts for the effect of temperature on the composition of the cathode deposit.

It is significant that the polarization curve for the standard electrolyte occupies a position intermediate between the curves for straight stannous chloride and for straight nickel chloride (Fig. 3). The ennobling action of nickel chloride when added to a stannous chloride-alkali fluoride electrolyte is not inconsistent with the formation of an intermetallic compound of nickel and tin. It is also noteworthy that an increase in the nickel content of the electrolyte from 60 to 75 g/l causes only a slight further ennobling of the cathode potential, and that over this nickel concentration range the nickel content of the deposit remains almost constant.

Effect of the Composition of the Electrolyte on the Composition of the Deposit

The cathodic polarization curves give some indication of the manner in which the composition of the deposit may be expected to change with variation in the concentration of each constituent of the electrolyte. The effects of the variables of the process on deposit composition have already been outlined by Parkinson. A fuller examination of the effect of varying the ratio of tin to nickel in the electrolyte and of varying the fluorine concentration of the electrolyte has since been made.

Effect of varying the tin-nickel ratio in the electrolyte.—A solution containing 50 g/l of stannous chloride, 28 g/l of sodium fluoride, and 35 g/l of ammonium bifluoride was prepared and varying amounts of nickel chloride were added thereto. Deposits were made over the current density range 5–40 amp/ft². The results obtained are summarized in Table I. The figures recorded are the average of from two to four tests in each case; there was very little scatter between the individual test results in each group.

TABLE I. *Effect of tin-nickel ratio in electrolyte on deposit composition*
(Temperature: 65°C)

$NiCl_2$, g/l	Per cent tin in deposit at a current density of:			
	5 amp/ft²	15 amp/ft²	24 amp/ft²	40 amp/ft²
20	92.3	88.8	—	—
60	70.5	76.5	79.0	—
100	69.5	72.5	82.3	—
150	66.8	69.8	72.3	—
200	65.5	66.5	68.5	—
300	63.3	64.8	65.8	63.3
400	62.8	64.8	62.3	63.0

Except at the lowest concentrations of nickel the composition of the deposit remains fairly constant over the range examined. Over the range 60–150 g/l of nickel chloride there is a tendency for the amount of nickel in the deposit to decrease as the current density is increased. Over the whole range the amount of nickel deposited increases, at first rapidly but later very slowly, as the concentration of nickel chloride is increased. For the standard solution containing 300 g/l of nickel chloride, changes in current density and in nickel chloride concentration have little effect on deposit composition.

Effect of varying the fluorine concentration in the electrolyte.—Using a solution containing 50 g/l of stannous chloride and 300 g/l of nickel chloride, the effect of varying the sodium fluoride concentration was studied. This solution contained no ammonium bifluoride and therefore no adventitious hydrofluoric acid; the effect of free hydrofluoric acid concentration was examined independently. The results obtained are shown in Table II from which it is seen that an increase in sodium fluoride concentration is accompanied by a decrease in the tin content of the deposit.

The effect of hydrofluoric acid concentration was determined by varying the concentration of acid in a solution containing the above amounts of stannous chloride and nickel chloride along with some ammonium bifluoride. The solution was initially made up to contain 38 g/l of ammonium bifluoride, corresponding to 12 g/l of free hydrofluoric acid; further additions of 2, 4, and 8 g/l of acid were made. Table III shows that variation in the free acid concentration over the range concerned has no marked effect on deposit composition; as the acid concentration increases the amount of tin in the deposit slightly diminishes.

Effect of varying the working temperature and current density.—The effect of these variables was dealt with in the original paper. Summarizing here, variation in the temperature from 45° to 70°C and in the current density from 18 amp/ft² to 36 amp/ft² has little effect on deposit composition. The brightness of the plate falls as the temperature is reduced, however, unless the current density is also reduced, and in practice the temperature should not be allowed to fall below 60°C.

TABLE II. *Effect of sodium fluoride concentration on deposit composition*

(Temperature: 58°C; current density: 24 amp/ft²)

Sodium fluoride, g/l	Per cent tin in deposit
20	72.5
40	68.0
60	62.5

TABLE III. *Effect of free hydrofluoric acid concentration on deposit composition*

(Temperature: 58°C; current density: 24 amp/ft²)

Free hydrofluoric acid, g/l	Per cent tin in deposit
12	73.0
14	71.5
16	71.0
20	70.0

From the above results it will be appreciated that it is not easy to deposit tin-nickel alloy plate over a wide composition range from the type of electrolyte under consideration. As information on the structure of deposits covering as wide a range of composition as possible was wanted, an attempt was made by modifying the composition of the electrolyte to deposit plate of other than the standard composition (65 per cent tin, 35 per cent nickel). By resorting to the solutions given in Table IV it was possible to obtain deposits having limiting tin contents of 42 per cent and 72 per cent, respectively; further work has since enabled the upper limit to be extended to 87 per cent of tin but not for bright plate. It is remarkable that the change in the composition of the deposit is always relatively much smaller than the change in the tin/nickel ratio in the electrolyte. Also, a change in the cathode current density does not greatly alter deposit composition, unless the solution is relatively low in total metal content. In Table IV the effect of current density is only marked for solution (a) which contains much less metal than solutions (b) and (c) and appreciably less than solution (d).

Throwing Power and Conductivity

Throwing power means rather more in alloy plating than it does in the deposition of a single metal. The term embraces the following considerations: (*a*) distribution of metal thickness over the surface of an irregular cathode, i.e., conventional throwing power; (*b*) variation in the composition of the deposit over the surface of an irregular cathode (hereafter referred to as composition throwing power); and (*c*) variation in the brightness of the deposit over the surface of an irregular cathode (hereafter referred to as brightness throwing power).

TABLE IV. *Effect of electrolyte composition and current density on deposit composition*

(Temperature: 65°C)

	Composition of electrolyte, g/l		Current density, amp/ft²	Per cent tin in deposit
(a)	$SnCl_2$, $2H_2O$	21	16	60
	NaF	11		
	NH_4HF_2	15	32	42
	$NiCl_2$, $6H_2O$	180		
(b)	$SnCl_2$, $2H_2O$	100		
	NaF	75	16	62
	NH_4HF_2	100		
	$NiCl_2$, $6H_2O$	500	32	59
(c)	$SnCl_2$, $2H_2O$	100	16	72
	NiF_2	75	40	72
	$NiCl_2$, $6H_2O$	325		
	KCl	100	64	66
(d)	SnF_2	50	24	64
	NaF	75	40	61
	$NiCl_2$, $6H_2O$	200	64	51

Previous work has established that the composition throwing power and brightness throwing power are excellent. No significant variation either in composition or brightness has been observed on irregular cathodes when plated in a clean solution. Contaminated electrolytes do not give fully bright deposits, but the variation in brightness is not then related to the unavoidable variations in surface current density but rather to the geometry of the

work insofar as certain surfaces are more favorably placed than others to collect foreign matter. Even under these conditions the composition throwing power remains at a high level.

The thickness throwing power was measured quantitatively by using the bent cathode test. Cathodes bent at a right angle were plated in the standard tin-nickel solution under conditions calculated to give a deposit thickness of 0.0005 in. based

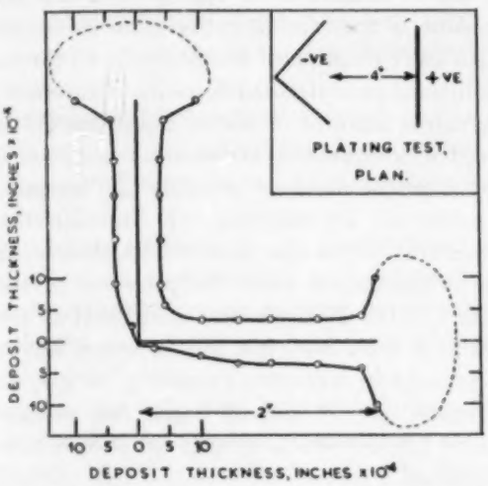

FIG. 7. Throwing power test, showing distribution of deposit on bent cathode placed symmetrically with respect to anode.

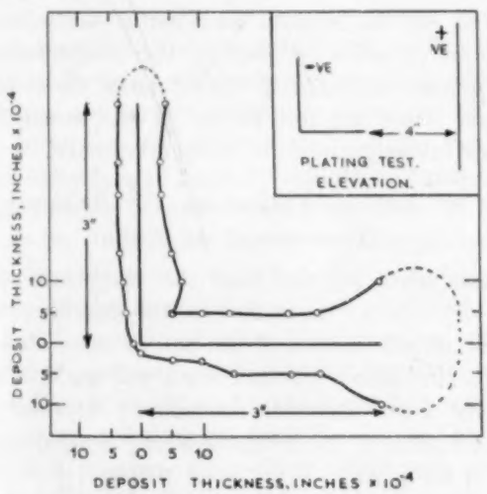

FIG. 8. Throwing power test, showing distribution of deposit on bent cathode placed unsymmetrically with respect to anode.

on the total cathode area. After plating, the tin-nickel coating was protected by an overlay of 0.02 in. of electrodeposited copper and the cathodes were then sectioned and the thickness of the alloy plate measured under the microscope.

The results obtained for two different sets of conditions are summarized in Fig. 7 and 8. Except at the extreme edges of the cathodes, where the thickness of the plate approaches twice the average, and at the back of the bend where the thickness diminishes to about 0.0001 in., the thickness distribution is seen to remain very constant; it is particularly noteworthy that so much alloy has deposited on the remote surfaces of the cathodes. Few, if any, other electrolytes are capable of simulating this performance.

It was decided to supplement these tests by calculating the throwing power and it was therefore necessary to determine the conductivity of the electrolyte. Conductivity measurements were made over the temperature range 40°–65°C with the results shown in Fig. 9 which includes a comparison curve for a straight nickel chloride solution. Of the

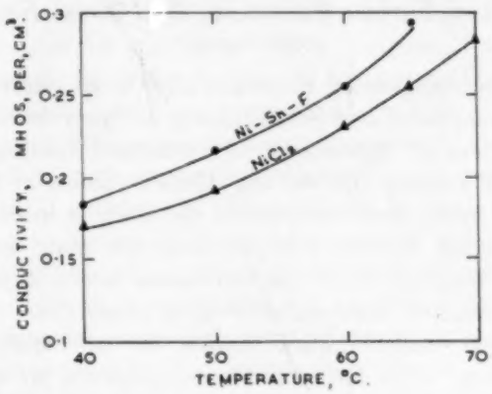

FIG. 9. Variation of conductivity with temperature for the standard alloy plating electrolyte and for a nickel chloride electrolyte.

TABLE V. *Throwing numbers for some common plating baths*

Electrolyte	*N*	Source of information
Tin-nickel	0.0145	Authors
Silver cyanide	0.023	Gardam (4)
Copper sulfate	0.0115	Wesley and Roehl (5)
Nickel chloride	0.0067	
Watts type nickel	0.0024	
Hard nickel	0.005	

two solutions the tin-nickel electrolyte has a somewhat higher conductivity, its specific conductivity at 65°C being 0.29 mhos per cm³.

Gardam's throwing number, N, was calculated from the formula $N = \frac{b}{2\rho}$ where ρ is the specific resistance of the electrolyte and b is a constant.[2] For the tin-nickel electrolyte at 65°C, $b = 0.1$ and $\rho \doteq \frac{1}{0.29} = 3.45$, hence $N = 0.0145$. This is a high value, as is evident from the values of N for various electrolytes given in Table V.

[2] The value of b is obtained from the formula $e_c = a - b \log d$, where e_c is the cathode potential at the current density, d.

For bright, or almost bright plate, as normally obtained from the standard electrolyte, the effect of current density on deposit composition is negligible. The composition throwing power in practice is so good that analytical checking of deposit composition is not necessary. If, through the electrolyte getting out of balance, the deposit becomes dull, plate composition may vary with current density to some extent, but even in extreme cases there is not much departure from the equi-atomic deposition rate.

The brightness throwing power is generally high. Slight variations in brightness may occur over the surface of irregular cathodes.

Effect of Various Cations on the Internal Stress in the Deposit

Electrodeposited tin-nickel alloy is an intermetallic compound and consequently is fairly hard, the hardness of deposits of the standard composition being around 700 on the Vickers diamond scale. Like many such compounds the alloy is inherently somewhat brittle, but provided the plate is free from internal stress the brittleness is not sufficient to impair its serviceability or to cause the coating to flake under impact. Owing to the brittleness, however, it is not possible to fabricate by sharp bending sheet material plated with tin-nickel as the compressive stress induced in the coating on the inside of the bend usually causes some of the plate to flake off.

To give serviceability the plate must be deposited in a stress-free condition. The amount of stress in the plate and also its brightness vary with the nature of the foreign cations that are necessarily present in the electrolyte. These cations are unavoidably introduced via the fluoride additions and may be H^+, Na^+, K^+, or NH_4^+; they may be present either individually or collectively, according to the nature of the fluoride or fluorides employed. Tin-nickel plate of constant composition can be deposited from a mixed chloride electrolyte containing any one or alternatively containing two, three, or even all of these cations, but an acceptable deposit from the viewpoint of stress and brightness is not obtained in every instance.

An examination was made of the effect of these cations on the properties of the plate. Tests were carried out using a solution containing 50 g/l of stannous chloride and 300 g/l of nickel chloride to which the following additions were made: (*a*) sodium fluoride, ammonium bifluoride, and hydrofluoric acid; (*b*) potassium fluoride and hydrofluoric acid; (*c*) sodium fluoride and hydrofluoric acid; (*d*) ammonium fluoride and hydrofluoric acid. In each case the solution was adjusted to a total fluoride content of 2*M* (38 g of F per liter) of which 12 g/l was present as hydrofluoric acid.

The magnitude and nature of the stress were estimated by depositing 0.0005 in. of tin-nickel alloy on one side of a copper strip measuring 6 x 1 x 0.005 in. The strip was held rigidly at the upper end and the stress was determined qualitatively from the curvature, if any, induced by the deposit. This test was reasonably reproducible and served as a useful indication of the relationship between the nature of the foreign cations and the stress.

With the exception of solution (*a*), all the remaining solutions gave stressed deposits. Solution (*b*) gave the greatest amount of stress. Solutions (*b*) and (*c*) induced a compressive stress while solution (*d*) induced a tensile stress of roughly the magnitude of that observed for solution (*c*). Solution (*a*) gave substantially stress-free deposits. It thus seems that stress is associated with the presence of the ions K^+, Na^+, NH^4. Hydrofluoric acid itself at the concentrations used does not induce stress but can do so if present in amounts exceeding 12 g/l, and for this reason care should be taken not to allow the free acid concentration greatly to exceed this limit in practice.

The fact that solution (*a*) does not induce stress is attributed to the presence of both Na^+ and NH^+_4. A balanced reaction results, the negative stress induced by the sodium ions being neutralized by the positive stress induced by the ammonium ions. The reasons underlying the effect of these foreign ions on stress are not known at the moment and further investigations are being conducted.

Effect of Various Cations on the Brightness and Appearance of the Deposit

These tests suggest that the brightness of the plate depends on the nature of the fluoride present, that is, on the nature of the cation associated with the fluorine anion. Further work was undertaken to find the most desirable fluoride or fluorides from the viewpoint of the brightness and general appearance of the plate.

Using an electrolyte containing 50 g/l of stannous chloride and 300 g/l of nickel chloride with some free hydrofluoric acid, the effects of (*a*) sodium fluoride, (*b*) ammonium bifluoride, (*c*) sodium fluoride and ammonium bifluoride in equal amounts, and (*d*) potassium fluoride, were examined. As previous work had shown that the presence of hydrofluoric acid was always desirable no tests were made in acid-free electrolytes. In each of the above groups tests were carried out at fluorine concentrations of 1.0*M*, 1.5*M*, and 1.75*M*; this does not include any fluorine derived from the hydrofluoric acid which,

for each concentration of alkali metal or ammonium bifluoride, was adjusted to 4, 8, 12, and 16 g/l. This makes 48 electrolytes in all. Brass panels, measuring 3 x 2 in., polished on one side, were plated at 9, 18, and 36 amp/ft² in each electrolyte; the temperature in every case was 64°C and the electrolytes were agitated during deposition. The appearance of the plate was assessed by visual examination.

Owing to the high reflectivity of many of the samples it is extremely difficult to obtain an informative photograph of them. The following comments, however, summarize the results of the visual examination.

1. For the metal concentrations used, the fluorine concentration, not including the fluorine from the hydrofluoric acid, must exceed 1.0*M* for satisfactory deposition.

2. Potassium fluoride at all concentrations, irrespective of the hydrofluoric acid concentration, gives a plate that is neither as bright as is desirable nor as bright as can be obtained from the use of other fluorides.

3. Ammonium bifluoride behaves similarly to potassium fluoride, but is less satisfactory.

4. Sodium fluoride along with free hydrofluoric acid over a certain concentration range for each gives excellent bright plate over the whole of the current density range investigated.

It thus appears that the sodium ion is at least partly responsible for the brightness of the plate. This is confirmed by the observation that solutions containing ammonium bifluoride alone, which normally produce semibright plate, can be made to deposit fully bright plate by adding to them either sodium fluoride or sodium chloride.

From the brightness viewpoint the presence of ammonium bifluoride is not really essential. The addition of the ammonium salt is advisable, however, for the reason given in the preceding section. Also, there is some evidence that solutions containing both sodium fluoride and ammonium bifluoride are rather more tolerant to metallic impurities, particularly to copper, than those containing sodium fluoride and hydrofluoric acid.

Anodic Replenishment of the Electrolyte

The tin-nickel process is at present being operated with tin and nickel anodes used simultaneously and supplied by separate circuits The difference between the anode potentials of the tin and nickel under properly balanced conditions does not exceed 0.1 volt which suggests that it might be possible to feed all of the anodes from a single current source. Some measure of success has been obtained with a single anode circuit but the dual circuit system is generally to be preferred. The dual system facilitates control and enables accurate replenishment of the electrolyte to be effected. There is a tendency for a tin-nickel alloy containing about 76 per cent of tin to deposit chemically on the tin anodes, whether the bath is working or not. These anodes must therefore be bagged to retain the resultant sludge. The amount of sludge formed in terms of work plated is comparatively small, and the sludging has no deleterious effect on the cathode deposit.

Alternatively, operation with alloy anodes is a possibility. Cast anodes containing the same amounts of tin and nickel as in the cathode deposit have a duplex structure, consisting of $Ni_3Sn_2 + Ni_3Sn_4$. Such a structure is unsatisfactory as the Ni_3Sn_2 is dissolved preferentially. A single phase structure appears to be essential, and this limits the available alloys to either Ni_3Sn_2 or Ni_3Sn. Neither of these compounds corresponds exactly in composition to the deposit (which is approximately NiSn), and although each compound dissolves smoothly in the electrolyte without the formation of sludge neither compound enables the electrolyte to be kept completely in balance. Alloy anodes have not been tested outside the laboratory where a true assessment of their performance is complicated by the high drag-out from small tanks. From work already done it is thought that anodes consisting of Ni_3Sn_4 might prove satisfactory in practice while the evidence is that Ni_3Sn_2 is less promising. The use of Ni_3Sn_2 anodes leads to a steady fall in the tin content of the electrolyte. On the other hand, Ni_3Sn_4 contains proportionately more tin than the deposit and would be expected to lead to enrichment of the electrolyte in tin, but since some tin is lost through oxidation the balance may prove to be partly redressed. Unfortunately, Ni_3Sn_4 cannot be made merely by casting. The cast alloy has a duplex structure and prolonged annealing out of contact with air is necessary to convert the cast structure wholly to Ni_3Sn_4.

Ideally, alloy anodes of composition NiSn are wanted, but apart from electrodeposition no means of making such an alloy is known at present. It is possible that powder metallurgical methods might enable a suitable alloy to be produced and this line of approach is being considered. The main advantages accruing from the use of alloy anodes are reduction or elimination of anode sludging and simplification of electrical control.

Structure of the Deposits

In an earlier publication, one of us (H. P. R.) showed that tin-nickel deposits containing around 65 per cent of tin and 35 per cent of nickel were characterized by a metastable nickel arsenide type of structure, similar to that of $\gamma' Ni_3Sn_2$ (2). It was

also shown that such deposited alloys recrystallized when heated above 300°C, and that in bright deposits of this composition there was strongly marked preferred orientation.

This preliminary work has now been extended to cover as wide a composition range as possible. From the authors' earlier remarks it is clear that chloride-fluoride electrolytes will only deposit tin-nickel alloys over a limited composition range. By resorting to the modified solutions given in Table IV it was possible to prepare deposits suitable for x-ray examination varying in tin content from 57 per cent to 82 per cent. The alloys were deposited on copper foil.

TABLE VI. *Summary of results of x-ray examinations of tin-nickel electrodeposits*

Ref. No.	Appearance of electrodeposit	Tin content, per cent	Structural constitution
1105	Bright	57	Sn/Ni phase; crystal structure similar to that of 875
875	Bright	65	Sn/Ni phase; hexagonal structure cell with lattice constants a = 4.15 Å, c = 5.10 Å, c/a = 1.23
570	Bright	69	Sn/Ni phase as above
544	Mainly bright but with local dull patches	75	Sn/Ni phase as above mainly, but in dull patches substantial concentrations of Ni_3Sn_4 are present.
526	Bright and dull regions	82	Substantial concentrations of Ni_3Sn_4 are present, but in bright regions hexagonal Sn/Ni phase is predominant.
1095	Very matte surface	87	Mixture of Sn with an alloy phase not specifically identified.
900	Dull	68	Hexagonal Sn/Ni phase as above, with lattice constants not noticeably different from those established for 875.

In order to provide direct reference standards of established tin-nickel alloys falling within the range of composition of the electrodeposits, alloys corresponding with the molecular formulas Ni_3Sn_4 and Ni_3Sn_2 were cast and aged for 48 hours at 625°C. Conventional x-ray powder examination confirmed that these gave crystal structure data corresponding with standard data published in the literature (6).

Two x-ray diffraction techniques were employed for examination of the electrodeposits themselves. Powder samples were obtained by severe deformation of the cathodes. The electrodeposit was fragmented in this way and the fragments could be collected to form a conventional cylindrical specimen for mounting in a 19 cm diameter x-ray powder camera. In the second method, rectangular sections, of dimensions 10 x 3 mm, were cut from the cathodes and these were arranged for examination by x-ray surface reflection utilizing a 10 cm diameter cassette. The sections were held on a single crystal goniometer head, so that it was a simple matter to change the angle of incidence of the x-ray beam on the electrodeposited surface. In most instances all the data required could be obtained with a single angular setting between 10° and 15°.

TABLE VII. *X-ray data on a typical bright tin-nickel electrodeposit (No. 875)*

$\frac{d}{n}$ (obs.)	I	hkl.	$\frac{d}{n}$ (calc.)
2.94	s	101	2.94
2.56	vw	002	2.55
2.076	vs	102	2.08
		110	
1.697	m	201	1.70
1.601	vw	112	1.61
1.528	vw	103	1.54
1.470	m	202	1.47
1.314	m	121	1.31
1.280	vw	004	1.28
1.198	m	122	1.20
		104	
		300	
1.085	w	114	1.09
		302	

The fourth column lists calculated interplanar spacing data based upon a hexagonal structure cell with lattice constants: a_o = 4.15 Å; c_o = 5.10 Å; c/a = 1.23.

Identity of the Deposits

The results of the x-ray examination of the electrodeposits are summarized in Table VI. It is seen that most of the bright deposits are composed of a single alloy phase with a characteristic crystal structure. Table VII gives interplanar spacing data for this phase

The preponderating alloy phase, corresponding approximately to the composition NiSn, has a structure similar to that of Ni_3Sn_2 but the difference in the dimensions of the unit cell for NiSn and Ni_3Sn_2 previously reported is confirmed. In particular, the axial ratio of 1.25 for NiSn is appreciably

smaller than the minimum value of 1.26 established for Ni_3Sn_2 richest in tin. A reference specimen of cast alloy, aged at 625°C, and containing 58 per cent of tin, gave values of $a_o = 4.13$ Å, $C_o = 5.20$ Å, $C/a = 1.26$ for its structure cell dimensions.

Another noteworthy feature is that the characteristic hexagonal phase persists in the bright electrodeposits for tin concentrations up to about 75 per cent by weight. The range of composition would appear to extend from about 57 per cent to nearly 75 per cent tin. The hexagonal phase is indeed found in specimen 526 which contains 82 per cent of tin. However, it is not certain that, for the specimens of higher tin content, the composition was absolutely consistent over the whole area. The x-ray investigation in any event proves that differences in phase condition from one point to another occur both in specimens 526 and 544. There is thus no conclusive evidence that the hexagonal phase condition in the electrodeposited alloy extends beyond a tin content of about 75 per cent.

The lattice dimensions of the hexagonal alloy characterizing the bright electrodeposits show only minor changes with alterations in tin content. As is mentioned below, the x-ray reflections exhibit some broadening associated with textural features of the deposits, so that the accuracy of lattice parameter determination is not high. Even so, direct comparison of the x-ray diffraction patterns of the series shows that differences in lattice spacings are not greater than one or two parts in a thousand over the range of compositions studied. The directions in which minor changes can be detected indicate that the structure cell dimensions increase slightly with increase of tin content.

All the electrodeposits characterized by the hexagonal crystal structure have been proved to be in a metastable condition. Heat treatments up to temperatures of about 300°C produce no detectable change, but above this temperature decomposition begins, and various mixtures of the normal $\gamma' Ni_3Sn_2$ phase and the Ni_3Sn_4 phase form, depending upon the chemical composition of the electrodeposit.

Texture of the Deposits

The x-ray reflection patterns reveal that in the majority of the bright electrodeposited specimens the crystallites are directionally orientated with respect to the surface of the cathode. The directionally orientated arrangement is normally found whenever the hexagonal phase condition occurs. It is found, for instance, on the bright areas of specimen 526 but on the dull areas, where the phase condition changes to Ni_3Sn_4, no directionality is disclosed.

Specimen 900, alone of those in the hexagonal phase condition, exhibited practically no directionally orientated features. It is significant that this specimen was specially prepared to possess a dull surface and that a random orientated texture resulted as a consequence.

The principal orientation texture in bright specimens appears to be one in which (110) planes of the hexagonal crystallites tend to lie parallel to the copper base surface. This texture is shown by specimens 1105 and 544 which represent the extremes of the bright composition range. On the other hand another texture is quite common as is disclosed in some photographs by a change in the arrangement of the strong arcs.

Line broadening effects on the x-ray diffraction patterns of specimens 1105 to 544 indicate that the average ultimate crystal size of the hexagonal alloy is below 0.1 μ. Some variations from one specimen to another were evident, but a reasonable estimate is that the average size lies about the 0.05 μ figure. No difference in this respect was disclosed by the dull specimen 900.

Appreciably larger crystal size features were displayed when the phase condition was not the characteristic hexagonal one. If the electrodeposit was composed largely of Ni_3Sn_4 for example, the crystal size appeared to be greater than 0.1 μ. The free tin constituent of the electrodeposit, specimen 1095, was composed of still larger crystallites, of average size between 1 and 5 μ.

General Discussion

Although some relevant information has been collected it is impossible at this stage to advance other than a tentative theory of the tin-nickel alloy plating process.

The following facts have been firmly established: (*a*) the chloride-fluoride electrolyte favors the codeposition of tin and nickel in equal atomic proportions; (*b*) an entirely different electrolyte containing the two metals as acetates when operated at temperatures above 65°C has been found to produce bright tin-nickel alloy plate of the same composition as that obtained from the chloride-fluoride electrolyte. Both of these electrolytes deposit a tin-nickel alloy chemically by direct immersion on tin.

It is difficult to explain the constancy of composition of the cathode deposit and the chemical deposition of tin-nickel on tin by any mechanism other than one involving the presence in these electrolytes of some complex ion containing both tin and nickel. There is some further evidence supporting this possibility. When making up the tin-nickel electrolyte it is customary first to dissolve the nickel chloride in water and then to add the fluorides and stannous chloride in that order. When about half

of the fluoride additions have been made the solution often becomes turbid and develops a tendency to precipitate nickel salts. On adding the stannous chloride the solution becomes clear and if more fluoride is added the turbidity does not reappear. It is suggested that this solubility effect is consistent with the presence of a tin-nickel complex.

The fact that a tin-nickel alloy cannot readily be deposited from a stannous chloride-nickel chloride bath except in the presence of fluorine suggests that the fluorine ion must in some way be bound up with the tin-nickel complex. Mixed fluorides of tin and nickel are well known, and it may be significant that light green crystals of a previously unreported compound of this type having the formula $NiF_2 2SnF_2 \cdot 6H_2O$ have been isolated from the tin-nickel electrolyte. The high throwing power of the tin-nickel electrolyte in respect of both thickness and composition further suggests that deposition does not occur directly from tin and nickel ions. Although the complexing effect of fluorides has been shown to be much more marked for a straight stannous chloride solution than for a straight nickel chloride solution there is evidence of complex formation in the latter case. The view that in the standard alloy plating bath both the tin ions and the nickel ions are complex is therefore not inconsistent with the experimental results obtained for straight solutions.

The postulate of a complex mixed metal-fluorine ion is believed to be entirely novel. There is not sufficient evidence available at present to enable the structure of the complex to be predicted with any degree of certainty. Both tin and nickel form fluorine coordination compounds with covalency numbers of four and six, and it is conceivable that the tin-nickel-fluorine complex has a structure modelled on similar lines. It is believed that the ion is in any case dimensionally large compared with the stannous ion and the nickel ion. It seems to be fairly certain that simple metal ions are present freely in the electrolyte in addition to the complex ion, but under normal conditions the simple ions are not discharged as their deposition potentials are too high. However, under certain circumstances it is possible to discharge at any rate the stannous ion in preference to the complex ion, the notable instance being when surface-active agents are present in the electrolyte. It has already been mentioned that such additions when present in other than very small amounts greatly favor the deposition of tin.

If 1 g/l of Lubrol W is added to a standard tin-nickel electrolyte, tin-nickel alloy plate cannot be deposited at current densities exceeding about 2 amp/ft^2. As the current density is increased the deposit rapidly becomes enriched in tin and very soon almost pure tin plates out. If the cathode is rotated rapidly, the tendency to deposit tin as the current density is raised diminishes markedly. This observation again tends to support the view that the tin and nickel are associated in a single, large complex ion. Of the three possible ions present, the stannous ion will probably be the smallest since the nickel ion is usually highly solvated. In the presence of the surface-active agent the easy diffusion of ions to the cathode is obstructed to an extent depending on the dimensions of the migrating ions. The molecule of the surface-active agent is itself large and would be expected to impede the complex ions far more than the stannous ions, and any film of these large molecules in the immediate vicinity of the cathode would cause the cathode layer rapidly to become impoverished in complex ions. Rotation of the cathode probably disrupts the film and allows the depleted cathode layer to be replenished. Rotation introduces centrifugal forces which act on all the ions present in proportion to their respective masses. At the rotational speeds used the tin-nickel alloy deposited was richer in tin than the standard alloy, the maximum nickel content not exceeding 25 per cent. It is suggested that this enrichment is the result of the larger mass of the nickel ion and the tin-nickel ion as compared with the stannous ion.

From the practical viewpoint, one of the most noteworthy features of the chloride-fluoride tin-nickel electrolyte is the constancy of composition of the deposits obtained from it. This property of the solution greatly simplifies the control of the process and makes it almost as easy to operate as a single metal plating process. The gamma structure which typifies these electrodeposits occurs under equilibrium conditions only when the atomic ratio of nickel to tin approaches 3:2. As the atomic ratio in the electrodeposit is close to 1:1, the indication is that under the conditions of electrolysis additional tin can be incorporated into the alloy lattice. It would appear that vacancies and defects in atomic packing characteristic of the structure are not necessarily associated only with one kind of atom, but can occur in the nickel layers as well as in the tin layers. The symmetry of the nickel arsenide type of structure cell is maintained, but the cell dimensions are modified and show little variation with tin content, the distinguishing feature being the decrease in axial ratio. Structurally, therefore, bright electrodeposited alloys may be considered to be identical over a composition range that is certainly wider than is likely to be encountered in practice.

The reason for this departure from structural equilibrium is probably to be found in the surplus activation energy of the discharging cations which causes the released atoms to penetrate into non-

equilibrium positions in the crystal lattice. An equilibrium condition is understood to exist when the potential energy of the atoms and ions in the crystal lattice of the deposit is at a minimum. This state can be approached (*a*) by maintaining the difference between the activation energy of the discharging cations and the crystal lattice energy at a minimum, and (*b*) by maintaining the rate of deposition at the lowest possible value, i.e., operating at the lowest possible cathode overvoltage. Under these conditions there is a close approach to thermodynamic reversibility. As the operating temperature is increased, however, the proportion of ions having an energy in excess of their activation value, E, for the process at temperature, T, increases exponentially, according to the equation $k = Ae^{-E/RT}$. At the working temperature of 65°C an adequate proportion of the discharging ions possess energy sufficient to surmount the potential energy barrier associated with the metastable crystal lattice. It is therefore significant that tin-nickel alloys cannot be deposited from the solutions under consideration at temperatures below 45°C. The high working temperature thus appears to be at least one factor responsible for these deposits being in a nonequilibrium state.

Conclusion

This paper describes the laboratory work that has been carried out on the codeposition of tin and nickel from chloride-fluoride electrolytes.

Although laboratory research is continuing, sufficient information has been obtained to enable industrial development to commence, and at the time of writing several plants are in operation. The largest of these plants has a capacity of 2000 gal and has now been working for about a year. Experience gained with this plant and with others since installed has indicated directions in which the process might be improved. Basically, the process has proved satisfactory. The brightness of the deposit, however, has not normally been quite good enough to enable all final finishing to be dispensed with, while pitting has occasionally proved a little troublesome. The further work now in hand is mainly directed toward finding suitable additions to improve brightness and to combat pitting, and progress is being made in each field. Practical experience has also suggested directions in which the chemical engineering of tin-nickel plating plant might be improved, and this applies in particular to the filtration and circulation of the electrolyte.

Considering the very short time that this new process has been in industrial use the results obtained to date can justly be regarded as most gratifying. The view has, in fact, been expressed by a user that in one year tin-nickel has made as much industrial headway as electrodeposited chromium made in the first ten years!

The tin-nickel process is being used for finishing a wide variety of articles, including automobile fittings, domestic goods, battery cases, etc. The plate is fully as tarnish resisting as chromium and has a more pleasing color. The blueness of chromium is entirely absent, tin-nickel being characterized by a faint rose-pink tint.

Acknowledgments

The bulk of the work described in this report was carried out in the Laboratories of The Tin Research Institute. Grateful acknowledgment is made to Dr. J. W. Price who did all the analytical work on deposits and electrolytes. The authors are indebted to The International Tin Research Council for permission to publish this paper.

Any discussion of this paper will appear in a Discussion Section, to be published in the December 1953 issue of the Journal.

REFERENCES

1. N. Parkinson, *J. Electrodepositors' Tech. Soc.*, **27**, 129 (1951).
2. H. P. Rooksby, *J. Electrodepositors' Tech. Soc.*, **27**, 153 (1951).
3. British Pat. 566,633.
4. G. E. Gardam, *Trans. Faraday Soc.*, **34**, 698 (1938).
5. W. A. Wesley and E. J. Roehl, *Trans. Electrochem. Soc.*, **86**, 419 (1944).
6. O. Nial, "X-ray Studies on Binary Alloys of Tin with Transition Metals," University of Stockholm (1945); T. Heumann, *Z. Metallkunde*, **35**, 206 (1943).

The Hot-Wire Process for Zirconium[1]

ROBERT B. HOLDEN AND BERNARD KOPELMAN

Sylvania Electric Products Inc., Bayside, New York

ABSTRACT

To better understand the hot-wire process for zirconium, a study has been made of the thermal decomposition of zirconium tetraiodide molecules which are isolated from the effects of interaction with other tetraiodide molecules and with the reaction products. It was found that the probability that a given zirconium tetraiodide molecule will decompose upon striking once upon a hot surface *in vacuo* is very high, approaching unity at 1400°C.

This work was supplemented and extended by a second series of investigations, which were based upon pressure measurements made inside of an operating de Boer bottle. From these two experimental approaches considerable information was gained about the hot-wire process, including a knowledge that the rate-determining step in most cases is that of gaseous transport, and that the initial synthesis of zirconium tetraiodide in the de Boer bottle is catalyzed, apparently photochemically, by the lighting of the filament.

INTRODUCTION

Although the hot-wire method for the preparation of pure metals has been known since the early part of the century, the process actually remains little understood from a fundamental standpoint, despite the fact than an appreciable amount of engineering data has been collected. Currently there is considerable interest in the application of this process to the preparation of ductile zirconium. Commonly known as the de Boer iodide process, it is conducted in the following manner (1). The zirconium which is to be purified, together with a small amount of iodine or zirconium tetraiodide, is loaded into a reaction chamber or "de Boer bottle." This de Boer bottle contains two sealed-in electrical leads capable of carrying a substantial current, and a long, thin "seed" filament which joins these leads within the bottle. The bottle is then evacuated (if free iodine is placed in the bottle, precautions must be taken to prevent loss during evacuation), and heated to a temperature such that the iodine will react with zirconium to form the tetraiodide at an appreciable rate. A current is then passed through the seed filament sufficient to heat it to 1300° to 1500°C. The volatile zirconium tetraiodide diffuses to the hot filament, where it is decomposed to metallic zirconium and iodine. The iodine thus liberated diffuses back to the crude "feed" zirconium, reacts with more of it to form the tetraiodide, which is in turn decomposed upon the hot filament, and so on. In this manner a heavy rod of ductile zirconium is built up on the seed filament.

It was decided to carry out a fundamental study of the iodide process in this laboratory to gain an improved understanding of the process in general and of the controlling or limiting factors in particular.

From a kinetic standpoint the process may be considered to consist of the following steps: (*a*) synthesis of zirconium tetraiodide at about 300°C from the zirconium feed material and iodine vapor; (*b*) transport of this tetraiodide to the neighborhood of the hot filament; (*c*) thermal decomposition of this tetraiodide on the hot filament; (*d*) transport of the iodine liberated at the filament back to the neighborhood of the feed zirconium. On further consideration it is seen that steps (*b*) and (*d*) are closely related, for they both proceed according to precisely the same mechanisms (diffusion and convection) and the only intrinsic differences between them are the greater speed and smaller kinetic collision diameter of the free iodine as compared with the tetraiodide. Hence a simplification is to be gained by lumping (*b*) and (*d*) together and terming it simply the gaseous transport step.

For our purposes the analysis into these three steps constitutes an adequate description of the de Boer iodide process.

The most important goal is a knowledge as to which of the steps in the process is rate-determining. This information is of importance in a fundamental sense, and engineering-wise is vital to an intelligent attempt to accelerate the process.

The problem, then, is to determine which is the slow step. The two sets of experiments described here clearly reveal the slow step in the process.

THE DECOMPOSITION COEFFICIENT

To begin with, it is not known what fraction of the gaseous contents of an operating de Boer bottle is zirconium tetraiodide and what fraction is free

[1] Manuscript received August 1, 1951. This paper was prepared for delivery before the Philadelphia Meeting, May 4 to 8, 1952. This work was done for the Atomic Energy Commission under Contract At-30-1-GEN-366.

iodine. For purposes of argument, however, consider a hypothetical cracking bottle containing only zirconium tetraiodide. The rate at which zirconium tetraiodide molecules strike the hot surface is easily computed from the kinetic theory of gases. This rate turns out to be enormously greater than the rate of deposition of metallic zirconium as determined from typical cracking runs. One explanation for this difference is that the average tetraiodide molecule must strike the hot surface many times before decomposing. This leads to a consideration of the probability that a given tetraiodide molecule will decompose upon striking the hot surface. A measurement of this probability offers a direct method for ascertaining whether the decomposition step (*c*) is rate-determining. Hence it was decided to perform a series of experiments which consisted in measuring the probability that a given zirconium tetraiodide molecule will decompose upon impinging once on a hot surface *in vacuo*. This probability, hereafter termed the "decomposition coefficient," may be considered to be characteristic of the limiting case of a de Boer bottle with a vanishingly small charge of zirconium tetraiodide.

Experimental

The apparatus used is shown in Fig. 1. It consists of a zirconium tetraiodide chamber, *a*, the neck of which is ground to accommodate a standard taper which is sealed to a conduit tube, *b*, a set of orifices, *c*, through which the tetraiodide effuses under essentially equilibrium conditions, and a hot target, *d*, which is struck by a portion of the effusing tetraiodide. The walls, *e*, are cooled by liquid nitrogen, *f*, in order to trap the tetraiodide which does not strike the target, that which rebounds from the target without having been decomposed, and any liberated iodine. The target is formed from a strip of sheet molybdenum and the desired temperature is obtained by resistance heating, the necessary current being supplied through the leads, *g*. The jigs, *h*, serve to secure the target to the leads and also to maintain rigidly the position of the target.

The target temperatures are measured through the window, *i*, by means of a Leeds and Northrup Optical Pyrometer, No. 8622-C. The system is attached to a D.P.I. air-cooled three-stage fractionating oil diffusion pump through a ball-type trap, *j*. The connecting tubes are 2 in. in diameter and as short as possible in order that the pumping speed might be as great as possible for the system.

The zirconium tetraiodide used in these experiments was prepared by a modification of the method of Stahler and Denk (2) and was distilled under high vacuum. This was analyzed for iodine and the stoichiometric amount was found. It is of critical importance never to allow this material to come in contact with atmospheric air, since it is immediately attacked by moisture.

To make a run, the entire apparatus is evacuated to a pressure of about 10^{-6} mm Hg, and the critical portions are baked out. Then the diffusion pump is shut off, the system filled with dry argon, and a flow of argon maintained through the apparatus while the tetraiodide chamber is loaded. The loading consists in placing a sealed thin-walled vial containing a weighed portion of zirconium tetraiodide in this chamber and then smashing it. The system is then evacuated, the target is degassed, the refrigerant space is filled with liquid nitrogen, the target is brought to the desired temperature, and the chamber, *a*, is heated by means of an oil bath to a temperature such that the tetraiodide effuses through the orifices, *c*. This temperature is maintained until all of the tetraiodide has effused.

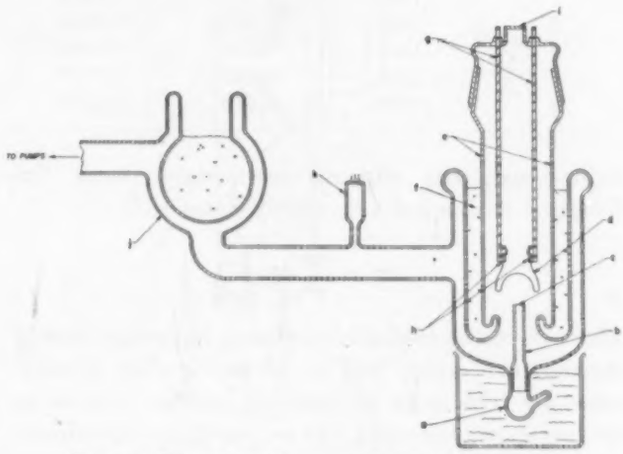

FIG. 1. Decomposition coefficient apparatus

During these runs the pressure in the system, as measured with the ionization gauge tube, *k*, was maintained $<1 \times 10^{-6}$ mm Hg and most of the time was of the order of 2×10^{-7} mm Hg. At the completion of a run the target was chemically analyzed for zirconium. The zirconium formed a bright, adherent plate upon one side of the molybdenum strip. The molybdenum strip was removed by dissolving it in nitric acid, leaving behind a thin, bright, highly ductile foil of zirconium. The only impurity which could be detected spectrographically in this foil was molybdenum, obviously the result of diffusion of the target material into the zirconium plate during the course of its build-up.

Treatment of Data

The experimental data are given in Table I.

In order to compute the decomposition coefficient, p_c, from these data, it is necessary to know the fraction of the effusing tetraiodide which actually

impinges upon the target. The conducting tube and orifices (*b* and *c*, respectively, in Fig. 1) were designed so that the resistance to molecular streaming offered by the orifices was of a higher order of magnitude than that of the conducting tube proper. Since the vapor pressure of crystalline zirconium tetraiodide is known as a function of temperature (3), it was possible to obtain any desired pressure in the zirconium tetraiodide chamber simply by choosing the proper temperature. This pressure was maintained at such a value that the mean free path was of a greater order of magnitude than the diameter of the effusion orifices. Under these conditions the tetraiodide effuses under essentially equilibrium conditions, and since the orifices are essentially

TABLE I

Run	Temp, °C corrected	ZrI_4 load, g	Zr on target, g
1	1382	0.7734	0.0087
2	1432	0.9530	0.0254
3	1372	2.2310	0.0605
4	1211	0.8416	0.0157
5	1152	0.5120	0.0030

knife-edged, the effusing tetraiodide obeys the Knudsen cosine law (4), which states that

$$ds = \frac{dw}{\pi} \cos x$$

where ds is the probability that a molecule coming through the orifice will be in an element of solid angle dw. The angle between dw and the normal to the orifice is given by x. (In an auxiliary experiment it was verified that this law was obeyed in this apparatus.)

The fraction, f, of the total tetraiodide which actually struck the target in any given run is then given by

$$f = \int_s ds = \frac{1}{\pi} \int_s dw \cos x$$

where the integration is performed over the entire solid angle intercepted by the exposed area of the target.

In these experiments the targets were in either of two shapes: one with the intercepting surface planar and the other with the intercepting strip bent into a semicircle. In calculating the intercepted fraction of the tetraiodide for the case of a flat target the integration was done graphically.

By bending the target strip into a semicircle so that its area closely approximated a portion of the surface of a sphere, and adjusting its height so that the orifice lay on the surface of this imaginary sphere defined by the target strip, the integral becomes (4)

$$f = \frac{A}{4\pi r^2}$$

where A is the exposed area of the target strip and r is the radius of this sphere.

The decomposition coefficient is then given by

$$p_c = \frac{1}{f} \cdot \frac{n_1}{n_2}$$

where n_1 is the number of moles of zirconium deposited on the target and n_2 is the total number of moles of zirconium which effuse through the orifice. In the calculations for the case of the semicircular target it was necessary to take into account the possibility that a given tetraiodide molecule might strike the target more than once before being trapped at the walls.

TABLE II

Temp, °C	Decomposition coefficient* p_c	Estimated error limit %
1432	1.0	10
1382	1.0	50
1372	0.8	10
1211	0.58	10
1152	0.32	10

* A value of 1.0 for p_c means that every zirconium tetraiodide molecule which strikes the hot surface is decomposed.

The results are given in Table II.

Discussion

The experimentally determined values of p_c demonstrate strikingly that the slow step in the cyclic iodide process is not the actual rate of decomposition. This result is an encouraging one from a practical standpoint, for it means that the slow step must be either the synthesis step (*a*) or the gaseous transport step (*b*, *d*), both of which appear to offer greater possibilities for acceleration than the actual rate of decomposition. The method chosen for deciding between these two follows.

Pressure Measurements

Outline of Method

One means of determining which of the remaining two steps is the slow one consists of making pressure measurements inside of an operating de Boer bottle. This method is, in principle, singularly simple and direct.

If the rate-determining step in the process were the synthesis step, it follows that most of the iodine present in the cracking bottle during a run would be in the uncombined form. On the other hand, if the gaseous transport step were rate-determining,

an appreciable fraction of this iodine would be in the form of the tetraiodide.

At the operating temperature of a de Boer bottle, iodine is a gas, whereas zirconium tetraiodide is a solid exhibiting a sublimation pressure of only a few centimeters. Consider a cracking bottle which is loaded with sufficient iodine to give a theoretical pressure, P_t, of, say, one-half of an atmosphere at the operating temperature prior to any reaction with metallic zirconium. The amount of free iodine present at any given time is given approximately by P, the measured pressure, and the amount of tetraiodide present in the bottle is approximately proportional to $(P_t - P)$. This affords a means of determining which of the steps is rate-determining.

In short, then, if the pressure in the bottle is substantially that which would be expected if the iodine were entirely uncombined, the synthesis step would be rate-determining. If the pressure were substantially less than this value, the gaseous transport step, which is the only remaining possibility, must be rate-determining. In principle the computation of the theoretical pressure, P_t, must include the effect of the nonuniformity of temperature inside the bottle. In practice, however, this turned out to be unnecessary.

Experimental

The bottle used in this work is of the conventional de Boer type (5), the bottle proper being Pyrex glass, 4 in. in diameter and about 20 in. high. The electrical leads, which were $\frac{3}{16}$-in. tungsten rods, were introduced through the bottom of the bottle in order to leave the top free for the installation of the pressure indicator.

A 0.010-in. tungsten seed filament was used in this work, and the feed zirconium consisted of sections of iodide zirconium. These sections were about a foot long, somewhat less than $\frac{1}{2}$ in. in diameter and had been cut from the end portions of "crystal bar" zirconium. They were held against the bottle wall by a cylinder of molybdenum screen.

The initial voltage applied across the bare tungsten seed filament was 12 volts, which gave a brightness temperature of 1240°C (not corrected for emissivity). As zirconium deposited, the voltage was reduced according to a set schedule by which the product $E^3\sqrt{I}$ was held approximately constant, so that the filament temperature was maintained at essentially the same value throughout a run.

The actual measurement of the pressure in the bottle is complicated by the fact that both the iodine and the zirconium tetraiodide are corrosive and are condensable. These difficulties were surmounted by using a glass Bourdon sickle-type gauge as a null indicator and balancing the pressure inside of the cracking bottle against air pressure in an external measuring system. This null indicator was mounted at the top of the cracking bottle as shown in Fig. 2. Since it did not appear to be feasible to observe the null indicator directly, an arrangement was used whereby the balance point could be detected electrically. This arrangement is also shown in Fig. 2. The sickle gauge, *a*, bears a movable gold-tipped contactor, *b*, which can make or break contact with the stationary gold-tipped contactor, *c*. This contact is detected by means of an auxiliary electrical circuit consisting of a battery and a microammeter with a series ballast resistor.

At some pressure difference, ΔP, between the de Boer bottle and the external pressure measuring system (regions A and B in Fig. 2) electrical contact

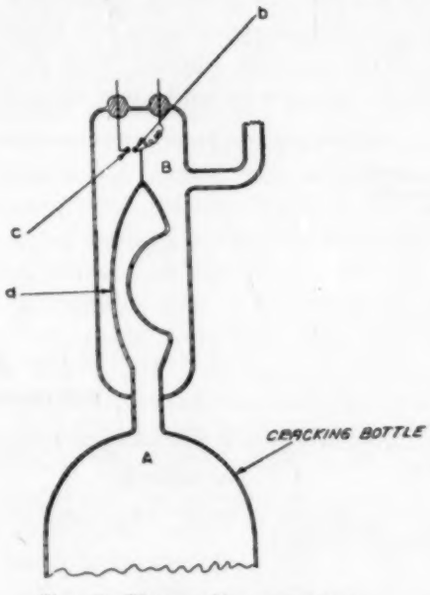

FIG. 2. Glass null manometer

will just be established. This pressure difference is determined by an initial calibration. In operation the pressure in the external measuring system, P', is adjusted until contact is just established (as shown by the microammeter) and then read on an ordinary mercury manometer. The actual pressure, P, in the cracking bottle proper is then given by $P = P' + \Delta P$.

At elevated temperatures this gauge was distinctly less accurate than at room temperature. The gauge constant, ΔP, is actually a function of temperature and displayed a tendency to slowly drift with time at the operating temperatures. Although the gauge used gave results with an accuracy better than ± 0.1 cm Hg at room temperature, the results obtained at the temperatures used in this work (300°–320°C) may be relied on only to ± 0.6 cm Hg.

Discussion

Typical results of pressure measurements made over the course of cracking runs are shown in Fig. 3 and 4. The ordinates give the total pressure in the bottle and the abscissas give the time elapsed after the bottle has reached the operating temperature (300°–320°C). In the run represented by Fig. 3 the filament was lighted two minutes after the bottle had reached the operating temperature whereas in the next run, represented in Fig. 3, the filament was not lighted until it had been held at the operating temperature for more than two hours. A small, sharp pressure increase followed the lighting of the filament in the run shown in Fig. 3, undoubtedly due to a temperature rise in the gas immediately surrounding the filament. In the run represented in Fig. 4 this rise was not detected, apparently because the pressure measurements were not taken at sufficiently short intervals. Shortly after the filament is lighted the pressure in both cases drops to a very

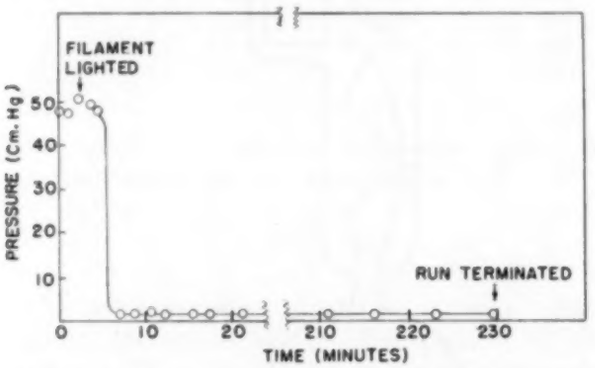

FIG. 3. Cracking run. (Time = 0 when bottle first reaches operating temperature.)

low value, indicating that the iodine has largely reacted to form the tetraiodide. The pressure remains low during the remainder of the run which shows that at steady-state operation most of the total iodine present is in the form of the tetraiodide. This result strikingly demonstrates that the synthesis step (*a*) is not the slow step in the process when conducted in this fashion. Strictly speaking, this result is applicable only when feed material is employed which is at least as reactive as crystal bar ends. The only material which would be expected to be consistently less reactive than crystal bar ends, however, is interior sections of crystal bar. In special cases other feed materials might become covered with a surface layer of oxide or otherwise passivated so that the rate-limiting step would be the synthesis step, (*a*), but this would not be the ordinary case.

The previously described work on the decomposition coefficient shows that the decomposition step (*c*) is also not the slow step. This implies that the rate-determining step in the iodide process for ductile zirconium is the transport of the gaseous reactants. This does not include the possibility of the special case involving highly passivated feed material, in which the synthesis step (*a*) could become controlling.

Once sufficient iodine has been added to the cracking bottle to cause solid zirconium tetraiodide to condense out during the steady-state operation, it is clear that further addition of iodine would have no effect on the rate of deposition of zirconium from a bottle which has essentially isothermal walls. From the fact that a large proportion of the iodine is in the form of tetraiodide during steady-state operation we can conclude that any addition of iodine beyond about one gram per liter of bottle volume (the exact value depending, of course, upon the actual temperature of the wall of the bottle), could not influence the rate and therefore would be pointless in a bottle with isothermal walls.

If the interior wall of the bottle were not essentially

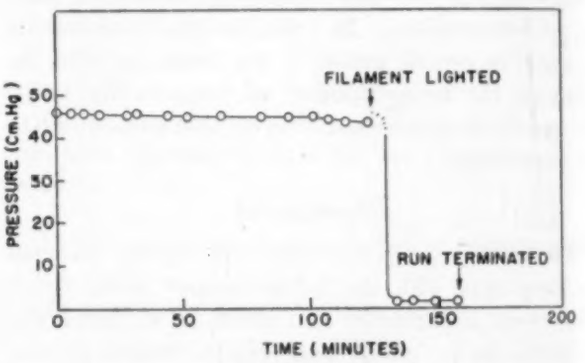

FIG. 4. Cracking run. (Time = 0 when bottle first reaches operating temperature.)

isothermal, zirconium tetraiodide would condense out preferentially on the colder portion and coat it with a layer of the tetraiodide, which would tend to thermally insulate this section. This, in turn, would effect a change in the temperature of the coldest exposed portion of the wall. Since the extent of this change would be dependent upon the actual amount of tetraiodide which condensed, the addition of iodine beyond a gram per liter of bottle volume could, in this case, indirectly produce an effect upon the actual rate of deposition of zirconium.

In view of the facts that most of the iodine is in the form of the tetraiodide and that the rate-determining step in the process is that of gaseous transport, it is at first curious that the iodide process does not proceed at a greater rate. The reason for this is as follows. For every molecule of zirconium tetraiodide which is reduced at the hot surface four atoms of iodine are liberated. These atoms remain unassociated as long as they remain in the hot region which immediately surrounds the filament. Since

the condition of pressure equality throughout the bottle must be fulfilled, it follows that there will be a net flow of molecules away from the filament whenever the process is taking place. This means that for a tetraiodide molecule to reach the hot filament it must proceed against this net flow gradient, i.e., it must, so to speak, swim upstream. With a circularly cylindrical filament it is easily shown from geometric considerations that the magnitude of this gradient increases exponentially as the filament is approached. This screening effect which is thus produced about the hot filament accounts for the observed rate for the process.

Since the rate for the entire cyclic process is determined by the rates of gaseous transport in the neighborhood of the filament, a method which suggests itself for accelerating the process is that of forcibly blowing the gaseous contents of the bottle over the filament. In view of the low pressure involved, however, this may prove to be impractical.

An unanticipated and very interesting result which is obtained from this data is that the synthesis of the zirconium tetraiodide proceeds very slowly before the filament is lit, and rapidly thereafter, i.e., the lighting of the filament enormously accelerates the reaction. Since iodine exhibits a high specific optical absorption in certain spectral regions, the most plausible hypothesis for the mechanism of this phenomenon is that molecules which absorb radiation in some frequency range become sufficiently excited to make them unusually reactive as compared to those molecules possessing only thermal energy. Reactions which proceed in this fashion, the so-called photochemical reactions, are common, particularly when one of the reactants is a halogen. A simple computation shows that between one and two per cent of the energy emitted by the hot filament under ordinary operating conditions is sufficiently energetic to completely dissociate the iodine molecule (D_o = 12,439 cm^{-1}) (6) into atomic iodine, which may well constitute the activated state for the reacting iodine.

However, since these reactive molecules (or atoms) will rapidly lose their excess energy, i.e., be "deactivated," this photo-excitation can only be effective in accelerating the reaction between zirconium and iodine when it takes place in the immediate neighborhood of the feed zirconium. Since the iodine absorbs the exciting radiation whether or not it is in the neighborhood of the feed, one would anticipate that the proximity of the feed material to the filament would be of critical importance in the initiation of the reaction. It would also be expected that as the photochemical synthesis proceeds and free iodine is consumed fewer blanketing iodine molecules would remain between the filament and the feed material so that the reaction would avalanche, i.e., it would be self-accelerating. On this basis one might expect some difficulty to be experienced in initiating the reaction in a case where the feed material is very far removed from the hot filament, which might be the case, say, in a very large de Boer bottle. Such a difficulty, if encountered, could be overcome either by (*a*) introducing the iodine very slowly after the filament is lit, or by (*b*) placing a few small "ignition" filaments near the feed zirconium, and operating them only until the synthesis is substantially complete. The first of these methods would operate by reducing the concentration of the blanketing iodine, and the second would depend upon the proximity of the auxiliary radiators to the crude zirconium.

Summary

A fundamental study of the hot-wire process for the production of ductile zirconium was conducted. Two complementary methods were employed. The first comprised a measurement of the probability that a zirconium tetraiodide molecule will decompose upon striking a hot surface. The second was based upon pressure measurements made in the interior of an operating cracking bottle. The more significant information gained is as follows:

1. The probability that a zirconium tetraiodide molecule decomposes upon impinging once upon a surface at 1300°–1500°C *in vacuo* is nearly unity.
2. The rate-determining step in the hot-wire process, when conducted with feed zirconium which is not appreciably less reactive than crystal bar ends, is the transport of the gaseous reactants.
3. The total amount of free iodine in an operating cracking bottle is very small.
4. The initial synthesis of zirconium tetraiodide in the cracking bottle is catalyzed, in all probability photochemically, by the lighting of the filament.
5. The iodide process could probably be accelerated by forcibly circulating the gases in the cracking bottle.

Any discussion of this paper will appear in a Discussion Section, to be published in the December 1953 issue of the JOURNAL.

REFERENCES

1. A. E. VAN ARKEL, "Reine Metalle," Julius Springer, Berlin (1939).
2. S. W. MELLOR, "A Comprehensive Treatise on Inorganic and Theoretical Chemistry," Vol. VII, pp. 150–1, Longmans Green and Company, New York (1947).
3. O. RAHLFS AND W. FISCHER, *Z. anorg. u. allegm. Chem.*, **211**, 349 (1933).
4. M. KNUDSEN, "The Kinetic Theory of Gases," p. 26, Methuen and Company, Ltd., London (1950).
5. J. H. DE BOER AND J. D. FAST, *Z. anorg. u. allgem. Chem.*, **153**, 2 (1926).
6. A. G. GAYDON, "Dissociation Energies," p. 65, Dover Publications. Inc., New York (1950).

The Electrochemistry of Gallium[1]

WILLIAM M. SALTMAN[2] AND NORMAN H. NACHTRIEB

Institute for the Study of Metals, University of Chicago, Chicago, Illinois

ABSTRACT

Electromotive force measurements were made on cells of the type Ga (s or l)/ $GaX_3 + HX/H_2$ (Pt) where X is chloride or perchlorate at 20°, 25°, 28°, and 35°C, for various gallic ion concentrations at several constant acidities. The standard electrode potential for the gallium-gallic ion electrode in aqueous solution at 25°C is found to be -0.560 ± 0.005 volt. The standard free energy at 25°C was calculated to be $-38{,}800$ cal mole^{-1}. The standard entropy and enthalpy for the cell reaction at 25°C were estimated to be -39.2 cal mole^{-1} deg^{-1} and $-50{,}500$ cal mole^{-1}, respectively.

The liquid gallium electrode behaved in an irreversible manner, but electroplated solid electrodes behaved satisfactorily.

INTRODUCTION

The purpose of this work was to attempt to determine the standard electrode potential, E^0, for the gallium-gallic ion couple:

$$Ga \rightarrow Ga^{+++} + 3e. \qquad (A)$$

Previous attempts (1–4) to measure the potential of cells with gallium electrodes led to results showing considerable variance. Results varied with time, equilibrium was apparently not obtained, and surface films were noted on the electrodes. Von Bergkampf (3), in a brief paper, reported potentials for two cells; from these measurements and with the assumption that the activity coefficients of gallium were equal to those of lanthanum, he calculated the value of E^0 to be -0.52 volts. This is the value generally accepted today. Von Bergkampf mentioned no precautions to exclude air, no corrections for hydrolysis, and no attempts to purify his materials.

Perhaps the most comprehensive work done was by Stelling (4). He found that the potential of gallium amalgam electrodes prepared under hydrogen varied erratically at first but became fairly constant after 2–4 days. In many cases, no steady state was observed and this was attributed to incomplete removal of air from the cells. Mechanical agitation of the electrodes increased the potentials. Using a dropping amalgam electrode he got more constant results. From these potentials Einecke (5) calculated the standard potential for equation (*A*) to be -0.56 volts.

Stelling also found that the potentials suddenly dropped about 300 mv when gallium melted. The potentials remained low as the liquid gallium supercooled until, at about 26°C, the potential rose suddenly to near its original value.

None of the above authors corrected his concentration data for the hydrolysis of the gallium salt. Fricke and Meyring (6) estimated the value of the first hydrolysis constant

$$K_1 = \frac{(GaOH^{++})(H^+)}{(Ga^{+++})} \qquad (B)$$

to be 1.4×10^{-3} at 18°C from *p*H measurements on gallium chloride solutions. More recent measurements (7) indicate a value of 4.03×10^{-3}.

EXPERIMENTAL

The experimental apparatus was conventional. A gas purification and saturation train was used so that gas might be bubbled through the cell arms to remove oxygen or to stir the solution. Tank hydrogen (or nitrogen) was bubbled through potassium permanganate solution and then passed up an oxygen absorption tower similar in design to one described by Meyer and Ronge (8). The gas was then passed through four saturators and then into the cells.

The bath was a 24 x 24 x 28 in. water bath with both cooling and heating arrangements. Temperature control was better than 0.01°C.

The electrical circuit for measuring the potentials was conventionally designed to give a null measurement. The potentiometer was a Leeds and Northrup Type K-2 potentiometer calibrated by the method of Young and Hartsuch (9). Appropriate shielding, grounding, and mechanical rigidity requirements were fulfilled.

Cells

Several types of cell construction were tried. The type used to obtain the data reported below was

[1] Manuscript received March 10, 1952. This paper was prepared for delivery before the Cleveland Meeting, April 19 to 22, 1950. Based on part of a thesis submitted to the Chemistry Department, University of Chicago, in partial fulfillment of the requirements for the degree of doctor of philosophy.

[2] Present address: Julius Hyman and Company, Denver, Colorado.

a three-arm H type with double cross tubes (to allow completely free circulation of gas and solution) and with a tungsten lead sealed into the bottom of each arm (platinum amalgamates with gallium). Each arm also contained an inlet for admission of gas or solution into the cell. In use, the cell held a total volume of 100 ml of solution. In a given experiment, the potential difference between any two of the three gallium electrodes used or between a gallium electrode and the reference electrodes could be measured.

Preparation of Materials

Gallium metal with an estimated initial purity of 99.8 per cent was repurified by the use of the method of Hoffman (10) with some variations. These variations involved the partition of chlorogallic acid between aqueous hydrochloric acid and isopropyl ether to separate gallium from most other elements (11). Analysis showed the final purity to be 99.992 per cent gallium with respect to metallic constituents. The method of analysis has been reported elsewhere (12).

A portion of the purified gallium metal was dissolved in *aqua regia* and the solution evaporated to a syrup four times, after repeated additions of concentrated nitric acid. It was then heated 16 hours at 250°–300°C to form the sesquioxide. The oxide was then dissolved in excess hydrochloric acid and the gallium precipitated as the hydroxide with ammonium hydroxide. The gelatinous precipitate was filtered, washed, and redissolved in slightly more than the calculated amount of hydrochloric acid. The gallium chloride solution was then analyzed for gallium as the oxide and for chloride as silver chloride.

Gallium perchlorate was prepared by addition of a measured small excess of silver perchlorate to the solution of gallium chloride. The excess silver ion was removed by the insertion of a gallium crystal in the solution.

Water and constant-boiling hydrochloric acid used to make up the several solutions were purified by redistillation from a quartz vessel.

Potential Measurements

Measurements made on cells with liquid gallium electrodes gave widely discordant results, and the potentials varied with time in an erratic manner. Since previous investigators (3, 4) had obtained variable results with the use of gallium crystals and amalgams, and in view of the steady potentials derived from the use of electrodeposited indium electrodes (14), we investigated the value of gallium electrodes prepared in this manner. Earlier workers used electrodeposition as a method of recovery of gallium from its solutions and were not generally concerned with the nature of the deposit.

Six tungsten electrodes were plated simultaneously, all connected in parallel. The external circuit consisted of a battery, a variable resistor, and a milliammeter. The anode for the electrolysis cell was made of platinum, since a tungsten anode soon decomposed.

Preliminary experiments showed that gallium was deposited as a gross, dull gray mass from a gallate solution about 0.01 molar in gallium and 2.5*N* in sodium hydroxide after 30 hours at 0.03 amp/cm² and 5 to 6 volts. On microscopic examination, the deposit was seen to consist of myriads of tiny bright crystals. The excess alkali was troublesome to remove, so the deposition in acid solutions was investigated.

At acidities above 1.0*N* hydrochloric acid the gallium did not deposit. In ice water with 0.1*N* acid and 0.002*M* gallium chloride and current densities of 0.03 to 0.45 amp/cm² the deposits were of a fragile tree-like structure. With 0.002*N* acid the electrolysis current soon dropped to zero and the region near the cathode was observed to contain a gelatinous white solid which appeared to be gallium hydroxide.

Good deposits similar to those obtained in alkaline solutions were obtained in solutions about 0.05*N* in hydrochloric acid and 0.003*M* (or greater) gallium chloride. The platinum anode was cut off to a 2-mm length and placed so it dipped below the surface of a liquid gallium pool, effectively forming a gallium anode. Nitrogen was bubbled through the solution. Electrolysis at current densities of 0.013 to 0.033 amp/cm² resulted in gross adherent polycrystalline deposits. When the electrolysis was performed at 28°C or higher, the deposits frequently showed partial melting.

All the electrodes used in these experiments were prepared at 25° or 20°C by electrolysis for 12 to 14 hours. The current was maintained as closely as possible to 15 ma, corresponding to a current density of 0.02 amp/cm². It was not necessary to keep a close check on the acidity. The solution was periodically tested for the presence of platinum and, if platinum was present, the solution was replaced. After one such electrolysis the current efficiency at the cathode was found to be 68.5 per cent.

The electrodeposited electrodes were tested in cells of the type:

$$Ga_{(s)}/GaCl_3 + HCl/H_2(Pt). \qquad (I)$$

Measurements were also made with electrodeposited gallium electrodes in cells of the type:

$$Ga_{(s)}/Ga(ClO_4)_3 + HClO_4/H_2(Pt). \qquad (II)$$

The following observations were made with regard to their behavior. (*a*) In solutions where the hydro-

chloric acid concentration was above 0.1*N*, a slow but steady evolution of gas from the electrode surface took place. In solutions below 0.05*N* acid, no gas evolution was observed. (*b*) The potentiometer null adjustment was easily made to about 0.03 mv. Readings were steady and reversible in the sense that the null setting could be approached from either side. (*c*) The potentials reached a constant value in 2 to 5 hours and maintained this steady state for from 2 to 12 hours. (*d*) The cell potentials generally exhibited an initial rise, leveled off, and then began a steady fall. (*e*) The average deviation from the mean steady state potential of three electrodes prepared and tested in the same solution was about 4 to 6 mv. (*f*) The average potentials of two sets of three electrodes prepared at different times and tested in the solution differed by less than the deviation within either set, i.e., the electrode preparation was generally reproducible. (*g*) Out of 223 electrodes prepared under the standard conditions, readings from 28 were rejected. (*h*) The potentials attained were independent of whether or not hydrogen bubbled over the gallium electrode. A temporary change occurred, but the potential soon returned to near its original value. This effect is discussed more fully below.

Concentration Series

Four series of experiments were performed, each with an approximately constant acid molality and varying gallic ion molalities. Three were in approximately 0.005, 0.01, and 0.03 molal hydrochloric acid. The fourth was in 0.025*M* perchloric acid. The three hydrochloric acid series were run at 20°, 25°, and 28°C. The perchloric acid series was run only at 25°C.

Three gallium electrodes were used for each experiment. The potentials reported are the averages for the three electrodes. Precautions were taken to exclude air and, at the end of an experiment, samples were taken for analysis and density determination. They were analyzed for gallium by the 8-hydroxyquinoline method, and for chloride gravimetrically as silver chloride. The perchlorate samples were titrated with standard base.

The precision of the measurements was too poor to permit any good assessment of the temperature coefficient of the potential. Whenever the stability of a set of electrodes permitted, they would be retained in the cell while the thermostat temperature was either raised or lowered. The solution was then allowed to reach equilibrium again. In this way several scattered measurements of the temperature coefficients were made.

Calculations and Results[3]

The first hydrolysis constants given in Reference (7) were recalculated with the use of the more rigorous equation:

$$K_1 = \frac{(GaOH^{++})(H^+)}{Ga^{+++})_s - (GaOH^{++})} \qquad (III)$$

where $(Ga^{+++})_s$ represents the stoichiometric gallic ion concentration. The calculated values range from 2.57×10^{-4} to 26.90×10^{-4} and averaged 5.83×10^{-4}. This last value was used to calculate the amount of hydrolysis of the various solutions used in this work. The difference between molarities and molalities as well as between molarities and activities was neglected in this calculation. The effect of further hydrolysis as well as complex formation (e.g., $GaCl^{++}$, etc.) was also neglected.

For a cell of type (I) where the reaction is $Ga + 3HCl \rightarrow GaCl_3 + \frac{3}{2}H_2$ the fundamental electrochemical equation leads to an expression:

$$E^{0\prime} = E - \frac{RT}{3F} \ln \frac{(M_{Ga^{+++}})}{(M_{H^+})^3}$$

$$= E^0 + \frac{RT}{3F} \ln \frac{(\gamma\pm)^4_{GaCl_3}}{(\gamma\pm)^6_{HCl}}$$

where $E^{0\prime}$ is, by definition, equal to the two expressions which follow; E is the observed cell potential (corrected to one atmosphere hydrogen pressure); M is the molality of the designated ion; E^0 is the standard potential of the gallium-gallic ion couple; and $\gamma\pm$ is the mean activity coefficient of the designated compound. A similar expression holds for cells of type (II).

If the second equality is plotted[4] against the square root of the ionic strength, the intercept at zero ionic strength is E^0.

The data were used to calculate best fitting linear equations of the form $-E^{0\prime} = a_0 + a_1\sqrt{\mu}$ by the method of least squares. Table I (columns 3 and 4) lists the coefficients a_0 and a_1 for the several equations. The standard error of estimate of the linear equation is given in column 5. The average of the standard errors is ±0.004 volts.

[3] For analytical results, densities, calculated $(GaOH^{++})$ concentration, corrected gallic ion and hydrogen ion concentrations, and the ionic strength, μ, order Document 3857 from American Documentation Institute, 1719 N Street, N. W., Washington 6, D. C., remitting $1.00 for microfilm (images 1 in. high on standard 35 mm picture film) or $1.35 for photocopies (6 in. x 8 in.), readable without optical aid.

[4] The data required for such plots have been microfilmed and are available from the American Documentation Institute, 1719 N Street, N. W., Washington 6, D. C. Order Document 3857, remitting $1.00 for microfilm or $1.35 for photocopies.

The values of a_0 are, of course, identical with the standard potential $-E^0$. Since these E^0 values, although at infinite dilution with respect to gallium, refer to various constant acidities, they were used together with the averages of the corrected acid concentrations to construct lines fitted by the least squares method. The constant term in each of these isothermal lines corresponds to a value (E'^{00}) which refers to zero gallic ion and zero acid concentrations.

The values of E'^{00} found for the three temperatures are listed in Table II along with the standard error of estimate. The values of the standard free energy $\Delta F'^{00}$ in cal/gram mole are also listed.

TABLE I. *Coefficients and standard error of estimate of least squares equations*

Acid series	Temp (°C)	a_0 (= $-E^0$) (volts)	a_1	Error of estimate (volts)
0.005 HCl	20	0.5459	+.02524	0.0050
	25	0.5467	+.02545	0.0032
	28	0.5411	+.06520	0.0064
0.01 HCl	20	0.5552	−.004077	0.0043
	25	0.5512	+.01098	0.0027
	28	0.5475	+.02061	0.0047
0.03 HCl	20	0.5241	+.02274	0.0053
	25	0.5182	+.04760	0.0047
	28	0.5192	+.05126	0.0038
0.025 $HClO_4$	25	0.5177	+.07331	0.0020

TABLE II. *Standard potential and free energy at infinite dilution*

Temp (°C)	$-E'^{00}$ (volts)	Error of estimate (volts)	$-\Delta F'^{00}$ (cal/mole)
20	0.599	±.006	38,700
25	0.560	±.005	38,800
28	0.553	±.005	38,300

TABLE III. *Activity coefficients*, $\gamma \pm GaCl_3$

μ	$\gamma \pm$ HCl	$\gamma \pm GaCl_3$	$\gamma \pm La(NO_3)_3$
0.10	0.906	0.800	0.772
0.15	0.873	0.729	0.688
0.20	0.844	0.668	0.620
0.25	0.821	0.617	0.563
0.30	0.803	0.575	0.523
0.35	0.791	0.542	0.497

The least squares linear equation for the 0.005M acid series at 25°C was used to calculate the mean activity coefficients for $GaCl_3$. Use was made of values for $\gamma \pm$ HCl interpolated from the data of MacInnes (15). Table III presents the calculated values and, for comparison, the activity coefficients of lanthanum nitrate interpolated from data given by Lewis and Randall (16).

The experiments to determine a temperature coefficient of the potentials allow only a rough estimation of its value. In every case where the bath temperature was raised, the potentials fell. When the bath temperature was lowered, the potentials of 30 out of a total of 53 electrodes increased in value. There appeared to be no correlation between increase in potential and acidity or gallic ion concentration. Nevertheless, since the potential trend was counter to what would be expected if the electrodes were simply deteriorating, this change was assumed to give a rough indication of the temperature coefficient. The over-all average of these changes was 0.566 mv degree^{-1}, corresponding to an entropy change for the reaction represented by cell (I) of −39.2 cal mole^{-1} degree^{-1}. This value can be compared with Latimer's estimate (17) of "at most, −50" in the infinitely dilute solution and with von Bergkampf's (3) value of −23.2 calculated from the heat of solution in 9N hydrochloric acid. If our entropy difference is assumed to be the standard entropy difference, the enthalpy, $\Delta H'^{00}$ at 25°C is −50,500 cal/mole.

Discussion

The analytical errors are small compared to the variability in the electrodes. In all but the most dilute solution the precision of the gallium analyses was better than 1.0 per cent. In the most dilute solution (0.000860M) the precision was 2.0 per cent. The chloride analysis errors averaged about 0.1 per cent and the perchlorate analysis errors about 1 per cent. These errors are not serious in the determination of E'^{0} since the analytical results enter only in the logarithmic term.

Gallium did not appear to be dissolving from the electrode into the solutions since the analytical results agreed fairly well with the calculated dilutions. Furthermore, inspection of the Nernst equation showed that the potential should fall if gallium were being dissolved.

If the gallium electrode were acting in part as a hydrogen electrode, the potentials would also be influenced. When a platinum wire was touched to a gallium electrode, the cell potential immediately fell to practically zero. The effect of the passage of hydrogen over the electrode varied with both gallic ion and acid concentrations. The higher the acid concentration and the lower the gallic ion concentration, the greater the potential rise on interruption of the hydrogen stream, or the potential fall on start of a hydrogen stream. In the 0.005M acid series, the potential rise on interruption of the gas stream averaged 1.9 mv. In the 0.03M acid series it ranged from 0.9 mv in the most concentrated gallic ion solution to 5.9 mv in the most dilute. These observations indicate that the gallium electrode was act-

ing to a minor extent as a hydrogen electrode, too. The potentials in the lower acid concentrations are more indicative of the true equilibrium potential of the gallium-gallic ion couple. The data presented in the previous section were, of course, obtained without passage of a gas stream over the gallium electrode.

The liquid electrodes showed considerable evidence of passivity, but the general trend of potentials shown by the solid plated electrodes was what might be expected from a reversible type of electrode. Previous investigators used crystals which must be prepared by supercooling the liquid (sometimes as much as 20°). It was recently reported (18) that a small transition in crystal form occurs at 18.9°C. This might well lead to strain in the crystal lattice and thus to potentials different from those found in this work. It has also been shown by Lewis (19) that while massive silver electrodes differed widely in their potential, electrodes prepared by electrolysis gave reproducible values.

Acknowledgment

The authors wish to thank the Aluminum Company of America for the gift of gallium used in some of the experiments.

Any discussion of this paper will appear in a Discussion Section, to be published in the December 1953 issue of the JOURNAL.

REFERENCES

1. J. REGNAULD, *Compt. rend.*, **86**, 577 (1878).
2. W. RICHARDS AND S. BOYER, *J. Am. Chem. Soc.*, **43**, 274 (1921).
3. S. VON BERGKAMPF, *Z. Elektrochem.*, **38**, 847 (1932).
4. O. STELLING, *Z. Elektrochem.*, **41**, 712 (1935).
5. E. EINECKE, "Das Gallium," p. 50, Leopold Voss, Leipzig (1937). Lithoprinted by Edwards Brothers, Inc., Ann Arbor, Mich. (1944).
6. R. FRICKE AND K. MEYRING, *Z. anorg. u. allgem. Chem.*, **177**, 325 (1928).
7. Office of Naval Research Contract 6N-ori-71, Chemistry Task XVII, University of Illinois Bimonthly Report No. 5.
8. F. R. MEYER AND G. RONGE, *Z. angew. Chem.*, **52**, 637 (1939).
9. T. F. YOUNG AND P. J. HAKTSUCH, "A Rapid and Precise Method for Calibration of Two Similar Potentiometers," University of Chicago; unpublished.
10. J. I. HOFFMAN, *J. Research Natl. Bur. Standards*, **13**, 665 (1934).
11. R. E. FRYXELL AND N. H. NACHTRIEB, *J. Am. Chem. Soc.*, **71**, 4035 (1949).
12. W. M. SALTMAN AND N. H. NACHTRIEB, *Anal. Chem.*, **23**, 1503 (1951).
13. F. DANIELS, J. H. MATHEWS, AND J. W. WILLIAMS, "Experimental Physical Chemistry," p. 195, McGraw-Hill Book Co., New York (1941).
14. E. M. HATTOX AND T. DEVRIES, *J. Am. Chem. Soc.*, **58**, 2126 (1936).
15. D. A. MACINNES, "The Principles of Electrochemistry," p. 167, Reinhold Publishing Corp., New York (1939).
16. G. N. LEWIS AND M. RANDALL, "Thermodynamics," p. 378, McGraw-Hill Book Co., New York (1923).
17. W. M. LATIMER, "Oxidation Potentials," p. 148, Prentice Hall, Inc., New York (1938).
18. E. C. KERR, G. B. ADAMS, N. C. HALLETT, AND H. L. JOHNSTON, Paper presented at 116th Meeting of American Chemical Society, September, 1949.
19. G. N. LEWIS, *J. Am. Chem. Soc.*, **28**, 158 (1906).

Electrodeposition Behavior of Cadmium and of Thallium at Mercury Cathodes[1]

L. B. Rogers and Charles Merritt, Jr.

Department of Chemistry and Laboratory for Nuclear Science and Engineering, Massachusetts Institute of Technology, Cambridge, Massachusetts

ABSTRACT

The deposition behavior from approximately millimolar solutions of thallium (I) and cadmium at a mercury cathode can be predicted from polarographic data within 10 mv. The variations in the deposition at a particular potential were usually smaller than that corresponding to ±5 mv when using instruments with control limits of about ±3 mv. The presence of about 0.02*F* copper or bismuth in the mercury appeared to have no effect on the deposition behavior of cadmium. During the course of this study, several incidental observations of practical importance were noted.

Introduction

The increased interest in controlled potential electrolysis made it desirable to examine more completely the applicability of polarographic data for predicting electrodeposition behavior (1) and to determine the experimental reproducibility of depositions performed with a suitable instrument. If experimental factors appreciably broadened the limits beyond those inherent in the instrument, the decrease in reproducibility would limit ones ability to separate elements having nearly the same deposition behavior (2). Thallium was selected as the first element to study because the amount deposited at a given potential for a one-electron reaction is least susceptible to variations in cathode potential. The results obtained with thallium encouraged the extension of the study to cadmium.

It is also important to know what effect, if any, the presence of one element in the mercury has on the deposition behavior of the second. Preliminary experiments were therefore carried out to test the effect of copper and bismuth in the mercury on the deposition behavior of cadmium. Cadmium was arbitrarily selected for this portion of the study.

Experimental

Apparatus.—The regulators for controlling the potential of the cathode were a line-operated unit of the type described by Lamphere (3) and a battery-operated regulator (4) both of which hold a preset potential constant to about ±3 mv. A portable Rubicon potentiometer having a range up to 1.6 volts, was connected across the reference half-cell and the cathode to adjust and measure the cathode potential to the closest millivolt. The potentiometer was also used to check the initial and final potentials of polarographic curves obtained with the Sargent Model XXI recording polarograph.

Measurements of *p*H were made with a Beckman Model G *p*H meter. Resistances of the salt bridges and polarographic cells were measured by means of a conductance bridge, Model RC-1B of Industrial Instruments, Inc.

The electrolytic cell shown in Fig. 1 consisted of a beaker fitted with a rubber stopper containing appropriate holes to receive the electrodes, stirrer, gas dispersion tube, and sampling tube. Electrical contact with the mercury cathode was made directly by means of a platinum wire sealed into glass. An "external" anode, a platinum wire, was placed in a saturated solution of potassium sulfate connected through an agar salt bridge, saturated with potassium chloride, to a vessel containing a saturated solution of potassium chloride which in turn was connected to the electrolytic solution by another agar salt bridge saturated with potassium chloride. A saturated calomel electrode (S.C.E.) was used as a reference half-cell and was also connected to the electrolytic solution by means of an agar bridge saturated with potassium chloride. The use of fritted glass dispersion tubes prevented contamination of the electrolytic solution with agar gel without unduly increasing the resistance of the cell. By using Tygon tubing for the major portion of the bridge, greater flexibility and ease of handling resulted. Because of the high currents drawn, an "internal" platinum anode was used only during the separations of copper and bismuth.

A motor-driven stirrer was constructed to permit simultaneous stirring of both the mercury and the solution. Deaeration of the solution prior to and during electrolysis was accomplished by passing

[1] Manuscript received May 2, 1952. This paper was prepared for delivery before the Philadelphia Meeting, May 4 to 8, 1952.

nitrogen through a solution of 0.1*F* hydrochloric acid and then through a fritted glass dispersion tube immersed in the solution.

Reagents.—Solutions were prepared from reagent-grade chemicals and distilled water. A stock solution of approximately 0.004*F* thallium (5) was prepared by saturating 0.1*F* hydrochloric acid with thallium (I) chloride and then decanting from the excess solid. The stock solution of cadmium was prepared by dissolving the required weight of cadmium oxide in enough hydrochloric acid to make the solution 0.05*F* in cadmium and 0.1*F* in hydrochloric acid. Solutions were prepared for electrolysis by ten-fold dilution with 0.1*F* hydrochloric acid to make the final concentration 0.005*F* in cadmium.

The copper-cadmium and bismuth-cadmium solutions were prepared from the required weight of the

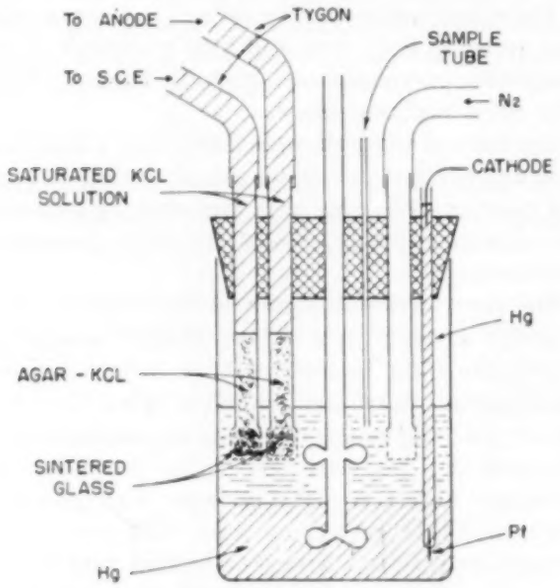

FIG. 1. Electrolytic cell

cupric or bismuth chloride and a suitable aliquot of the cadmium stock solution by dilution with 0.1*F* hydrochloric acid solution to make the final concentrations 0.02*F* in copper or bismuth and 0.005*F* in cadmium. In the case of bismuth, the bismuth chloride dissolved, but later reprecipitated as a milky suspension of the oxychloride. A well-shaken sample of this suspension was used in the electrolytic experiment.

Polarographic procedures.—The diffusion current (i_d) for each solution was determined prior to electrolysis. By measuring the i_d after electrolysis, one could calculate the distribution of the element between the two phases.

The determination of the values for $E_{\frac{1}{4}}$ of each element was made from appropriate polarograms taken with a total span of 0.5 volt on the slidewire. The initial and final voltages were determined to ±0.1 mv with a potentiometer. The observed $E_{\frac{1}{4}}$ was always corrected for *IR* drop.

Electrolytic procedures.—Depositions from known volumes of solution into a known volume of mercury (usually a total volume of 200 ml) were carried out at various potentials until equilibrium was reached. Using about a 20 ml sample which had been withdrawn through the sampling tube into a pipet, each solution was analyzed polarographically for thallium or cadmium to determine the percentage of the element remaining in solution. The sample was returned to the electrolytic cell after each polarogram so that an electrolysis at a new potential could be made without concern for changes in volume. By maintaining the potential on the cathode during the analysis of each sample, dissolution of any metal from the mercury could be prevented and the time required to reach equilibrium at a more negative potential decreased. The time required to reach equilibrium was different at each volume ratio and was determined by making a polarographic analysis at fixed time intervals until a constant value for the polarographic diffusion current was reached.

Several points on the deposition curve for a 1:1 volume ratio were determined by successive electrolyses at various potentials. For volume ratios other than 1:1, only a single electrolysis was performed at an appropriate potential. In all cases the value for the potential at which half of the element was in the mercury ($E_{50\%}$) was calculated by means of the Nernst equation (2) from the value of the percentage of the element remaining in the aqueous phase.

The solutions containing copper or bismuth together with cadmium were first electrolyzed at a potential sufficiently negative to deposit only the copper or bismuth and to leave the cadmium in solution.[2] When essentially all of the copper or bismuth had been deposited, the potential was made more negative and the $E_{50\%}$ for cadmium determined.

No attempt was made to control the room temperature which was approximately 27°C during most of the runs. Since only very small currents passed through the electrolytic cell, there was no appreciable heating effect on the solution.

RESULTS

Thallium.—The $E_{\frac{1}{4}}$ for thallous ion in 0.1*F* hydrochloric acid was found to be −0.461 volt vs. S.C.E. which agrees within the estimated experimental

[2] Polarograms taken of the copper-cadmium and bismuth-cadmium solutions after electrolysis at the first potential were used to determine when all of the copper or bismuth had been plated out and gave, at the same time, a reference i_d to use for the cadmium analysis. The values of i_d obtained were the same, within the limits of error, as those obtained for solutions of cadmium alone thereby

error with the value of −0.460 in the literature (6). As shown in Table I, an $E_{50\%}$ of −0.464 volt vs. S.C.E. was obtained for a volume ratio of 1:1 which also agrees well[3] with the $E_{\frac{1}{4}}$.

The reversibility of the thallium amalgam system was tested by allowing essentially complete deposition (about 99%) followed by dissolution of some thallium at an applied potential of −0.455 volt vs. S.C.E. At equilibrium 56.5 per cent of the metal ion was found in solution giving a calculated value for $E_{50\%}$ of −0.462 volt which agrees with the deposition result.

In view of the suggestion (2) that certain separations should be facilitated by using ratios of phases other than 1:1, experiments were run to check the shift of $E_{50\%}$ when the ratio of the volumes of mercury and solution are changed. The results, which are

TABLE I. *Deposition of thallium from 100 ml of 0.1F hydrochloric acid into 100 ml of mercury*

Applied potential ± 0.003 v (v vs. S.C.E.)	Percentage of thallium in aqueous phase	E_{50} per cent calc. (v vs.S.C.E.)
−0.390	93.5	−0.460
−0.410	88.7	−0.464
−0.430	79.5	−0.465
−0.450	63.7	−0.465
−0.470	42.8	−0.463
−0.490	22.5	−0.468
−0.510	10.5	−0.454
−0.530	8.1	−0.467

Mean = −0.464 ± 0.003 v[3]

TABLE II. *Effect on $E_{50\%}$ of using different volume ratios of mercury to aqueous phase*

Volumes of phases	Applied potential ± 0.003 v (v vs. S.C.E.)	Percentage of thallium in aqueous phase	E_{50} per cent (v vs. S.C.E.)	
			Found	Calc.*
150 ml mercury 50 ml aqueous	−0.430	57.0	−0.437	−0.435
50 ml mercury 150 ml aqueous	−0.510	36.2	−0.495	−0.493

* $E_{50\%}$ calculated from the $E_{50\%}$ for a ratio of 1:1.

summarized in Table II, are in good agreement with theory.

Cadmium.—An $E_{\frac{1}{4}}$ of −0.606 volt vs. S.C.E. for cadmium ion in 0.1*F* hydrochloric acid was obtained in the present study, and it agrees satisfactorily with the literature value of −0.599 volt (6). As shown in Table III, the $E_{\frac{1}{4}}$ agrees with $E_{50\%}$ within the assigned limits of error.[4]

When equilibrium was approached by dissolution from mercury for 8 hours, 31.8 per cent of the metal was found in the solution at an applied potential of −0.620 volt vs. S.C.E. This gave a calculated value for $E_{50\%}$ of −0.611 volt which shows that the cadmium system, as expected, is also reversible.

The shift of $E_{50\%}$ for the cadmium solutions for volume ratios other than 1:1 and the effect of copper and bismuth are summarized in Tables IV and V.

TABLE III. *Deposition of cadmium from 100 ml of 0.1F hydrochloric acid into 100 ml of mercury after 8 hours*

Applied potential ± 0.003 v (v vs. S.C.E.)	Percentage of cadmium in aqueous phase	E_{50} per cent (v vs. S.C.E.)
−0.605	60.4	−0.611
−0.600	69.4	−0.610
−0.616	48.2	−0.615
−0.630	19.0	−0.611

Mean = −0.612 ± 0.003 v.

TABLE IV. *Effect on $E_{50\%}$ of using different volume ratios of mercury to aqueous phase*

Volumes of phases	Applied potential ± 0.003 v (v vs. S.C.E.)	Percentage of cadmium in aqueous phase	E_{50} per cent (v vs. S.C.E.)	
			Calc.	Found
150 ml mercury 50 ml aqueous	−0.580	60.5	−0.586	−0.586
50 ml mercury 150 ml aqueous	−0.640	22.5	−0.624	−0.624

TABLE V. *Effect on the $E_{50\%}$ of cadmium of other metals deposited in mercury using 75 ml each of mercury and −0.1F hydrochloric acid*

Metal present	Potential (v vs. S.C.E.) applied to deposit		Percentage of cadmium in aqueous phase	E_{50} per cent (v vs. S.C.E.)	
	First element	Cadmium		This expt.	From Table III
Copper	−0.4	−0.628	23.6	−0.613	−0.612
Bismuth	−0.2	−0.620	42.2	−0.616	−0.612

Discussion

In general, the results indicate that, if an instrument is used which is inherently capable of controlling the potential to ±3 mv, an over-all experimental error of the same size can be attained. The present study also indicates that the position of the deposition wave can be predicted closely from polarography and that its exact position can be pre-

indicating that essentially no cadmium was deposited during the deposition of copper or bismuth.

[3] The limits of uncertainty are expressed in terms of a probability of 90 per cent in accordance with the recommendations set forth in ASTM Manual on the Presentation of Data, Supplement A, American Society for Testing Materials, Philadelphia (1940).

[4] Kolthoff and Lingane (6) have given the limits of uncertainty of $E_{\frac{1}{4}}$ for cadmium in 0.1*F* chloride solution as −0.599 ± 0.005 volt. The limits for the experimental value given here are also ±0.005 volt for a probability of 99 per cent.

dicted from a knowledge of the volumes of the two phases.

Although these studies involving prior deposition of copper or bismuth into the mercury showed no effect of the presence of these elements on the deposition behavior of cadmium, the limited amount of data does not rule out the possibility of finding effects under extreme conditions, i.e., high concentrations of copper or bismuth in the mercury during the deposition of a small amount of cadmium. Certainly the data cannot be extrapolated to other systems although it is encouraging to find that interference may not always be found.

Although it has been known that elements deposit at different rates, it was interesting to observe that the rate of attainment of equilibrium was very much slower with cadmium than with thallium. In contrast to the time of 3 hours for thallium, 9 hours were required for cadmium to attain equilibrium at a 1:1 volume ratio. If constant times of electrolysis are used which fail to allow for equilibrium to be established, a deposition curve can be obtained with nearly the same limits of experimental error as the curve obtained under equilibrium conditions but with an appreciably different value for $E_{50\%}$. Such a case is given in Table VI for which the electrolysis time was two hours.[5] Furthermore, it is important to note the pronounced effect of the volume ratio on the time required to reach equilibrium. In depositing cadmium at volume ratios of 1:3 and 3:1, the time was 29 hours compared to 9 hours for the 1:1 ratio. This can be attributed in part to the fact that a single stirrer of the type used in these experiments cannot stir both phases efficiently if the volumes are very different, i.e., the solution phase was poorly stirred when its volume was large whereas a large volume of mercury noticeably slowed down the stirrer. The use of a separate stirrer for each phase should minimize this difficulty.

TABLE VI. *Deposition of cadmium from 100 ml of 0.1F hydrochloric acid into 100 ml of mercury after 2 hours*

Applied potential ± 0.003 v (v vs. S.C.E.)	Percentage of cadmium in aqueous phase	$E_{1\%}$ per cent (v vs. S.C.E.)
−0.580	92.1	−0.612
−0.600	80.0	−0.618
−0.620	59.7	−0.625
−0.640	25.1	−0.626
−0.660	6.9	−0.626
−0.680	1.2	−0.623

Mean = −0.621 v ± 0.005 v.

During the early runs, it was found that hydrogen peroxide produced by reduction of dissolved oxygen in the solutions made it impossible to measure the polarographic diffusion currents of cadmium and thallium. After providing for deaeration of the solutions no further difficulty was encountered. The fact that other workers (7) have generally used an internal platinum anode, which probably causes catalytic decomposition of hydrogen peroxide, may account for the fact that no previous reports of the interference of hydrogen peroxide have been given.

It was found that the polarograms of thallous ion before electrolysis showed a slight maximum. Since this maximum did not appear in polarograms on electrolyzed solutions, it was obviously due to the presence, initially, of some reducible impurity, probably traces of oxygen. By electrolysis at a potential of −0.3 v vs. S.C.E. where less than 1 per cent of the thallium was deposited, the maximum was successfully eliminated so that a flat plateau could be obtained for the reference point of 0.0 per cent deposited.

A determination of *p*H before and after electrolysis showed no change and it was concluded that there was essentially no appreciable discharge of hydrogen from the acidic solutions of either thallium or cadmium.

Summary and Conclusions

From the depositions of thallium and cadmium into mercury at controlled potentials, one can conclude that the $E_{50\%}$ values for reversible half-cell reactions involving elements soluble in mercury is essentially equal to the polarographic half-wave potential when the volumes of mercury and aqueous phase are the same. For the two cases studied it has been shown that the prior separation of copper or bismuth effects no change in the value of $E_{50\%}$ for cadmium. The position of the deposition wave will be shifted by the value $\frac{.06}{n} \log \frac{V_{Hg}}{V_{sol'n}}$ [in accordance with predictions (2) from the Nernst equation] when the relative volumes of mercury and solution are different from 1:1. If complete separation is to be achieved, one must electrolyze for a much longer time than anticipated in order to insure attainment of equilibrium whenever the volume ratio differs appreciably from unity.

Acknowledgment

The authors are indebted to the Atomic Energy Commission for partial support of this study.

[5] A less striking case is presented in Table III where the time of eight hours allowed for the electrolysis gives a value for the amount of element remaining in solution which is only 99 per cent of the equilibrium value. Therefore the resulting value for $E_{1\%}$ will be slightly more negative than the $E_{1\%}$ at equilibrium.

Any discussion of this paper will appear in a Discussion Section, to be published in the December 1953 issue of the JOURNAL.

REFERENCES

1. J. J. LINGANE, *Ind. Eng. Chem., Anal. Ed.*, **16**, 147 (1944).
2. L. B. ROGERS, *J. Electrochem. Soc.*, **99**, 267 (1952).
3. R. W. LAMPHERE, *Anal. Chem.*, **23**, 258 (1951).
4. R. W. LAMPHERE AND L. B. ROGERS, *Anal. Chem.*, **22**, 463 (1950).
5. A. SEIDELL, "Solubilities of Inorganic and Metal Organic Compounds," 3rd ed., Vol. I, p. 1545, D. Van Nostrand Company, New York (1940).
6. I. M. KOLTHOFF AND J. J. LINGANE, "Polarography," Interscience Publishing Company, Inc., New York (1946).
7. J. J. LINGANE, private communication.

A New Electrochemical Process for Indium[1]

J. R. Mills, B. G. Hunt, and G. H. Turner

Research and Development Division, The Consolidated Mining and Smelting Company of Canada, Limited, Trail, British Columbia

ABSTRACT

Metallurgical operations on products containing indium result in its concentration in a slag containing 2.5 per cent In. This slag is reduced electrothermically to produce a bullion containing lead, tin, indium, and antimony. This bullion is treated electrolytically by a modification of the Betts process to yield a lead-tin alloy cathode and a high-indium (30–35%) anode slime. The anode slime is treated chemically to give a crude (99%) indium metal, which is refined electrolytically. The properties and uses of indium are discussed.

Introduction

The widespread association of indium with zinc blende is the general basis for the commercial recovery of this element, which is obtained as a by-product of zinc reduction. In the electrolytic process which is used at Trail, B.C., the indium remains with the iron content of the zinc concentrates through the roasting and leaching operations. Leaching plant residues containing this iron and indium are transferred to the adjacent lead smelter for the recovery of the contained lead and residual zinc values. In the lead blast furnaces the indium becomes divided between the slag and the lead bullion in roughly equal proportions. The indium content of the slag is removed along with the zinc in the slag fuming furnaces. The zinc oxide fume is treated in a separate leaching plant, residues from which are returned to the lead smelter along with the residues from the leaching plant treating the primary zinc calcine.

Earlier efforts to recover indium were based on the treatment of this zinc oxide fume by extraction with H_2SO_4, followed by the precipitation of a crude indium sludge containing 10 to 20 per cent In by neutralizing with Na_2CO_3. A similar method has been used by other producers of indium.

The indium content of the lead bullion reports almost quantitatively in the dross which separates from the lead before the casting of the latter into anodes for electrolytic refining. Since the indium-containing residues from the leaching of the zinc oxide fume are recirculated to the lead smelter, this dross provides an eventual outlet for practically all of the indium entering the operations. Customary treatment of this dross is a reverberatory liquation which yields the typical copper matte and speiss, along with a slag. This slag, as recovered in normal operations, contains 2.5 to 3.0 per cent In and 4 to 5 per cent Sn. This is the highest concentration of indium encountered in the Trail operations. For this reason the economic recovery of the metal from this source seemed promising, particularly if a process by which the lead and tin contents could be recovered simultaneously were found. Potential production of indium is approximately one million ounces (35 tons) per year from current operations while stockpiled by-products contain an additional reserve of some 10 million ounces. Fig. 1 shows the movement of indium through the Trail lead and zinc reduction plants.

[1] Manuscript received August 12, 1952. This paper was prepared for delivery before the Montreal Meeting, October 26 to 30, 1952.

Production of Indium

Electric Furnace Reduction of Indium-Bearing Slag

Slag resulting from dross treatment contains sufficient copper to make a preliminary copper separation advantageous. (See Table I.) Flotation is employed to remove the bulk of the copper as a saleable copper concentrate. This leaves the indium, tin, and lead in a finely divided tailings product as a wet filter cake. This material is processed to a suitable furnace feed by drying and sintering in a rotary kiln. The accompanying flowsheet (Fig. 2) shows the flow of indium from the above stage through to refined metal.

The smelting equipment consists of an electric furnace and its auxiliary gas and fume recovery system. The furnace is a shaft type of rectangular shape. There is a steel plate shell lined with fire brick which is in turn lined with carbon paste baked into position. Power is supplied to the furnace by a single phase transformer through two vertically suspended graphite electrodes. The rated power input is 75 kw at about 50 volts and 1500 amperes. There are two tapholes, the higher one for tapping slag and the lower one for removing metal or slag or for draining the furnace. Gases and fume are withdrawn from the furnace, mixed with air and burned in a combustion chamber, then cooled and passed through a baghouse unit for dust recovery.

The furnace charge is prepared by mixing each

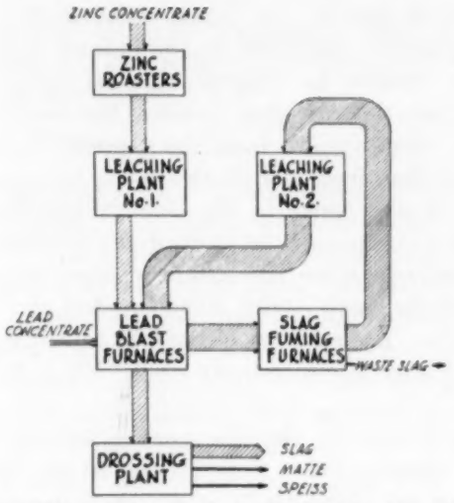

FIG. 1. Flow of indium through Trail lead and zinc reduction plants.

to the furnace and smelting continued until the reactions are completed as established by previous experience. The melt is then tapped out into a cast steel pot where the slag and metal constituents separate before freezing. When cold, the button is broken and the slag separated and discarded. The metallics are reheated in a melting pot, allowing separation of a speiss from the lead-tin-indium bullion. The melting point of the speiss is sufficiently high to prevent its melting and it is returned to the lead smelter. The bullion is allowed to cool to near its melting point, whereupon a soft crust collects on the surface and is removed by skimming. These skimmings contain appreciable indium and are recycled to the electric smelting furnace. The final bullion obtained after removing the skimmings contains about 80 per cent Pb, 4–5 per cent In, 10 per cent Sn, and 4–5 per cent Sb and is cast into suitable anodes for subsequent steps.

TABLE I. *Typical analyses of materials*

	Pb %	Cu %	Sn %	In %	As %	Sb %	Fe %	Zn %	S %	CaO %	SiO_2 %
Dross retreatment slag...	35.0	5.5	4.4	2.5	2.0	1.8	10.7	5.4	1.1	2.5	13.8
Sintered tailings.....	32.0	1.9	4.8	2.7	2.1	1.9	11.5	5.8	0.6	2.7	14.9
Bullion.....	78.0	0.8	10.0	4.6	0.2	4.3	<0.1	—	—	—	—
Slag.....	0.6	0.2	0.3	0.2	0.1	0.1	13.4	1.5	0.5	23.2	36.8
Speiss.....	6.5	6.2	6.2	1.7	13.7	2.9	49.6	1.5	—	—	—
Fume.....	37.8	—	2.8	3.1	3.9	0.5	0.6	29.8	1.5	0.3	1.4

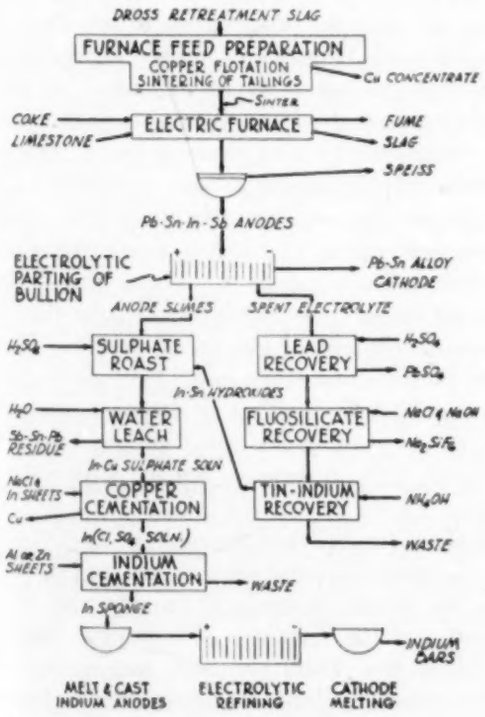

FIG. 2. Flowsheet of indium recovery process

100 lb of sinter with 17 lb limestone as a flux, and 8 lb coke as a reducing agent.

The operation as conducted at present is essentially batchwise. A batch of mixed feed is charged

The indium and tin are not readily reduced, so in order to obtain a slag acceptably low in both these metals, it was found necessary to carry the smelting temperature of each batch up to 2700°–2900°F (1480°–1590°C) before tapping the batch from the furnace. This type of operation, carried out on a relatively small scale and requiring such temperatures, can only be successfully accomplished by the use of an electric furnace. Under these conditions the major part of the indium and tin appear in the lead bullion where they are amenable to further treatment.

Some indium, tin, and lead together with most of the zinc are evolved from the furnace as a fume. This is burned to the oxide, collected in a baghouse, and recycled to the furnace until the zinc builds up to about 40 per cent when it begins to give trouble by causing excessive furnace blows. This high zinc fume is then removed from the circuit and the cycle repeated.

The speiss largely results from the reduction of part of the iron in the feed due to the prevailing reducing conditions and high temperatures. The iron forms the major constituent of an alloy containing arsenic, lead, tin, copper, antimony, and indium. Unless care is exercised, an excessive amount of indium appears in this speiss, lowering the recovery.

However, this indium is not necessarily lost as the speiss is returned to the lead smelter circuit. By ensuring that the proper amount of metallic iron is formed, there is reasonable assurance that most of the indium reports in the lead bullion.

The net recovery of indium and tin from sintered tailings to bullion is about 65 per cent, while that of lead is 70 per cent. The remainders are not lost as they are returned to the main metallurgical circuits for reprocessing. It is expected that, with continued operation, modifications will be developed that will result in higher recoveries and minimize the proportions of the materials that must be recycled.

Electrolytic Parting of the Bullion

The bullion was found to behave in an interesting way when subjected to anodic oxidation. Lead, tin, and indium were expected to go into solution, from which the lead and tin could be deposited at the cathode, leaving the indium to build up in the electrolyte. The oxidation-reduction potential of indium is considerably more negative than that of tin and lead, −0.34 volts as compared with −0.13 for tin and −0.12 for lead, which would suggest the probability of indium dissolving readily at the anode and not depositing at the cathode. Instead, as much as 90 per cent of the indium was found to remain at the anode in the form of an anode slime containing 30–35 per cent indium and 35–40 per cent antimony. Such a sharp upgrading of the indium content of the bullion, concurrent with the separation of the lead and tin as a lead-tin alloy cathode deposit seemed a very promising approach to the recovery of the lead, tin, and indium values of this metal.

The lead fluosilicate electrolyte from the Betts process lead refinery, being readily available and suitable, was chosen for the electrolyte in this operation. Lead starting sheets used in the lead refinery are also suitable for this process. The current density is not critical, but a value of 12 amp/ft² was chosen. Anode slimes are removed on a three-day cycle. The addition agents used in the lead refinery also satisfy this process. In general, this process may be operated in a manner almost identical to that of electrolytic lead refining. A typical anode slime composition is: In—33%; Sb—37%; Cu—12%; Sn—8%; Pb—3%; As—1%.

The cathode deposit contains 90–92 per cent lead, with the remainder being tin.

The lead content of the electrolyte gradually falls, as indium and tin enter it. The tin content levels off at about four g/l while the indium continues to rise. The lead content, which is initially in the range 50–60 g/l, is not allowed to fall below 15 g/l. It is maintained at this level by the addition of a lead refinery by-product, a crude lead fluoride, which is soluble in this electrolyte. The conductivity of the electrolyte gradually decreases as the indium content increases, which is objectionable. However, it is suspected that in this process the conductivity change results more from the increase in fluorine content than from any change in the metal content. There is no change in the chemically determined free acid content of the electrolyte. The electrolyte is withdrawn when the indium content reaches 35 g/l and the conductivity about one-half of the original value. The recovery of the indium, tin, and lead content from the withdrawn electrolyte is described later.

The reason for the retention of indium in the anode slimes appears to be related to the nature of the system Pb-Sn-Sb-In when its composition is approximately that produced in the electric furnace, namely, Pb—80%, Sn—10%, Sb—5%, In—5%. This system consists largely of a lead-tin alloy of the relative composition 80-10, upon which is superimposed the compound InSb. Some SnSb is also present, accounting for the retention of some tin in the anode slimes and the loss of some indium to the Pb-Sn alloy and thence to the electrolyte. The stability of the compound InSb is evidently sufficient to prevent indium from being oxidized at anodes operating close to the reversible potential of lead, and thus 0.2 volt more positive than the standard potential of indium. Polarographic studies of the electrochemical behavior of indium have shown that the electrolyte has a strong influence on the rate of electrochemical processes involving this element. In hydrofluosilicic acid, among many others, reactions involving indium appear to exhibit a distinct element of slowness, or in other words, moderate activation energies. This factor, in combination with the chemical association of indium and antimony, described earlier, may combine to render the bulk of the indium content of the anode passive. The electrolyte factor alone is not capable of preventing the oxidation of indium. This is demonstrated by the 10 to 15 per cent of the total indium content, not associated with antimony, which enters the electrolyte.

For these reasons it is desirable to keep the molar ratio of indium to antimony in the bullion close to unity. As indium exceeds antimony, the excess is oxidized and the recovery of indium in the slimes falls below the 80–90 per cent maximum. As the indium content of the electric furnace charge exceeds the antimony content, the bullion product usually contains more indium than antimony. This has been corrected by the addition of a high antimony content (28%) antimonial lead. In the future it is planned to recirculate a portion of the antimony-tin residue from the anode slimes treatment (see

below) to keep the indium-antimony ratio of the bullion at unity. This step will also increase the tin recovery of this process.

Treatment of Indium Slimes

The high indium slimes are treated for indium recovery as follows. Weighed amounts of the dried slimes mixed with the indium-tin hydroxides from the electrolyte recovery (see below) are mixed with concentrated sulfuric acid, and the mass is roasted to about 300°C. The metals are thoroughly oxidized; indium, copper, and lead to their sulfates, antimony, tin, and arsenic to oxides. The sulfated mass is leached with water. Indium, copper, and a small amount of arsenic are taken into solution. Antimony, tin, lead, and most of the arsenic remain in the residue, and this is filtered off.

Sodium chloride (50 g/l) is added to the acid sulfate extract at this point, the *p*H is adjusted to 1.0, and sheets of crude indium are placed in it. Cementation of the copper, which carries the arsenic with it, takes place rapidly. When it is complete, the copper-coated indium sheets are removed and replaced with zinc or aluminum sheets and the *p*H is adjusted to 1.5, whereupon cementation of the indium content of the solution proceeds rapidly. It has been found desirable when using aluminum to limit the indium content of the solution to about 50 to 60 g/l before cementation of the indium. At higher indium concentrations, the formation of aluminum sulfate in excess of its solubility lowers the indium recovery by coating the aluminum sheets with crystals of this salt. The sponge indium is removed from the solution, washed, compacted, melted under a caustic soda solution, and cast into slabs, which form the anodes for the electrolytic refining operation. At this stage, the indium has a purity in excess of 99.5 per cent. The major impurities present are lead, tin, iron, copper, and zinc or aluminum, depending on the metal used for cementation.

The addition of sodium chloride to the sulfated slimes water extract may merit an explanation. Electrochemical reactions of indium are very sensitive to the solutions in which they are carried out. Of the common inorganic anions, only the halides, excluding fluoride, allow these reactions to take place reversibly. The chloride was chosen because of its low cost.

Electrolyte Recovery

The electrolyte from the electrolytic parting of the bullion when discarded has the following composition: Pb, 15 g/l; Sn, 4 g/l; In, 35 g/l.

Lead is precipitated with sulfuric acid, and the sulfate returned to the lead smelter. The fluosilicate content is precipitated as sodium fluosilicate using sodium chloride and sodium hydroxide. The caustic sludge from the melting of indium sponge, which contains some indium, can be used at this point. The indium and tin are then precipitated as the combined hydroxides, using ammonium hydroxide. These are mixed with the anode slimes for further treatment.

Electrolytic Refining of Crude Indium

The most critical feature in the electrolytic refining of this metal is the choice of electrolyte. As indicated above, halides, other than fluoride, allow the electrochemical reactions of indium to take place reversibly. Polarographic studies of indium demonstrated this, and also showed why some previous attempts to refine the metal, using a soluble anode, had failed. It is noteworthy that previous successful attempts to deposit indium electrolytically were achieved with electrolytes containing citrate and tartrate (1). Both of these anions have been shown by polarography to allow the reversible reduction of indium from solution.

The electrolyte chosen for this refining operation and other features are as follows:

Details of electrolytic refining of indium

Indium (as chloride or sulfate)	40 to 60 g/l
Sodium chloride	90 to 100 g/l
*p*H	2.0 to 2.5
Temperature	less than 40°C
Current density	10 to 20 amp/ft²
Addition agent	glue, 1.0 g/l satisfactory
Anodes	bagged (cotton)
Tanks	rubber-lined steel
Product	99.98% indium

The indium content of the electrolyte is not critical. 40 to 60 g/l was the level chosen. Sodium chloride was added to provide the chloride ion necessary to ensure reversible anode and cathode behavior, and also to increase the conductivity of the electrolyte. As the temperature must be maintained below 40°C to ensure 100 per cent cathode current efficiency, a minimum generation of heat in the bath is necessary. This temperature requirement has been achieved without the aid of supplementary cooling. In combination with the temperature, the acidity of the electrolyte contributes to the cathode current efficiency. The *p*H is maintained in the range 2.0–2.5, in which range it is very stable. The current density has not been found to be critical. Values, higher than those indicated, might necessitate supplementary cooling in warm weather. Little work on addition agents for this process has been done, but a small amount of glue (1 g/l) gives an adequately smooth deposit. The anodes are bagged to prevent the small amounts of very fine lead, tin, and copper formed upon them from being mechanically carried

into the cathode deposit. The rubber-lined steel tanks are easily fabricated, and have proven satisfactory. Typical impurities in the cathode metal are: Pb, 0.007%; Sn, 0.007%; Cu, <0.001%; Fe, <0.001%; Cd, <0.001%. By careful re-electrolysis a metal of 99.999 per cent purity has been prepared. The cathodes are melted under a caustic soda solution cover and cast into large bars.

Analysis of Indium

Polarographic methods are used for all indium analyses in these operations. Analyses of refined indium metal for impurities use polarographic, spectrographic, and colorimetric methods.

The adoption of polarographic procedures for the analyses of and for indium has led to a greater knowledge of the electrochemistry of this element, which was of considerable value in choosing and developing this process.

Electrochemistry of Indium

This subject has been treated by others (2). The tendency of compounds of indium to be relatively nonionic or covalent in their bonding is felt to be one of the more important properties of this element which influences its metallurgy. The electrochemistry of indium in many electrolytes is affected by the high activation energies of the electrode processes. Kinetic factors also appear to influence the behavior of indium in high temperature reactions, such as the passage of indium through the lead blast furnaces, and in the electric furnace smelting of the indium-bearing slags previously described. In many respects the chemical behavior of indium is similar to that of tin, which accounts for the close association of these two elements in the lead-zinc metallurgical operations.

Properties and Uses of Indium

Indium is characterized by its extreme softness and ductility, relatively low melting point (156°C) and high boiling point (2.000°C), and its resistance to atmospheric and alkaline corrosion. It will be appreciated that a metal with these properties would find little use as a structural metal, but that its value would be found in special applications. Moreover, at a price of about 2½ times that of silver, uses are restricted to those in which small quantities of indium are effective. Outstanding is the use of a diffused layer of indium in high speed bearing alloys. Other applications are in alkali resistant solders (3) fusible alloys, and glass-to-glass and glass-to-metal sealing preparations (4).

Certain properties of indium and indium compounds hold promise of useful applications in the electrical and electronics industries.[2] These include the use of indium as a component of junction-type transistors (5), and of indium alloys as a solder in glass capacitators and as low resistance contacts with oxides such as TiO_2 and $BaTiO_3$, suggesting its value in piezoelectric units.

Other uses suggested for indium metal are for a counterelectrode in selenium rectifiers, and as an impurity addition in semiconductors for the purpose of stabilizing them in prepared electrical states. The oxides, sulfides, selenides, and tellurides of indium are all semiconductors and photoconductors. The oxide, either in film form or as a sintered compact of In_2O_3, has the characteristics that make it potentially useful as a resistor, either in the form of a film resistor heating element or a printed circuit resistive element.

Indium sulfide (In_2S_3) has a large negative temperature coefficient of resistivity, and is chemically and electrically stable at fairly high temperatures, which makes it a potential component for use in a thermistor. It also exhibits distinct phosphorescent properties.

Any discussion of this paper will appear in a Discussion Section, to be published in the December 1953 issue of the JOURNAL.

REFERENCES

1. L. R. WESTBROOK, *Trans. Electrochem. Soc.*, **57**, 289 (1930).
2. T. MOELLER AND B. S. HOPKINS, *Trans. Electrochem. Soc.*, **93**, 84 (1948).
3. S. M. GRYMCO AND R. I. JAFFEE, *Materials & Methods*, **31**, (3) 59, (1950).
4. R. I. JAFFEE AND S. M. WEISS, *Materials & Methods*, **36**, (3), 113 (1952).
5. L. D. ARMSTRONG, *Proc. Inst. Radio Engrs.*, **40**, 1341 (1952).

[2] From studies made at Battelle Memorial Institute, Columbus, Ohio.